Universität Rostock Traditio et Innovatio

Thermal and photocatalytic C-C and C-N bond formation by atom-transfer radical additions and photocycloadditions

Dissertation

in kumulativer Form

zur Erlangung des akademischen Grades

Doctor rerum naturalium

(Dr. rer. nat.)

an der Mathematisch-Naturwissenschaftlichen Fakultät

der Universität Rostock

vorgelegt von

Rajesh Dasi

geb. in Warangal, Indien

Rostock 2023

https://doi.org/10.18453/rosdok_id00004745

Die vorliegende Dissertation entstand an der Universität Rostock, am Institut für Chemie in der Abteilung Organische Chemie, in der Arbeitsgruppe von Prof. Dr. Malte Brasholz in der Zeit von März 2020 bis Juni 2023.

This dissertation was created at the University of Rostock, at the Institute of Chemistry, in the Department of Organic Chemistry, from March 2020 to June 2023 under the supervision of Prof. Dr. Malte Brasholz.

1. Gutachter: Prof. Dr. Malte Brasholz, Universität Rostock

2. Gutachter: Prof. Dr. Robert Francke, Leibniz-Institut für Katalyse

Datum der Einreichung: 2023

Datum der Verteidigung: 2024

Selbstständigkeitserklärung

Ich versichere hiermit an Eides statt, dass ich die vorliegende Arbeit selbstständig angefertigt und ohne fremde Hilfe verfasst habe. Dazu habe ich keine außer den von mir angegebenen Hilfsmitteln und Quellen verwendet und die den benutzten Werken inhaltlich und wörtlich entnommenen Stellen habe ich als solche kenntlich gemacht.

I hereby affirm that I have written the present work myself without any other assistance. No other resources were utilized than stated. All references as well as verbatim extracts were quoted, and all sources of information were specifically acknowledged.

Rostock, den 06.05.2024
Rajesh Dasi

कर्मण्येवाधिकारस्ते मा फलेषु कदाचन। मा कर्मफलहेतुर्भूर्मा ते सङ्गोऽस्त्वकर्मणि॥

-भगवद् गीता २-४७

"You are only entitled to the action, never to its fruits"

-Bhagavad Gita, 2-47

Acknowledgment

I would like to take this opportunity to express my sincere gratitude to my supervisor Prof. Dr. Malte Brasholz for his outstanding guidance during my doctoral journey and for providing me with excellent support, encouragement and an optimistic research environment. His enormous motivation and assistance always helped me throughout my research studies. I am extremely honored to be a part of his research group and to work under his supervision.

I would like to express my sincere thanks to Dr. Alexander Villinger for carrying out the X-ray crystallographic analysis and Prof. Dr. Julia Rehbein for our collaboration work as a part of my thesis. I would like to acknowledge my sincere thanks to all of the analytical service members of the University of Rostock. Specially, Dr. Dirk Michalik, and Ms. Heike Borgwaldt for the NMR services.

I would like to thank the members of our group Dr. Malte Gallhof, Dr. Eva Schendera, Dr. Mario Frahm, Paul Seefeldt, Saikumar Banda**,** and Felix Lorenz for your kind, helpful and valuable research discussions and pleasant working environment. A very special thanks to Dr. Lisa Marie Gronbach for your professional and personal support. Thank you also for the funny conversations and friendly meetings. I would like to express my sincere thanks to Mrs. Alice Voß for all the technical assistance. I am grateful to Mrs. Adelgunde Fifelski for the administrative support.

I would like to thank my dear friends Vijay, Anju, Vicky, Dinesh, Dr. Priyanka, Dr. Shital, Dr. Vishwas, Dr. Thiru, Sai, Dr. Manual Gronbach, Fairoosa, Shamna, Soumya, Maria, Alex, Johanna, Rashma, Veeda, Vidhi, Rokhya, Dr. Andhranik, Arpine, and Neeraja for their encouragement and support each and every time.

My heartfelt thanks to my parents for their unwavering love, constant support, and for being as my major source of motivation and strength. Last and most importantly I would like to thank my family members, Tharun, Prooja Priya, Haritha, and Ganesh for their love, encouragement and always being there for me to support. I would like to extend my sincere thanks to each and every one who is constantly there to support me each and every time.

Table of content

List of Abbreviations

Ac	Acetyl
AIBN	Azobis(isobutyronitril)
AQ	Anthraquinone
Ar	Aryl
ATRA	Atom transfer radical addition
ATRP	Atom transfer radical polymerization
BHT	Butylated hydroxytoluene
Bn	Benzyl
Boc	*tert*-Butyloxycarbonyl
bpy	2,2'-Bipyridyl
c.f.	confer
Cat.	Catalyst
CCDC	Cambridge Crystallographic Data Centre
CD	Circular dichroisms
CFL	Compact fluorescent lamp
d.r.	Diastereomeric ratio
DCE	Dichlorethane
DCM	Dichloromethane
DDQ	2,3-Dichlor-5,6-dicyano-1,4-benzochinon
dF{CF_3}ppy	2-(2,4-difluorphenyl)-5-trifluormethyl)pyridyl
DFT	Density Functional Theory
DMF	N,N-Dimethylformamid
DOD	Dual oxidative dehydrogenation
d*t*bbpy	4,4'-Di-tert-butyl-2,2'-dipyridin
e.r.	Enantiomeric ratio
EDG	Electron Donating Group
EnT	Energy transfer
eq.	equivalent
et al.	*et alii* (lat.)
EWG	Electron Withdrawing Group
HOMO	Highest occupied molecular orbital

IC	*Internal conversion*
ISC	*Intersystem crossing*
LED	Light-emitting diode
LUMO	Lowest unoccupied molecular orbital
M	Molar Mass
mL	Millilitre
mmol	Millimole
mol	Mole
NBO	Natural Bond Orbital
NBT	Nitro-blue tetrazolium
°C	Degree Celsius
PC	Photocatalyst
ppy	2-Phenylpyridin
r.r	Regioisomeric ratio
r.t.	Room temperature
SCE	*Saturated calomel electrode*
Sens	Sensitizer
SOMO	Singly occupied molecular orbital
Temp.	Temperature
TEMPO	2,2,6,6-Tetramethylpiperidinyloxyl
THF	Tetrahydrofuran
UV	Ultraviolet
μmol	Micromole

Abstract

This cumulative dissertation presents the development of new thermal and photochemical methods for formation of carbon-carbon and carbon-heteroatom bonds. The first example of radical functionalisation of biomass-derived 5-chloromethylfurfural (CMF) was described. A highly efficient triethylborane/oxygen-mediated atom transfer radical addition (ATRA) reaction between CMF and styrene derivatives was developed. Additionally, *in-silico* studies were performed on the CMF-derived 2-formyl-5-furfuryl radical intermediate, for characterizing its electronic properties and its behaviour in radical addition reactions. Further, a series of ATRA products were synthesised using a variety of substituted alkenes with high yield and selectivity.

In the second part, visible light-mediated triplet-sensitized [2+2] and [3+2] photocycloadditions of 2-cyanochromone with several alkenes were developed, using (Ir $[dF(CF_3)ppy]_2(d$*t*$bpy))PF_6$ as the photosensitizer. The method allowed to access the corresponding cycloadducts with high regio- and diastereoselectivity. The use of mono- di- and trisubstituted styrenes as a reactants led to [2+2]-cycloadducts exclusively. Employing trialkyl-substituted alkenes as reaction partners resulted in the formation of [3+2]-cycloaddition products.

Finally, a photocatalytic one-pot dehydrogenative Aza Paternò-Büchi reaction of dihydroquinoxalinones with substituted styrenes and acrylonitriles was developed. The method was successfully applied for the synthesis of diverse functionalised azetidine derivatives with high overall yields. In addition, structurally diverse amino acid-derived dihydroquinoxalinones were employed for the synthesis of the corresponding azetidines. In-depth mechanistic investigations were performed to elucidate the reaction mechanism.

Kurzfassung

In dieser kumulativen Dissertation wird die Entwicklung neuer thermischer und photochemischer Methoden zur Bildung von Kohlenstoff-Kohlenstoff- und Kohlenstoff Heteroatom-Bindungen vorgestellt. Das erste Beispiel einer radikalischen Funktionalisierung von 5-Chlormethylfurfural (CMF) aus Biomasse wurde beschrieben. Es wurde eine hocheffiziente Triethylboran/Sauerstoff-vermittelte Atomtransfer-Radikaladdition (ATRA) zwischen CMF und Styrolderivaten entwickelt. Darüber hinaus wurden *in-silico*-Studien an dem von CMF abgeleiteten 2-Formyl-5-furfuryl-Radikal durchgeführt, um seine elektronischen Eigenschaften und sein Verhalten in radikalischen Additionsreaktionen zu beschreiben. Darüber hinaus wurde eine Reihe von ATRA-Produkten mit verschiedenen substituierten Alkenen in hoher Ausbeute und Selektivität synthetisiert.

Im zweiten Teil wurden durch sichtbares Licht vermittelte Triplett-sensibilisierte [2+2]- und [3+2]-Photocycloadditionen von 2-Cyanochromon mit verschiedenen Alkenen unter Verwendung von (Ir [dF(CF3)ppy]2(dtbpy))PF_6 als Photosensibilisator entwickelt. Diese Methode ermöglichte die Synthese der entsprechenden Cycloaddukte mit hoher Regio- und Diastereoselektivität. Bei der Verwendung von mono- di- und trisubstituierten Styrolen als Reaktionspartner wurden ausschließlich [2+2]-Cycloaddukte als Reaktionsprodukte erhalten. Die Verwendung von Trialkyl-substituierten Alkenen als Reaktionspartner führte zur Bildung von [3+2]-Cycloaddukten.

Schließlich wurde eine photokatalytische dehydrierende Aza Paternò-Büchi-Reaktion von Dihydrochinoxalinonen mit substituierten Styrolen und Acrylnitrilen entwickelt. Die Methode wurde erfolgreich zur Synthese verschiedener funktionalisierter Azetidin-Derivate mit hohen Ausbeuten eingesetzt. Darüber hinaus wurden strukturell diverse, von Aminosäuren abgeleitete Dihydrochinoxalinone für die Synthese der entsprechenden Azetidine erfolgreich eingesetzt. Eingehende mechanistische Untersuchungen wurden durchgeführt, um den Reaktionsmechanismus aufzuklären.

Introduction

1.1 Carbon-centered radicals and methods for their generation

Radical carbon-carbon or carbon-heteroatom bond formation is one of the most fundamental transformations in organic chemistry. Over the years, the application of free radical reactions has gained significant attention in the synthesis of various organic compounds.[1] The generation of carbon-centred radicals from feedstock chemicals and their subsequent addition to unsaturated compounds offers a wide range of synthetic applications.[2] The use of organotin reagents for radical generation is a classical approach that has had a significant impact on synthetic radical chemistry. The majority of tin-mediated radical formation reactions have been carried out by employing trialkyl/triaryl tin hydrides in the presence of radical initiators such as 2,2'-Azobisisobutyronitrile (AIBN).[1a-d,2a,3] Utilization of photochemical activation in this context has been predominantly been demonstrated for ditin reagents due to their effective homolysis of the Sn-Sn σ-bond.[4]

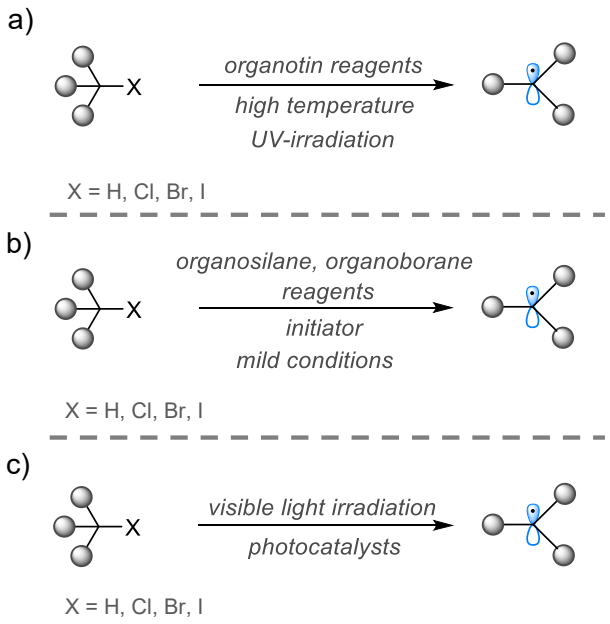

Scheme 1: Classical and modern methods for radical generation.

Even though organotin reagents have proven their significant importance in chemical transformations, concerns about their toxicity and metal contamination in the final product had led to identifying alternative approaches for radical generation.[5] In this context, organoboranes and organosilanes have been established as potent initiators for radical chain reactions with their superiority in reactivity and safety compared to organotin reagents. Among them, tris(trimethylsilyl)silane [$(TMS)_3SiH$] and triethylborane (Et_3B) are widely recognised

radical promoters in the development of synthetic radical chemistry and these reagents can be easily initiated using AIBN, UV-irradiation, or oxygen-dosing (**Scheme 1b**).[6] Particularly, the autoxidation of organoboranes has demonstrated their potential as potent radical initiators in a wide range of applications.[7] Compared to classical initiators, triethylborane in combination with oxygen provides a great advantage in the generation of more complex and functionalised radicals even at low temperatures.[6a-c,8]

1.1.1 Thermal methods for the generation of C-centered radicals

As mentioned earlier, the generation of carbon-centered radicals has been extensively performed using organotin, silane and borane reagents along with radical initiators such as peroxides and diazo compounds under thermal conditions. **Scheme 2a** and **2b** illustrate the general mechanistic pathways of organotin and silane reagent-mediated carbon-centered radical generation and subsequent radical addition to the alkenes.[3,6d,e] The radical chain reaction proceeds via an initial generation of tin- or silicon-centered radicals under thermal conditions along with the initiators. Subsequently, the tin or silicon radicals abstract the X atom from the organic substrate (R-X), leading to the generation of carbon-centered radicals. The resulting radical ($R^{\bullet}$) undergoes subsequent radical addition with alkenes. In radical chain propagation process, the newly generated radical intermediate abstracts the hydrogen atom from the organotin or organosilane reagent to deliver the desired final product.

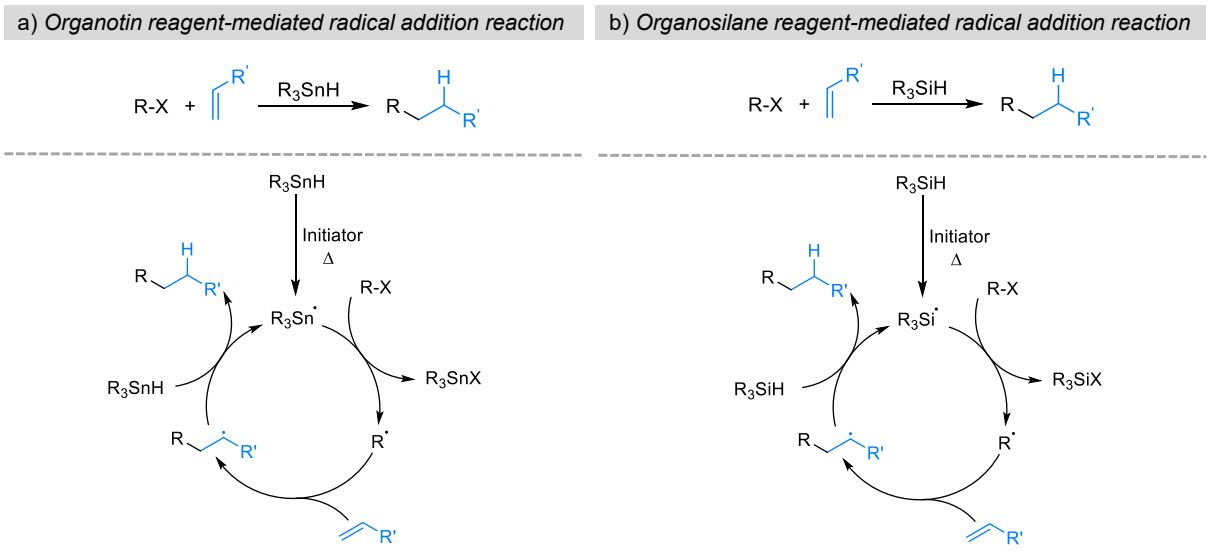

Scheme 2: General representation of organotin and organosilane-mediated radical addition reactions with their respective mechanism.

In comparison to the organotin and silane-medicated radical addition reaction, the general mechanism of organoborane reagent-mediated radical addition to alkenes is represented in **Scheme 3**.[6a-c] In the radical chain process, primarily organoboranes react with oxygen for the generation of an alkyl radical ($R^{\bullet}$) and dialkylborylperoxy radical ($R_2BOO^{\bullet}$). Formed ($R^{\bullet}$) radical subsequently reacts with the alkene (R'-X) through the abstraction of the X, resulting in the formation of a radical intermediate ($R'^{\bullet}$). The generated radical intermediate ($R'^{\bullet}$) participates in an addition reaction with an alkene and a subsequent transfer of hydrogen atom from a proton source leading to the formation of the final product. On the other hand, formed dialkylborylperoxy radical ($R_2BOO^{\bullet}$) propagates the radical chain process by reacting with organoborane reagent (R_3B) to give alkyl radical ($R^{\bullet}$).

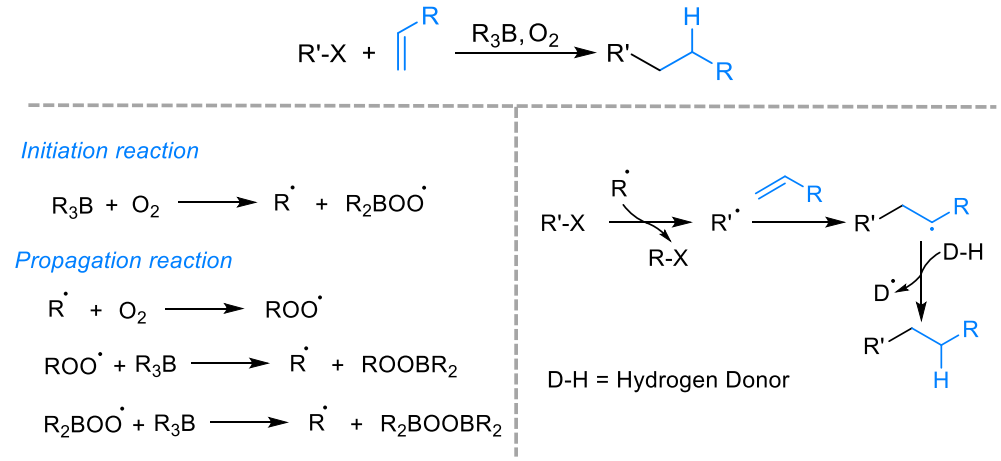

Scheme 3: General representation of organoborane-mediated radical addition reactions and mechanism.

1.1.2 Thermally induced radical addition reactions

The Giese[2a,9] and Kharasch[10] reactions are widely recognised as an effective approach for carbon-carbon bond formation via a radical pathway. Over the decades, these radical addition reactions have offered numerous advantages over organometallic ionic addition reactions.[9-13] In particular, halogen atom-transfer radical addition to alkenes (also known as ATRA reaction) takes advantage of radical reactivity for the simultaneous formation of C-C and C-X bonds.[11-13]

The general mechanism of Giese and ATRA reaction mediated by an organoborane reagent is depicted in **Scheme 4a** and **4b**, respectively.[2a,6a-c] In the classical process, a radical ($R^{\bullet}$) is generated from an alkyl halide (R-X) through the abstraction of heteroatom (X) by ethyl radical. The generated radical ($R^{\bullet}$) subsequently adds to the unsaturated substrate, which

results in the formation of a second radical intermediate. In the final stage, the carbon-centred radical intermediate abstracts the hydrogen atom from the proton source or a halogen atom X to deliver the corresponding final product.

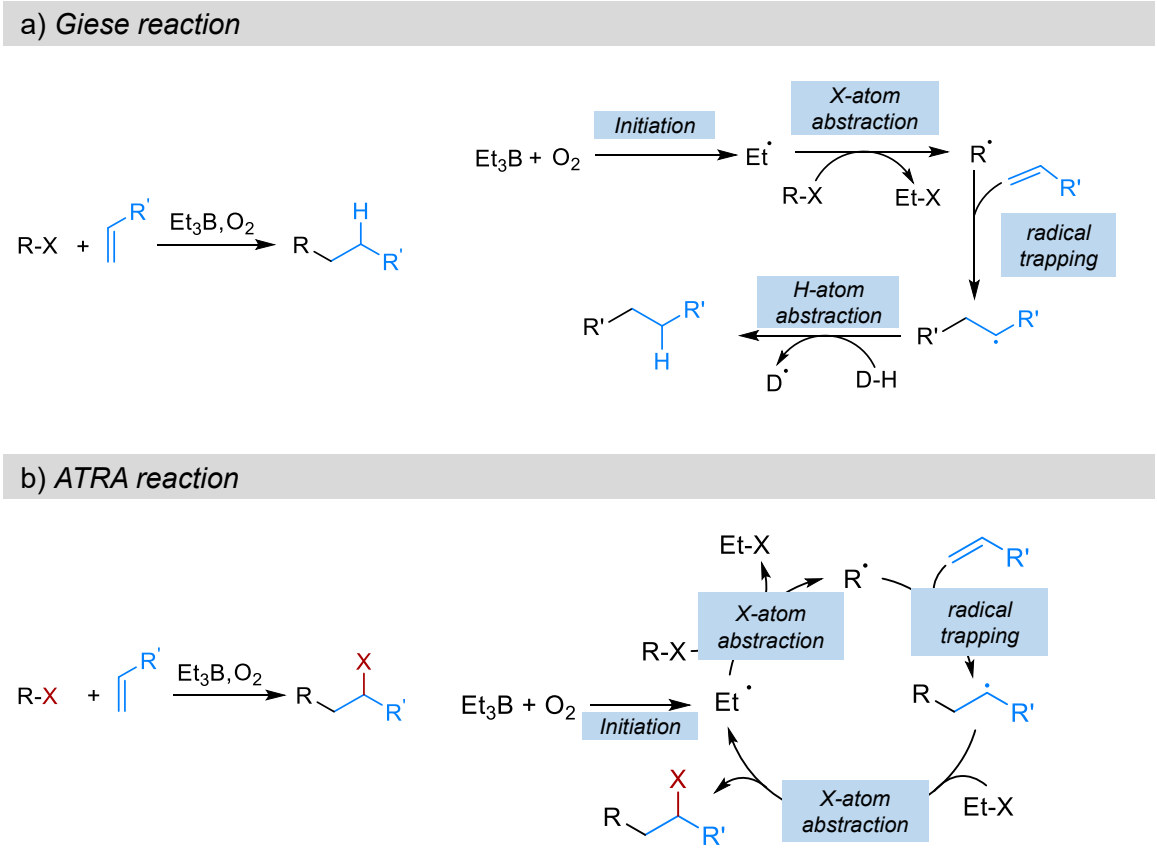

Scheme 4: General representation of Et_3/O_2-mediated Giese and ATRA reactions with their respective mechanism.

1.1.3 The Kharasch reaction and its variants

Since the discovery of ATRA reactions by Kharasch and co-workers, an unprecedented *anti*-Markovnikov addition of hydrogen bromide to alkenes with peroxides as radical initiators (**Scheme 5**),[10a] this reaction found widespread applications in the synthesis of complex halogenated compounds, natural products such as prostaglandins, alkaloids and including the synthesis of polyhalogenated compounds.[10,13,20d]

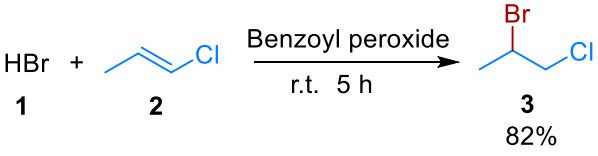

Scheme 5: First historical ATRA reaction developed by Kharasch *et al.*[10a]

In 1945, Kharasch *et al*. reported the addition of a polyhalogenated compounds such as tetrachloromethane, trichloromethane to 1-octene in the presence of dibenzoyl or diacetyl peroxide as radical initiators.[10b] In this radical addition reaction, a carbon-centered radical intermediate **6** is generated and subsequently undergoes addition to 1-octene (**7**), leading to the formation of another radical adduct **8**. Adduct **8** either abstracts the chlorine atom from **4** in a chain propagation step to give ATRA product **9** or it may react with another molecule of 1-octene (**7**) to form oligomeric products **10** (**Scheme 6**).

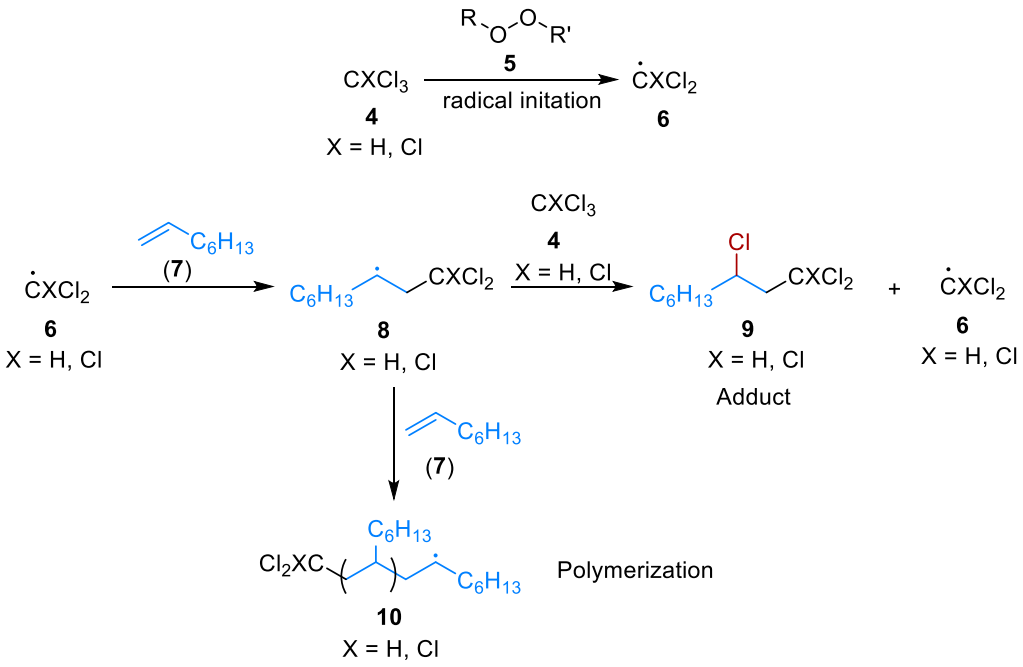

Scheme 6: Kharasch reaction of chloroform or tetrachloromethane with 1-octene (**7**).[10b]

Following the pioneering work of Kharasch, Curran and co-workers demonstrated the utility of the ATRA reaction by way of the introduction of new side chains on β-lactam rings (**Scheme 7a**).[13] Another advantage of ATRA reactions demonstrated by Curran and co-workers is known as atom transfer radical cyclisation (ATRC). Using $(Bu_3Sn)_2$ as a radical initiator, the cyclisation of α-iodo-carbonyl compounds **14** with terminal olefins was achieved. However, the reaction showed poor selectivity with a mixture of *cis*- and *trans*-isomers of the 5-*exo* and 6-*endo* products (**Scheme 7b**).[14]

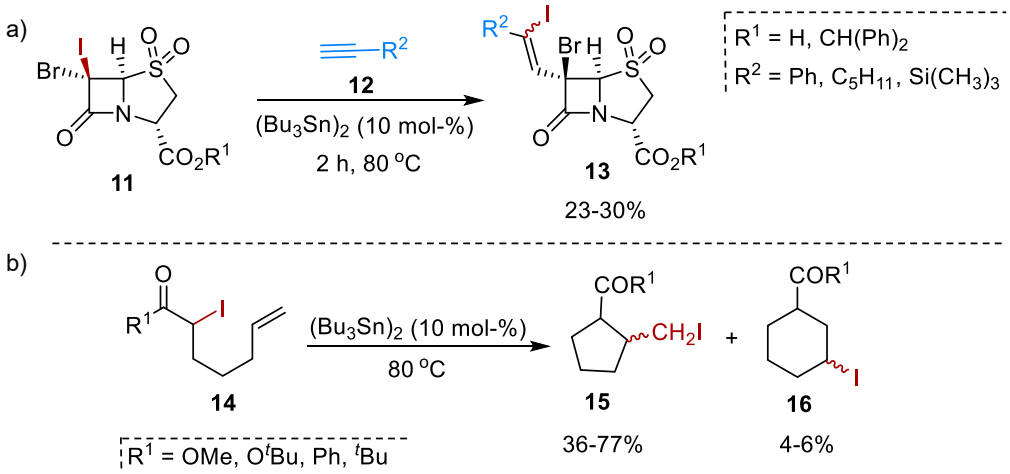

Scheme 7: a) ATRA reaction of α-iodocarbonyls with alkynes.[13] b) Atom transfer cyclisation of α-iodocarbonyls.[14]

In addition to organotin- and organosilane-mediated ATRA reactions, Oshima and co-workers developed a triethylborane-induced ATRA reaction along with oxygen as an initiator.[15] The desired ATRA products **19** was accessed in a high yield using ethyl bromoacetate, benzyl bromoacetate, bromomalonate and bromoacetonitrile along with various olefins **18** and Et_3B in the presence of air (**Scheme 8**). Another report from the same group demonstrated an Et_3B/O_2-mediated ATRC of iodoacetals and iodoacetates in water for the synthesis of corresponding lactones.[16]

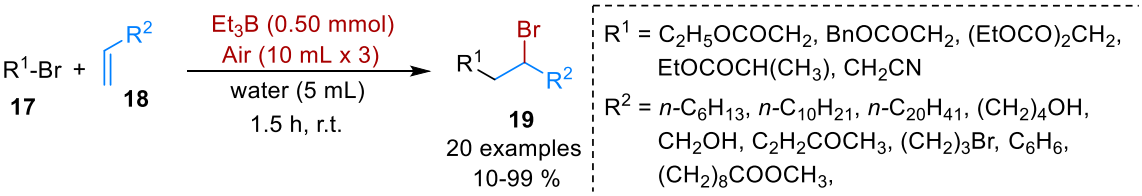

Scheme 8: Et_3B/O_2-mediated ATRA reactions by Oshima *et al*.[15]

In 1998, Oshima *et al.* reported another example of an Et_3B/O_2-mediated ATRA reaction of α-iodo-γ-butyrolactone **20** with several alkenes **21** in various acidic and basic aqueous solutions (**Scheme 9**). [17] The reaction between halogenated compounds **20** with terminal alkenes **21** or terminal alkynes led to the synthesis of corresponding ATRA products **22** in good yields. Moreover, it was found that triethylborane can initiate a radical reaction even under high acidic reaction conditions.

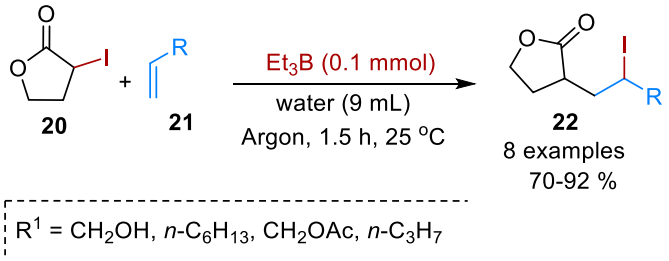

Scheme 9: ATRA reactions of iodo-γ-butyrolactone mediated by triethylborane.[17]

Porter and co-workers demonstrated a diastereoselective synthesis of ATRA products by a reaction between N-(α-bromoacetyl) oxazolidinones **23** and alkanes **24** employing the Et_3B/O_2 reagent system in combination with Lewis acids (**Scheme 10**).[18] The diastereoselective synthesis can be achieved with the use of chiral oxazolidinones as auxiliaries. While the reported method showed excellent control of the configuration in the generated stereogenic centers, it exhibited limitations with internal alkenes and tertiary bromides which did not furnish the desired ATRA products.

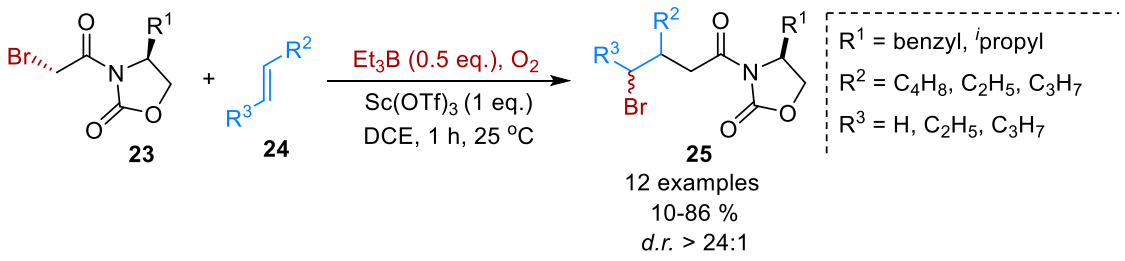

Scheme 10: Et_3B/O_2-mediated ATRA reactions developed by Porter *et al.*[18]

Following the initial discovery that ATRA reactions can also be carried out by transition metals, several efforts have been made to catalyse ATRA reactions using different transition metal complexes. Asscher and Vofsi reported the first metal catalysed ATRA reaction using iron (III)- or copper(II)-chloride in 1963.[19] Subsequently, many groups reported the use of copper,[20] iron,[21] and ruthenium[22] complexes to catalyse the ATRA reactions.

1.1.4 Photocatalytic generation of C-centered radicals

In contrast to thermal methods for generating C-centered radicals, and considering the need for mild methods to generate reactive radicals from polysubstituted substrates, there is a constant need to develop new, efficient, and green methods for their generation. The rapidly emerging field of visible light-driven photocatalysis has gained significant interest due to its

efficacy and specificity in chemical transformations along with its ability to generate organic radicals under mild conditions.[23,24] Moreover, visible light-driven reactions are less prone to side reactions and enable the reduction in toxicity and the danger associated with radical generation using thermal and UV-initiation methods.

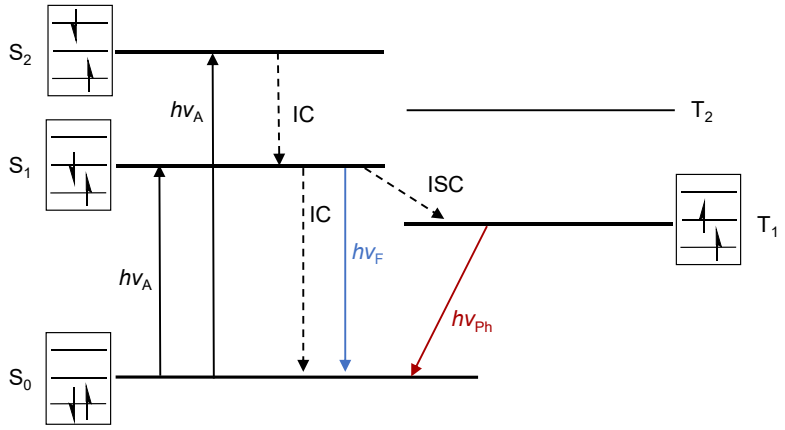

Scheme 11: JABLONSKI-Diagram: $h\nu_A$ = Absorption, $h\nu_F$ = Fluorescence, $h\nu_{Ph}$ = Phosphorescence, IC= *Internal Conversion*, ISC = *Intersystem Crossing*. [24,25]

Since most organic compounds do not absorb visible light, the addition of photocatalyst (PC) is necessary to access a variety of open-shell radicals, radical ions, and electronically excited species. Initially, the photocatalyst (PC) is excited to a higher singlet excited state (S_1 or S_2) from the ground state (S_0) through the absorption of light (**Scheme 11**). The higher singlet excited states (S_2) rapidly transition to the first singlet excited state (S_1) by *internal conversion* (IC). The relaxation of singlet excited (S_1) to the ground stage (S_0) can occur by further IC or fluorescence ($h\nu_F$). Alternatively, the singlet excited state (S_1) can convert into the first triplet excited state (T_1) through *intersystem crossing* (ISC). From there the first excited triplet state (T_1) can further undergo chemical reactions with a given reactant or relax to the electronic ground state (S_0) by phosphorescence ($h\nu_{ph}$).[24,25] More generally, a photochemical reaction can take place from the first excited singlet state (S_1) as well as from the first excited triplet state (T_1) and this reaction can be initiated by several mechanisms such as energy transfer (EnT), photoinduced electron transfer (PET) or atom transfer (AT) of the catalyst with a reactant.[25,26]

Photoinduced Energy Transfer (EnT)

The energy transfer (EnT) mechanism is one of the important and fundamental pathways in preparative photocatalysis. In this process, energy transfer occurs from the triplet-excited photocatalyst to the substrate and here photocatalyst (PC) is referred to as a sensitizer

(Sens).[27] Triplet-triplet energy transfer, also referred to as collisional or Dexter energy transfer, is the energy transfer pathway most relevant in synthetic organic chemistry.[28-30]

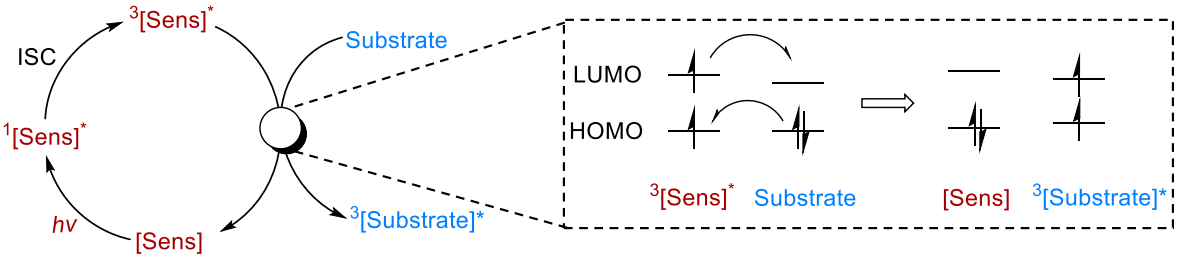

Scheme 12: Schematic representation of Dexter energy transfer.

During a collisional triplet energy transfer, a ground state acceptor molecule is excited to its triplet state via electron exchange with a triplet excited donor molecule. The excited donor molecule, i.e. the triplet sensitizer, transfers an electron from its LUMO to the LUMO of the acceptor molecule and another electron is transferred from the HOMO of the acceptor molecule to the HOMO of the donor molecule (**Scheme 12**).[28,31] Therefore, it is important to consider the relative triplet energies of both the triplet sensitizer and substrate before combing them in a reaction. Photoinduced energy transfer can be used in synthetic chemistry to perform various types of reactions such as cycloadditions,[28-30] isomerisation of double bonds,[32,33] generation of reactive singlet oxygen species,[34] sensitisation of azide or diazo compounds,[35,36] cleavage of sulfur-sulfur bonds,[37] oxa-di-π-methane rearrangement,[38] methyl or phenyl group migration,[39] alkylation[40] and sensitised atom transfer radical additions.[41]

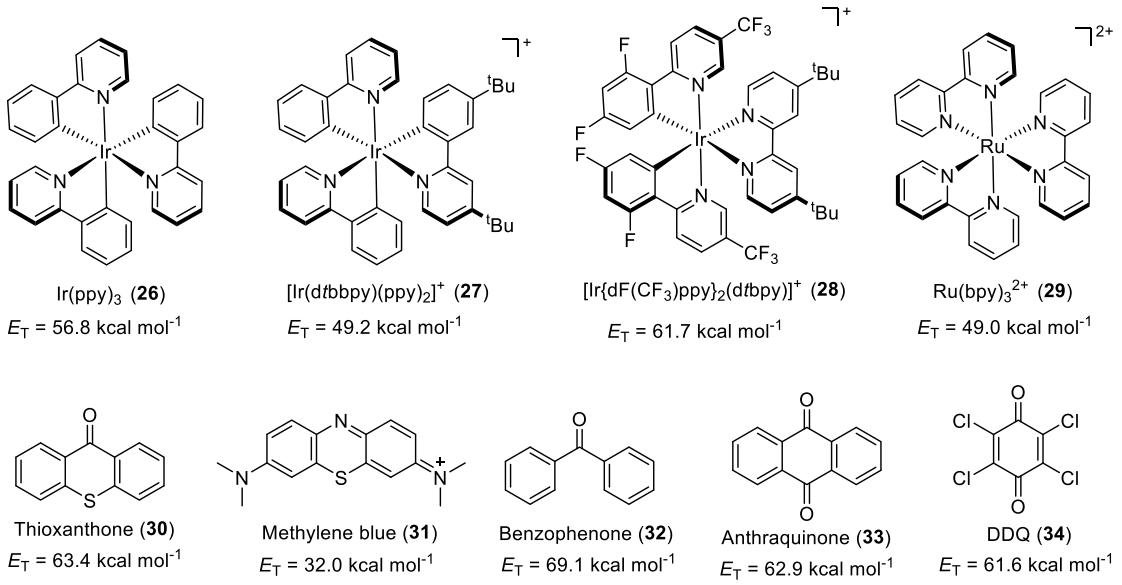

Figure 1: Common transition metal-based and organophotosensitizers with respective triplet energies.

The utilization of visible light-induced energy transfer has found widespread application in various cycloaddition reactions.[29-30] Liu and co-workers reported an energy transfer-mediated intermolecular [2+2] photocycloaddition of coumarin-3-carboxylates **35** with acrylamide analogues **36** using a iridium (III) complex **38** as a sensitizer to afford several cyclobutanbenzopyranones **37** with excellent yields (**Scheme 13**).[42] Furthermore, the synthesised cyclobutanbenzopyranones can be employed in the synthesis of biologically active tetrahydrodibenzofurans.

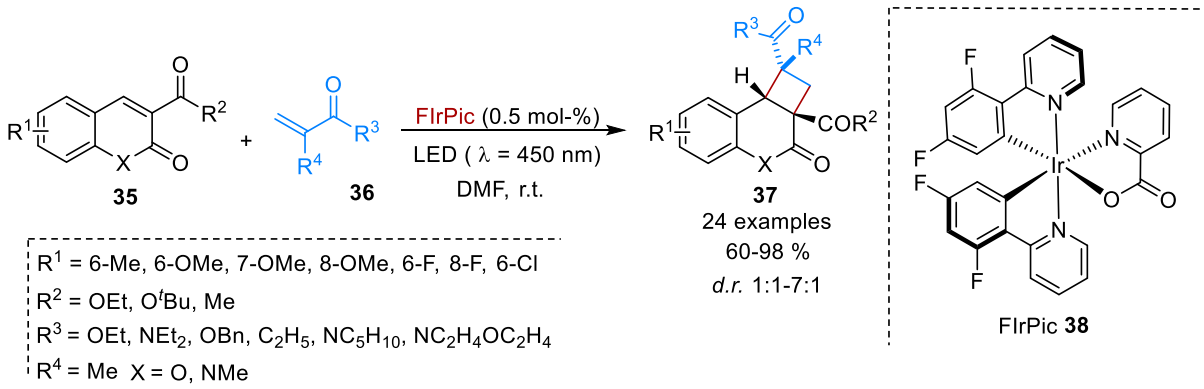

Scheme 13: Energy transfer-mediated Intermolecular [2+2] cycloaddition of coumarins by Liu. [42]

Yoon *et al.* demonstrated an intramolecular [2+2] cycloaddition of 3-alkoxyquinolone **39** by using a chiral iridium photosensitizer functionalised with a hydrogen-bonding domain **41** (**Scheme 14**).[43] This method provided an access to synthesis corresponding quinolone cycloadducts **40** with excellent enatioselectivities and it was found that enantiocontrol of the reaction was provided by the key interactions between pyrazole moiety of the catalyst and quinolone carbonyl group.

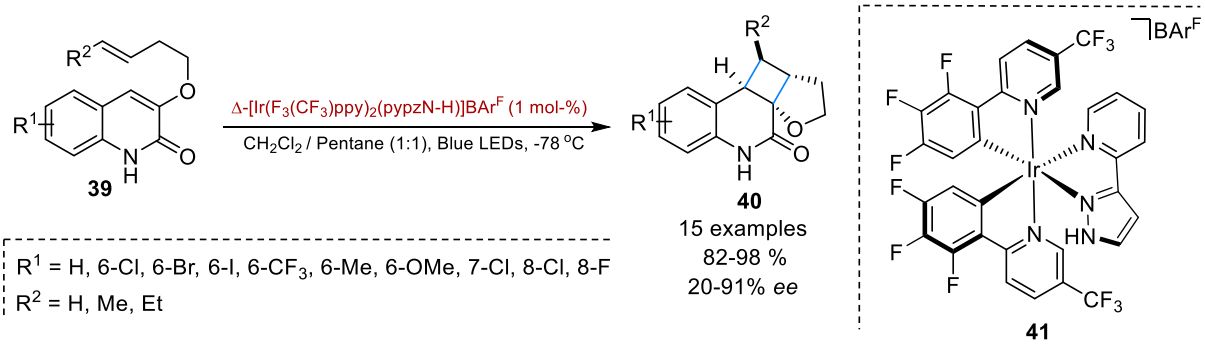

Scheme 14: Intramolecular [2+2] cycloaddition of 3-alkoxyquinolone by triplet energy transfer.[43]

Glorius and co-workers reported a novel photocatalytic dearomatization of pyridines by energy transfer-initiated intramolecular [4+2] cycloaddition (**Scheme 15**).[44] Employing a heterogeneous iridium based photosensitizer a variety of alkylated pyridines **42** were

converted in to highly functionalized isoquinuclidine analogs **43** with excellent yield. Moreover, this method showed an excellent regioselectivity and high functional group tolerance.

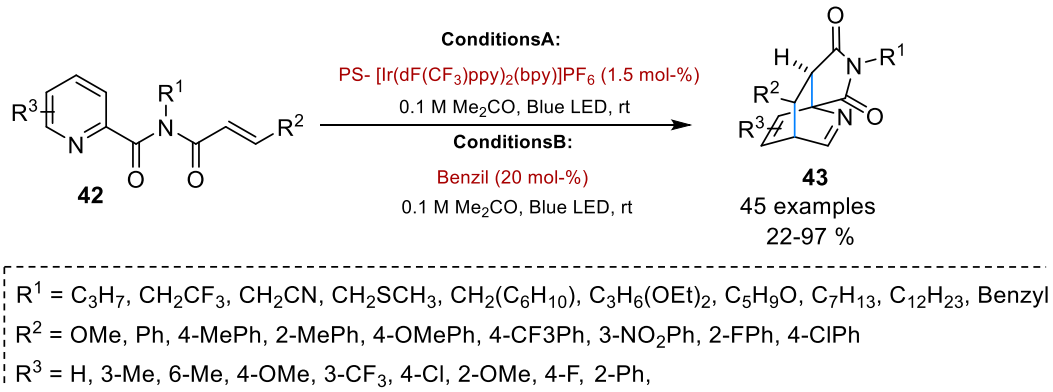

Scheme 15: Energy transfer-catalysed Intramolecular [4+2] cycloaddition.[44]

Further examples of energy transfer-induced cycloaddition reactions are provided in section 1.2.1

Photoinduced Electron Transfer (PET)

As mentioned earlier a photocatalytic reaction may take place by the mechanisms such as EnT, PET or AT. In the case of the photoinduced electron transfer mechanism, absorption of a photon in the visible light region by a photocatalyst leads to the generation of its excited state. Following the excitation, the photocatalyst exhibits two distinct independent electron transfer pathways which are known as oxidative quenching and reductive quenching (**Scheme 16**). The majority of metal photocatalyst typically exhibit short-lived singlet excited states, which rapidly undergo *intersystem crossing* (ISC) to generate their triplet excited state. Consequently, the oxidative and reductive quenching occurs from their triplet excited state. In reductive quenching, the transfer of an electron takes place from the electron donor (D) to the excited photocatalyst, resulting in the single electron reduction of the catalyst and the single electron oxidation of the donor, and generating the radical ions $PC^{\bullet-}$ and $D^{\bullet+}$ respectively. The reduced catalyst subsequently reacts with an electron acceptor (A) to return to its ground state and to generate the radical anion $A^{\bullet-}$. On the other hand, oxidative quenching occurs through an electron transfer from the catalyst to the acceptor, followed by the reaction of the oxidised catalyst with the electron donor, resulting in the catalyst returning to its ground state.[25,45]

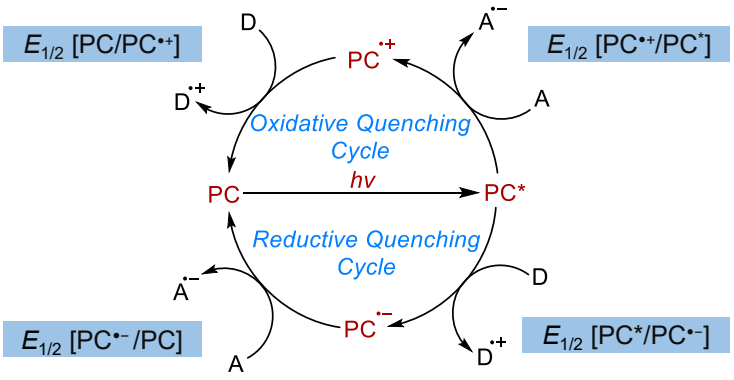

Scheme 16: General mechanism of photoredox catalysis through PET. A = Acceptor, D = Donor, $E_{1/2}$ = redox potential.[25,45]

The respective redox behaviour of the photocatalyst is described by the redox potentials of the excited state E^*_{Red} and E^*_{Ox}, which are derived from redox potentials of ground state E_{Red} and E_{Ox}, and the excitation energy ($E_{0,0}$) (Eq. 1 and 2).[25]

$$E^*_{Red} = E_{Red} + E_{0,0} \quad \text{(Eq. 1)}$$

$$E^*_{Ox} = E_{Ox} - E_{0.0} \quad \text{(Eq. 2)}$$

Different types of commonly used transition metal and organophotoredox catalysts with their excited state redox potentials are depicted in **Figure 2**. As examples of strongly reducing photocatalysts, the excited state redox potential [PC•+/PC*] of the iridium(III)-complex *fac*-Ir(ppy)$_3$ **44** is $E_{1/2}$ [PC•+/PC*] = -1.73 V *vs*. SCE (*saturated calomel electrode*) in MeCN, and for the organophotocatalyst 10-phenylphenothiazine (PPT) **49** the excited state redox potential [PC•+/PC*] is $E_{1/2}$ [PC•+/PC*] = -2.10 V *vs.* SCE in MeCN. As examples of oxidizing photocatalysts, the excited state redox potential [PC*/PC•−] of [Ir(d*t*bbpy)(ppy)$_2$]$^+$ **45** is $E_{1/2}$ [PC*/PC•−] = +0.66 V *vs.* SCE in MeCN and that of [Ir{dF(CF$_3$)ppy$_2$}(d*t*bpy)]$^+$ **46** is $E_{1/2}$ [PC*/PC•−] = +1.21 V *vs.* SCE in MeCN.[45-49] However, in addition to redox potentials, other properties such as respective absorption range (λ_{max}), excited state lifetime (τ), and triplet yield (Φ_T) are further important factors in the effectiveness of a photoredox catalyst.[25,45]

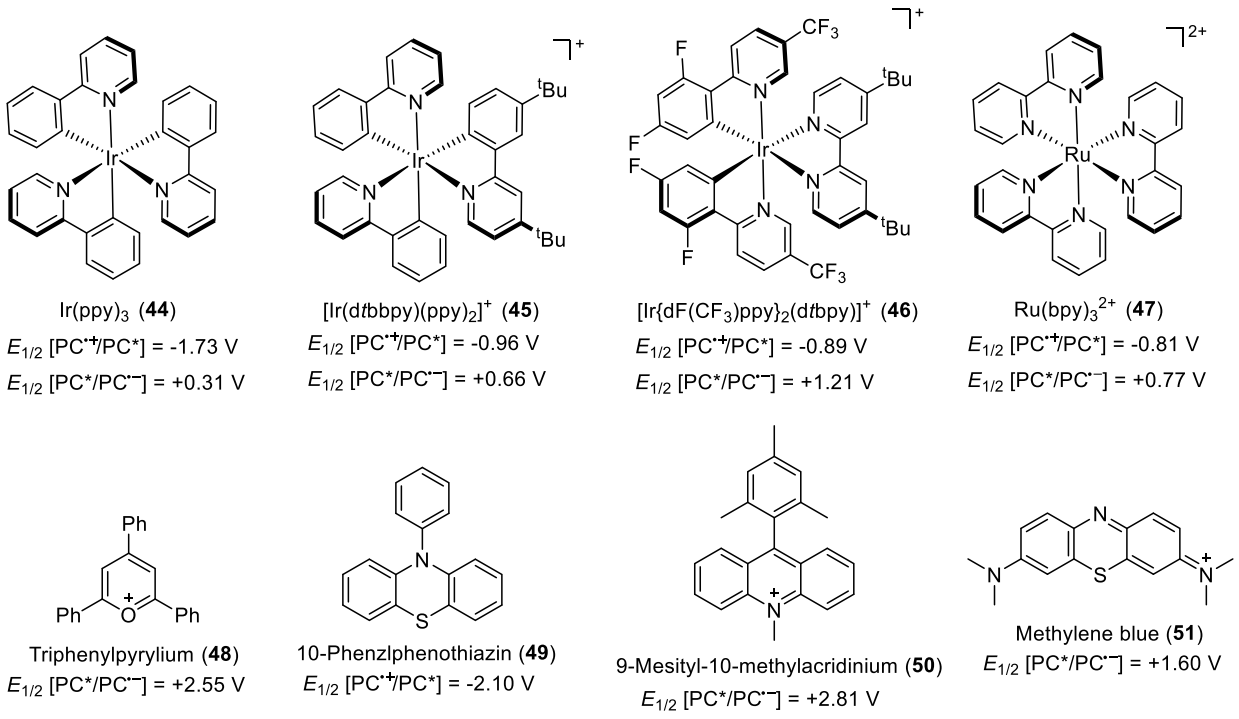

Figure 2: Common transition metal-based and organophotocatalysts with key excited-state redox potentials.

The generation of radical ions through photoinduced electron transfer (PET) provides several advantages over the classic methods of performing radical reactions, and this will be discussed here for exemplary transformations such as cycloaddition reactions (*cf.* Chapter 1.2) and atom transfer radical addition (ATRA, *cf.* Chapter 1.1.3) reactions.

In 2008, the group of Yoon reported a photoredox-induced intramolecular [2+2] cycloaddition using the ruthenium-based photocatalyst $Ru(bpy)_3^{2+}$ (**Scheme 17**).[50] Visible light irradiation of (bis)enone substrates **52** in the presence of $Ru(bpy)_3Cl_2$, $^iPr_2NEt$ and $LiBF_4$ provided access to cycloadducts **53** in a high yield with good diastereoselectivity. The reaction proceeds via initial reductive quenching of $*Ru(bpy)_3^{2+}$ by $^iPr_2NEt$ and subsequent one-electron reduction of the enone by $Ru(bpy)^{3+}$ to deliver cyclobutanes **53** through an intramolecular radical anion cyclisation.

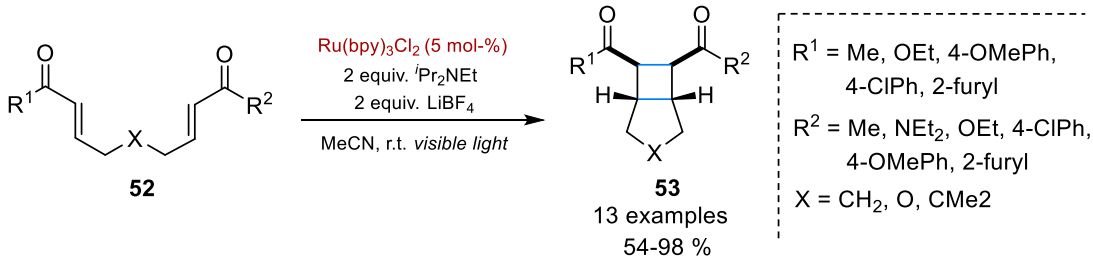

Scheme 17: Visible light photocatalysed Intramolecular [2+2] cycloaddition.[50]

The same group in 2010 reported an example of crossed intermolecular [2+2] cycloadditions of acyclic enones using the same catalytic system employed in earlier intramolecular [2+2] cycloadditions (**Scheme 18**).[51] Irradiation of aryl enone **54** in the presence of methyl vinyl ketone (**55**), $Ru(bpy)_3Cl_2$, $^iPr_2NEt$ and $LiBF_4$ gave the desired intramolecular formal [2+2] cycloaddition products in high yields with excellent chemo- and stereoselectivity. Importantly, only trace amounts of homodimerization products were observed and this was achieved by selectively employing more reactive Michael acceptors as the second reaction partner.

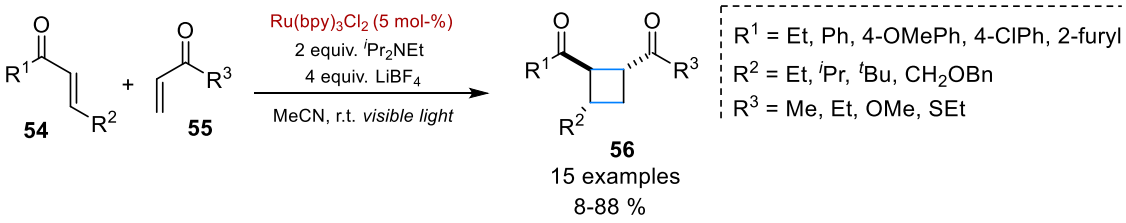

Scheme 18: Visible light-mediated Intermolecular [2+2] cycloaddition of enones **54**.[51]

In addition to reductive intra- and intermolecular cycloadditions of radical anions, a radical cationic Diels-Alder cycloaddition was developed by Yoon and co-workers (**Scheme 19**).[52] The reaction between substituted dienes **57** and electron-rich dienophiles **58** in the presence of $Ru(bpz)_3^{2+}$ under visible light led to [4+2] cycloadducts **59**. Further, the usefulness of this method was demonstrated in the total synthesis of natural product heitziamide A.

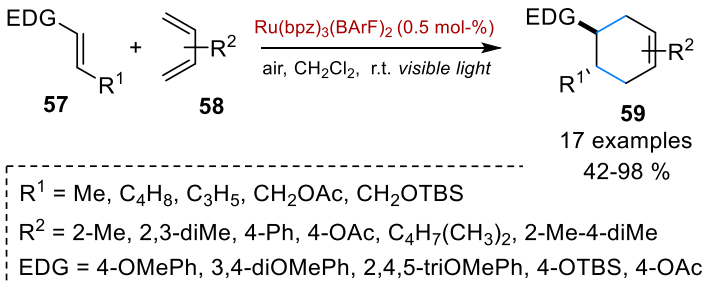

Scheme 19: Radical cationic [4+2] cycloaddition by visible light photocatalysis by Yoon *et al*.[52]

[3+2]-Photocycloadditions are well-known for the synthesis of polysubstituted pyrrole derivatives, which have numerous applications in organic synthesis as well as medicinal chemistry. Xiao and co-workers reported a visible light-induced [3+2]-photocycloaddition between 2*H*-azirines **60** with the electron-deficient alkynes **61** to synthesise pyrroles **62** under metal-free conditions and demonstrated this metal-free photocatalytic transformation provides access to the synthesis highly functionalized pyrroles and their corresponding drug analogues (**Scheme 20**).[53]

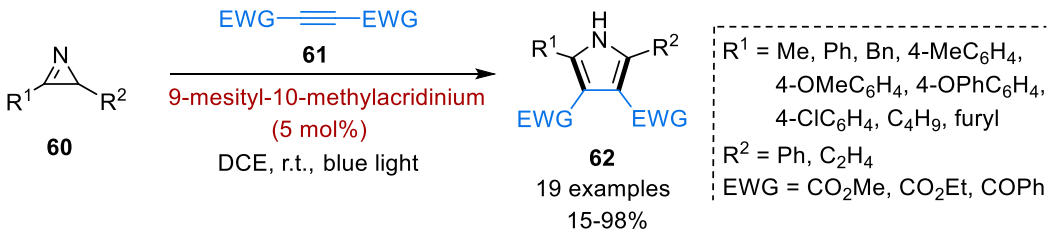

Scheme 20: Formal [3+2]-cycloaddition induced by visible light for the pyrroles synthesis.[53]

Visible light-induced ATRA reactions

Although atom transfer radical additions have been established as a powerful tool in synthetic chemistry, there are still limitations such as using high-temperature or UV-light sources. In light of recent developments, visible light catalysis has emerged as a promising alternative to radical addition reactions mediated by organotin and silane reagents. A number of metal complexes under visible light catalysis have proven to be exceptionally effective and versatile catalysts for ATRA reactions and have been applied to many useful transformations in organic synthesis.[54-56]

ATRA reactions generally may proceed via two different pathways, namely the radical chain pathway and the radical-cationic pathway (**Scheme 21)**. In the radical chain pathway, the X-atom abstraction from the substrate **63**, typically an alkyl halide, by the catalyst results in the generation of radical **64**. Radical **64** subsequently undergoes addition with alkenes **65**, followed by X atom abstraction from **63** in a radical propagation step which leads to the formation of the ATRA product **67** and regeneration of radical **64**.

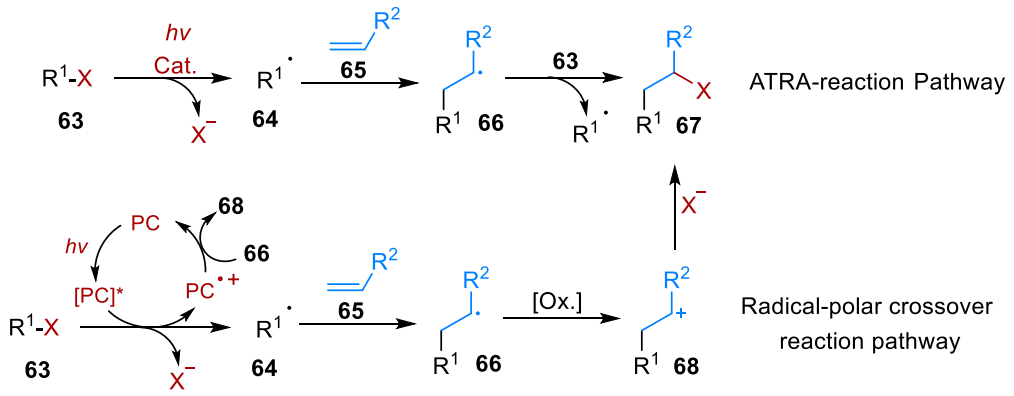

Scheme 21: General reaction mechanism of ATRA reactions by radical chain and radical-polar crossover pathways.[54]

In the radical-cationic pathway (also called radical-polar crossover pathway) a single electron transfer (SET) between photoredox catalyst and substrate R^1-X **63** leads to the formation of a radical **64**, the anion (X^-) and the catalyst radical cation $PC^{\bullet+}$. Subsequently, the formed radical **64** adds to the alkene **65**, and the newly generated radical intermediate **66** is oxidized to the carbocation **68** by the catalyst radical cation $PC^{\bullet+}$. The reaction of nucleophile (X^-) with the cation leads to the formation of the ATRA product **67**.[54]

Following the pioneering work by Kharasch and co-workers[10] who developed the thermal ATRA reaction, in 1994, Barton and co-workers reported the earliest example of a visible light-mediated ATRA reaction between phenylselenium sulfonate **69** and vinyl ethers **70** employing $Ru(bpy)_3Cl_2$ as the catalyst to synthesise β-phenylselenosulfones **71** (**Scheme 22**).[57] In the proposed mechanism, a tosyl radical was generated from the phenylselenium sulfonate via single electron transfer with the excited-state catalyst. Subsequently, the generated radical adds to the alkene **70**, leading to the formation of another radical intermediate. The resulting radical intermediate can react with the **69** to give desired ATRA product.

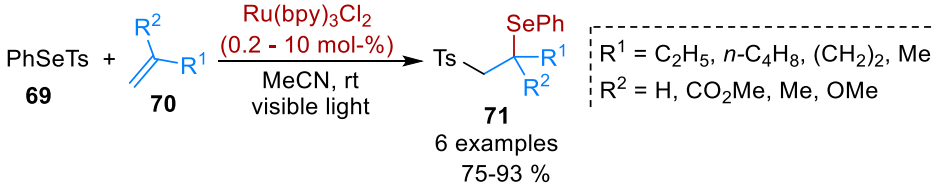

Scheme 22: Visible light-mediated ATRA reaction by Barton *et al.*[57]

In 2012, Stephenson *et al.* reported the first photoredox-catalysed ATRA reaction for the incorporation of a (per)fluoroalkyl moiety **72** into alkenes **73** (**Scheme 23**).[58] When alkyl halides **72** with fluorinated side chains are employed in ATRA reaction, the cleavage of the reactive carbon-halide bond by single electron transfer from the excited state photocatalyst is much facilitated. Although this synthetic transformation has demonstrated its effectiveness in the preparation of perfluorohalogenated products **74** from unactivated alkenes **73**, it still suffers from the application of perfluoroalkyl iodides as ATRA reagents.

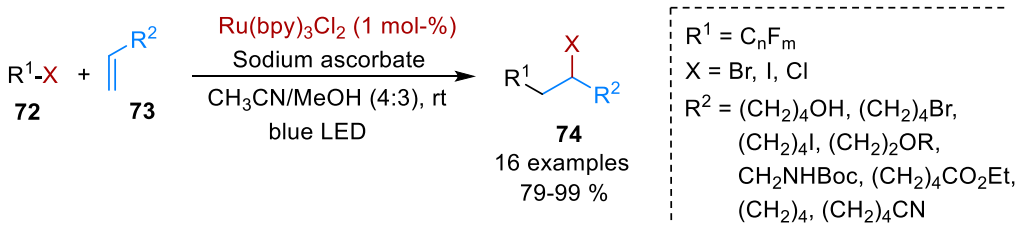

Scheme 23: Iodofluoroalkylation of alkenes by visible light-mediated ATRA-reaction by Stephenson *et al.*[58]

Subsequently, Reiser and co-workers introduced copper-based photocatalysts for wide applications in the photoinduced ATRA reaction (**Scheme 24**).[59] By using Cu^{I}-phenanthroline complex $[Cu(dap)_2]Cl$ as a catalyst, haloalkanes **75** such as α-bromoacetophenone, bromomalonate and perfluorobutyl iodide were successfully added to different alkenes **76** under visible light irradiation for the synthesis of corresponding ATRA products **77**.

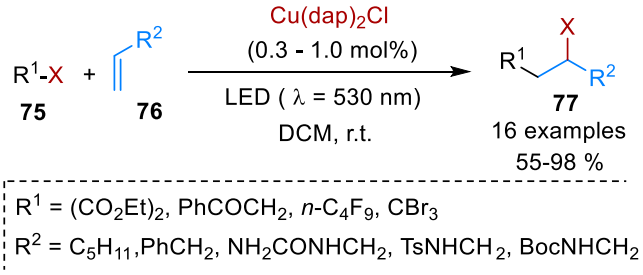

Scheme 24: Visible light-mediated copper(I)-catalysed ATRA-reaction by Reiser et al. [59]

1.2 Photocycloaddition reactions

Cycloaddition reactions are widely recognized for their ability to form carbon-carbon and carbon-heteroatom bonds with high stereoselectivity and atom efficiency.[60] During the last decades, photocycloaddition reactions have gained significant attention as they complement conventional (thermal) cycloadditions, and as they can allow for the synthesis of three- to eight-membered ring skeletons from simple precursors.[61-68] Importantly, photocycloadditions facilitate the synthesis of complex and distinctive natural products and molecules with high stereocontrol and increased ring strain. Moreover, it is possible to use visible light or sunlight as a sustainable energy source to carry out certain cycloaddition reactions.

Proco and co-workers reported a synthesis of the tetrahydrocyclopenta[*b*]benzofuran core of the rocaglamides (**81**) and (**82**) employing photoinduced [3+2] cycloadditions as key step (**Scheme 25**).[69] Upon irradiation at λ = > 350, 3-hydroxyflavone underwent an intramolecular proton transfer, leading to the formation of an oxidopyrylium betaine intermediate. Subsequently, betaine underwent [3+2]-dipolar cycloadditions with methyl cinnamate to afford the cycloadduct **79** along with the small amount of [2+2] cycloadduct. A subsequent base-induced rearrangement of intermediate **79** led to the desired scaffolds **80.**

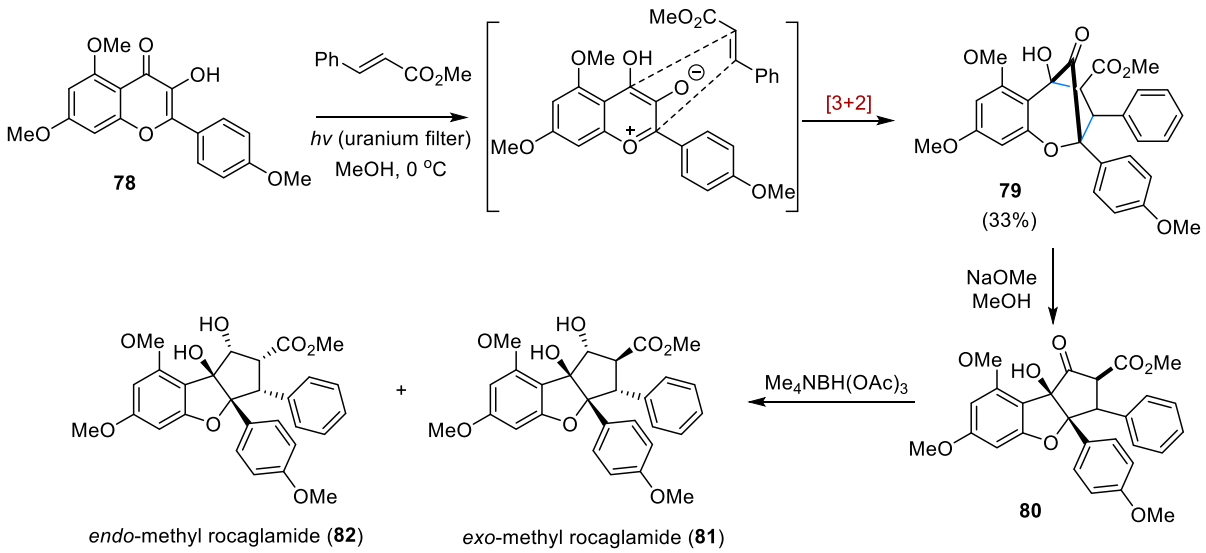

Scheme 25: Total synthesis of methyl rocaglamides by photoinduced [3+2] cycloaddition.[69]

Nicolaou and co-workers utilized a photointiated [4+2]-cycloaddition in their synthesis of the natural product (-)-Hamigeran A (**Scheme 26**).[70] In their synthetic pathway, initially, the enantioenriched alcohol **83** was transformed in to ester intermediate **84**, to enable an intramolecular photoenolisation to the *o*-quinodimethane followed by Diels-Alder-cyclisation to tricycle scaffold **85**.

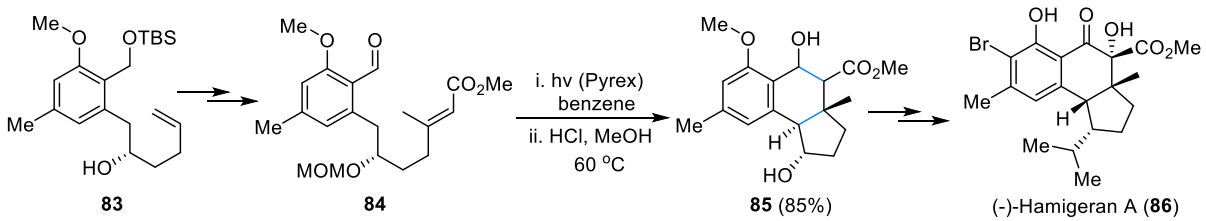

Scheme 26: [4+2] photocycloaddition as a key step in the total synthesis of (-)-Hamigeran A (**86**).[70]

A total synthesis of the naturally occurring anti-cancer agent Taxol reported by Sieburth *et. al* by employed a [4+4]-photocycloaddition as a key step (**Scheme 27**).[71] Hence, (bis)2-pyridone **87** was transformed into cyclooctadiene **88** as single isomer, in a single step. Subsequent transformations eventually led to Taxol (**89**) as a final product.

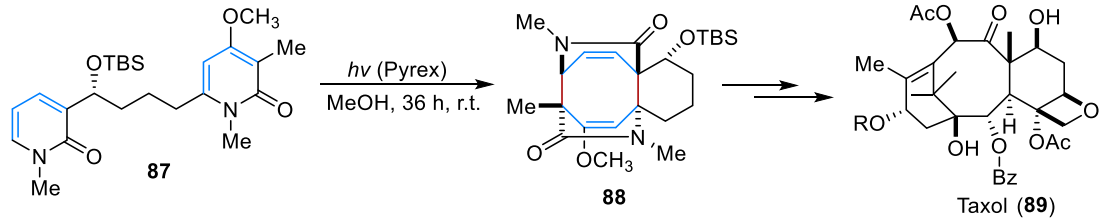

Scheme 27: Total synthesis of Taxol by [4+4] photocycloaddition approach.[71]

Feldman and co-workers reported a highly efficient approach for the synthesis of the sesquiterpene (±)-dactylol (**93**) (**Scheme 28**).[72] Their method involved an initial intramolecular [6+2]-photocycloaddition of tropone **90** to afford the cyclooctadiene **91**. The resulting cycloadduct **91** was then transformed to into final targeted molecule (**93**).

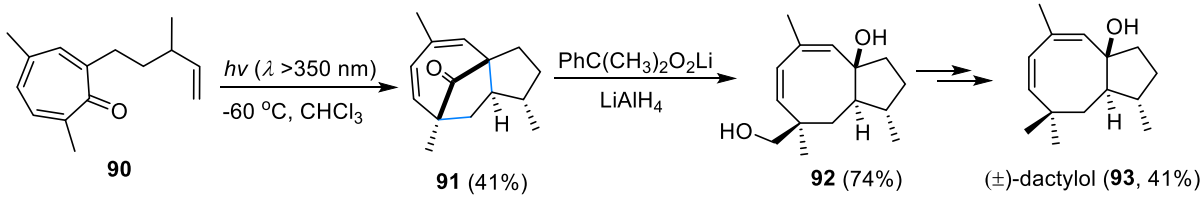

Scheme 28: Intramolecular [6+2] photocycloaddition in the total synthesis of (±)-dactylol.[72]

1.2.1 [2+2]-photocycloaddition reactions

Among the various photocycloadditions, [2+2]-photocycloaddition reactions played a significant role in the synthesis of natural products. Moreover [2+2]-photocycloaddition demonstrated as a one of the simple and straightforward approach for the synthesise of complex multi-substituted cyclobutanes.[67,68]

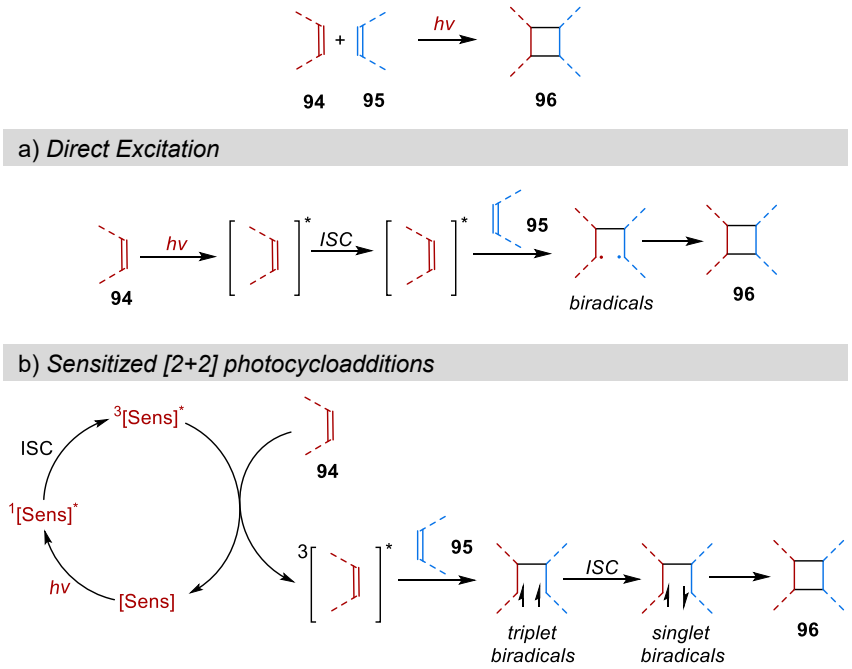

Scheme 29: General scheme of [2+2] photocycloaddition under a) direct excitation or b) triplet sensitization.[73,67]

Corey and co-workers demonstrated the utilization of the [2+2]-photocycloaddition in the synthesis of the natural products (±)-caryophyllene (**101**) and (±)-isocaryophyllene (**Scheme 30**).[74] An intramolecular [2+2]-photocycloaddition reaction between 2-cyclohexenone (**97**) and isobutylene (**98**) led to the formation of cyclobutane **99**. From there, further steps including ring annulation C-C bond fragmentation at the ring fusion eventually led to the formation of caryophyllene (**101**) as a final product.

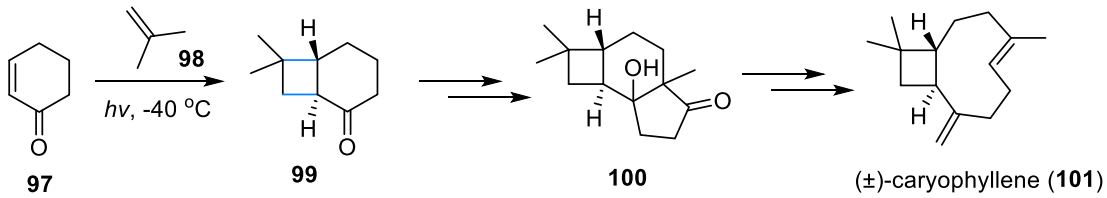

Scheme 30: Synthesis of caryophyllene (**101**) by using [2+2] photocycloaddition.[74]

The total synthesis of the tricyclic sesquiterpene isocomene (**105**) using intramolecular [2+2]-photocycloaddition was reported by Pirrung (**Scheme 31**).[75] Dienone **102** underwent [2+2]-addition to generate cyclobutane **103**. Subsequently, isocomene was obtained in a good yield from Intermediate **103** after a Witting reaction followed acid-catalysed rearrangement.

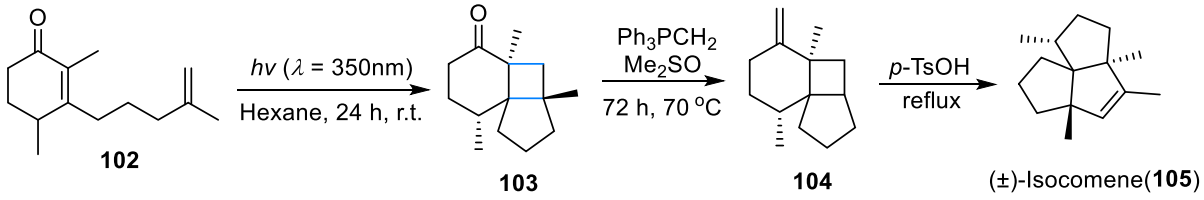

Scheme 31: Intramolecular [2+2] photocycloaddition in the total synthesis of (±)-isocomene (**105**).[75]

While the first historic examples of [2+2]-photocycloadditions were induced using direct excitation by UV light, sensitization of these reactions with aryl and alkyl ketones under long-wave irradiation has been utilized for many decades since.[65,76,77] During the last decades, visible light-absorbing triplet sensitizers have been introduced and shown be highly effective promoters, even for asymmetric [2+2]-additions.[62,67,68] In 1961, Schenck *et al.* reported a photosensitised intermolecular [2+2] cycloaddition by employing benzophenone as a photosensitizer under UV light excitation (**Scheme 32**).[76] A reaction between 2,3-dimethylmaleic anhydride **106** and furan (**107**) led to cyclobutane adduct **108** in a moderate yield.

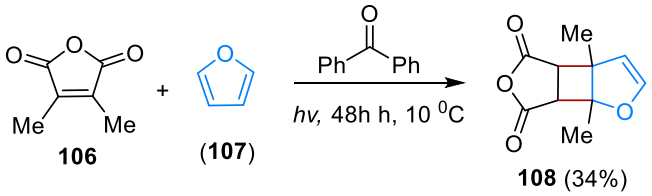

Scheme 32: Photosensitised [2+2]-cycloaddition by Schenck *et al*.[76]

Corey and co-workers reported an example of a selective triplet-sensitized [2+2] photocycloaddition of 2-allyl-1,3-butadiene **109** as a key step in the total synthesis of the natural product bergamotene (**111**), using benzophenone as photosensitizer (**Scheme 33**).[77]

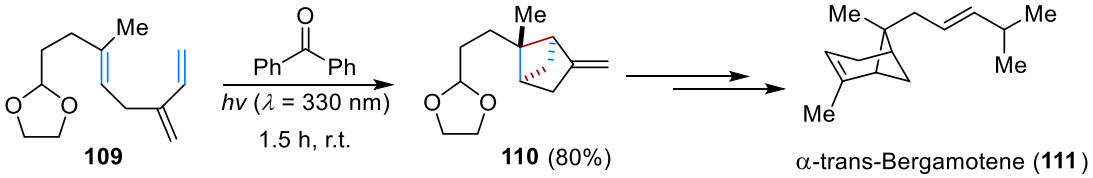

Scheme 33: Triplet-sensitised [2+2]-cycloaddition in the synthesis of α-*trans*-Bergamotene (**111**). [77]

A highly enantioselective triplet-sensitized intramolecular [2+2] photocycloaddition using a chiral thioxanthone **115** as photosensitizer was developed by the Bach group (**Scheme 34**).[78] In their method, quinolone **112** underwent the [2+2]-addition to deliver two regioisomeric cycloadducts **113** and **114** with high enantioselectivity.

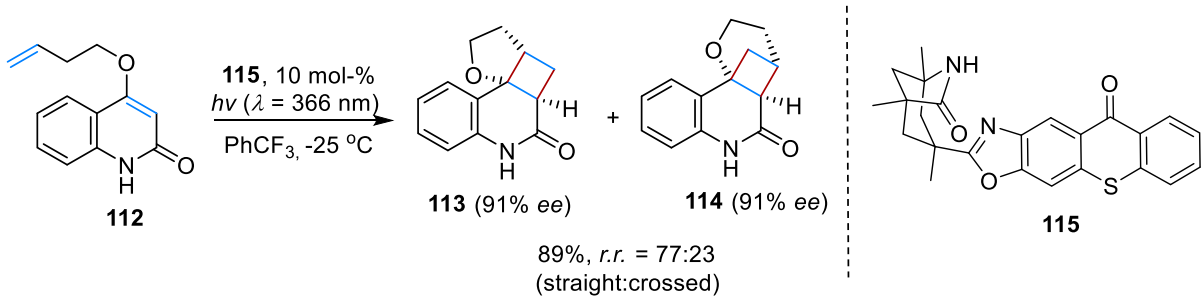

Scheme 34: Enantioselective triplet-sensitised intramolecular [2+2]-cycloaddition by Bach *et al*.[78]

Lu and Yoon reported an intramolecular [2+2]-photocycloaddition reaction of styrenes through an EnT pathway using an iridium-based complex, $[Ir(dF(CF_3)ppy)_2(dtbbpy)]PF_6$ as a sensitizer to access cyclobutane adducts **117** (**Scheme 35**).[79] This method was further utilized in the total synthesis of (±)-cannabiorcicyclolic acid (**122**).

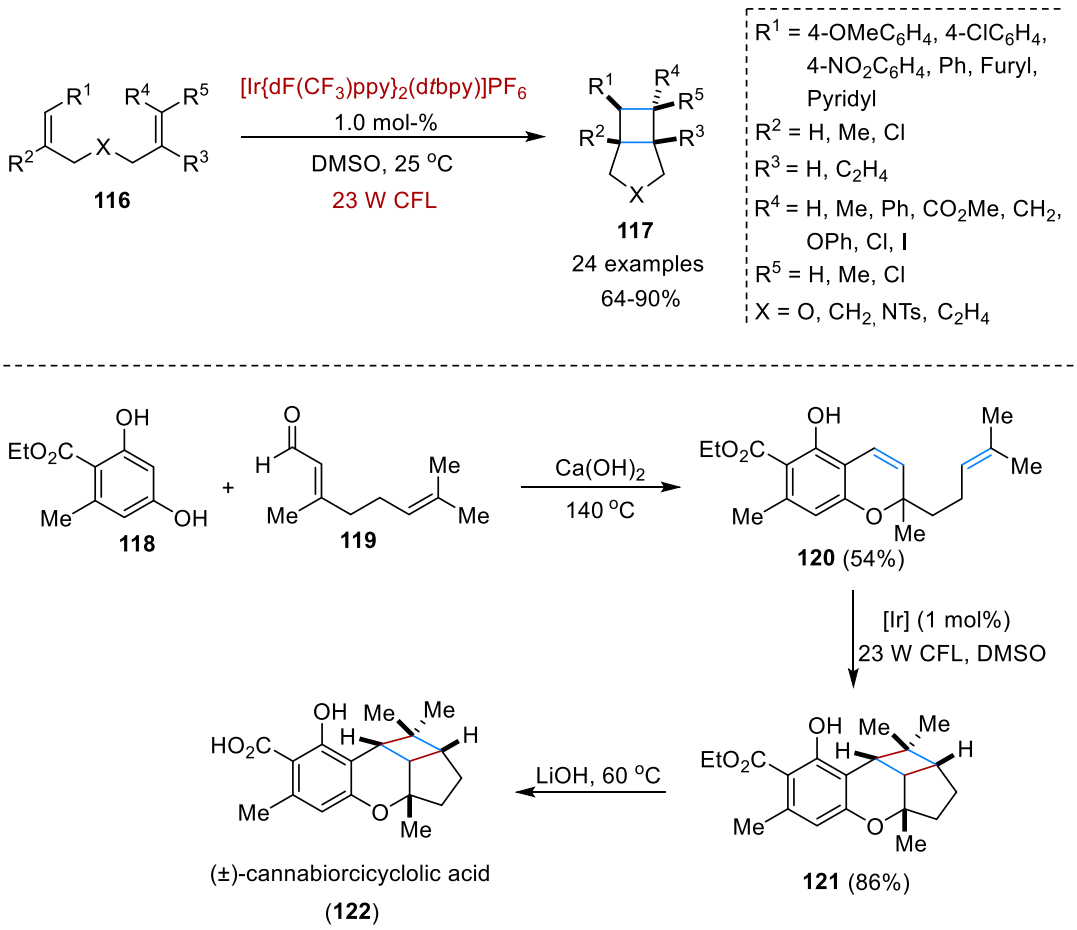

Scheme 35: Visible light-mediated [2+2]-cycloaddition of styrenes and its utility in total synthesis of (±)-cannabiorcicyclolic acid (**122**).[79]

Recently, the Kwon group demonstrated a visible light-mediated triplet sensitized intramolecular [2+2] photocycloaddition of dienones **123** using a polypyridyliridium(III) complex as a sensitizer to afford bridged benzobicycloheptanones **124** with excellent regioselectivity (**Scheme 36**).[80] Moreover this novel approach showed its superiority over previously reported methods for the synthesis of benzobicyclo[3.1.1]heptanones, which can be further transformed into B-norbenzomorphan analogues.

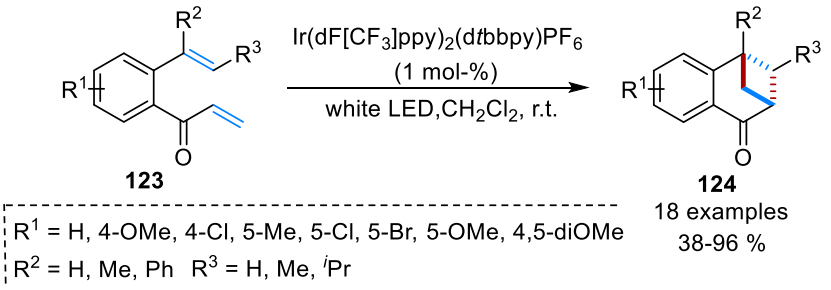

Scheme 36: Triplet-sensitized intramolecular [2+2] photocycloaddition.[80]

An example of enantioselective intermolecular [2+2] photocycloaddition of quinolones under visible light-irradiation using a chiral thioxanthone catalyst **115** was reported by Bach and co-workers (**Scheme 37**).[81] Upon irradiation, the sensitized reaction between 2(*1H*)-quinolones **125** and different electron-deficient olefins **126** delivered the corresponding cyclobutane adducts **127** with high regio- and diastereoselectivity. Moreover the respective cycloadducts were obtained in high enantiomeric excess (up to 95% *ee*) as a result of efficient energy transfer facilitated by hydrogen bonding between the chiral photosensitizer and substrate.

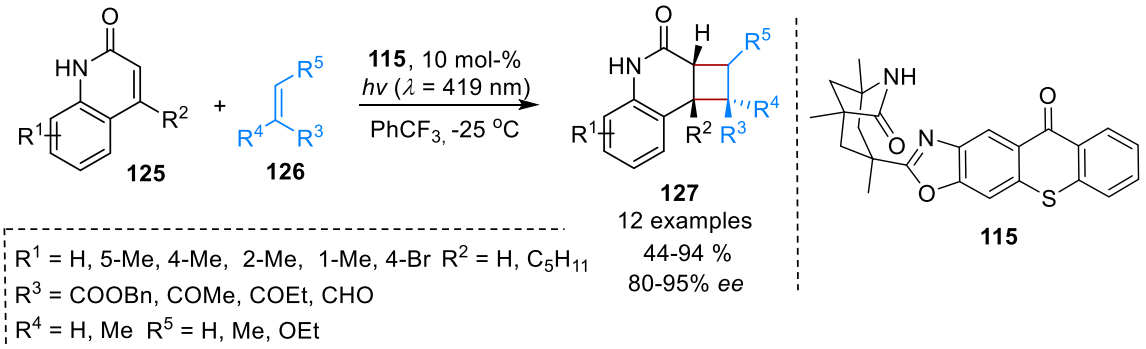

Scheme 37: Enantioselective intermolecular [2+2] photocycloaddition of quinolones by Bach *et al.*[81]

1.2.2 The Paternò-Büchi reaction

The [2+2]-photocycloaddition between a carbonyl compound and an alkene is commonly referred to as the Paternò-Büchi reaction (**Scheme 38**).[82] Several elegant synthetic applications of the Paternò-Büchi reaction in the synthesis of natural products have also been reported.[83] Generally, the Paternò-Büchi reaction involves an initial excitation of the carbonyl compound **128** through direct excitation or triplet sensitization. Subsequently, the singlet or triplet excited carbonyl moiety cyclizes with an alkene **129** to form an oxetane **131**. Even though *n,π**-absorption of the carbonyl moiety initially leads to the singlet state, the majority of the reactions occur via the triplet state of the carbonyl group, which is accessed by *intersystem crossing* (ISC) and which is particularly efficient with aromatic aldehydes and ketones. On the other hand, if an alkene has a lower triplet energy than the carbonyl compound, the reaction may proceed via the *π,π** triplet state of the alkene rather than the excited state of the carbonyl compound.[82]

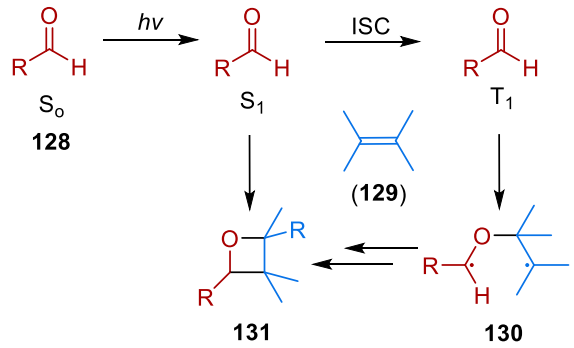

Scheme 38: Schematic representation of the Paternò-Büchi reaction between an aldehyde **128** and 2,3-dimethylbut-2-ene (**129**).[82]

Photochemical oxetane synthesis can be combined with several subsequent transformations of the oxetane products such as ring-opening reactions. The Schreiber group reported a total synthesis of the natural product (±)-Asteltoxin (**138**) starting form 3,4-dimethylfuran (**132**) using the Paternò-Büchi reaction and consecutive ring-opening as a key transformations. (**Scheme 39**).[84]

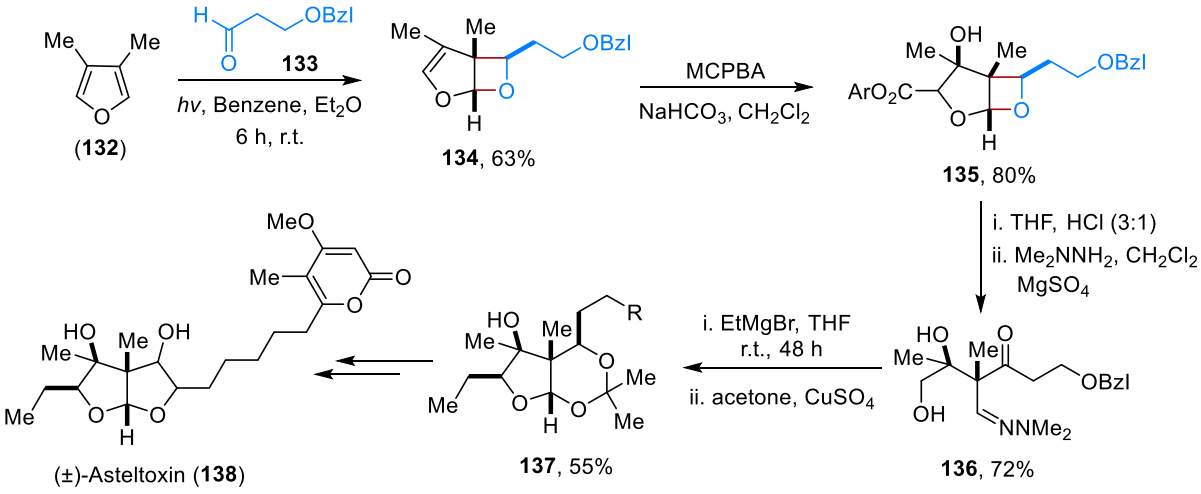

Scheme 39: Synthesis of (±)-Asteltoxin (**138**) using Paternò-Büchi reaction by Schreiber *et al*.[84]

In another example, Bach and co-workers demonstrated the synthetic significance of the Paternò-Büchi reaction and subsequent ring-opening of an oxetane in the synthesis of enantiomerically pure (+)-preussin (**142**) (**Scheme 40**).[85] A photochemical reaction of dihydropyrrole **139** with benzaldehyde afforded 3-aminoxetane derivate **140** with a good yield and further, it was transformed into (+)-preussin (**142**) by hydrogenolytic ring-opening and *N*-deprotection.

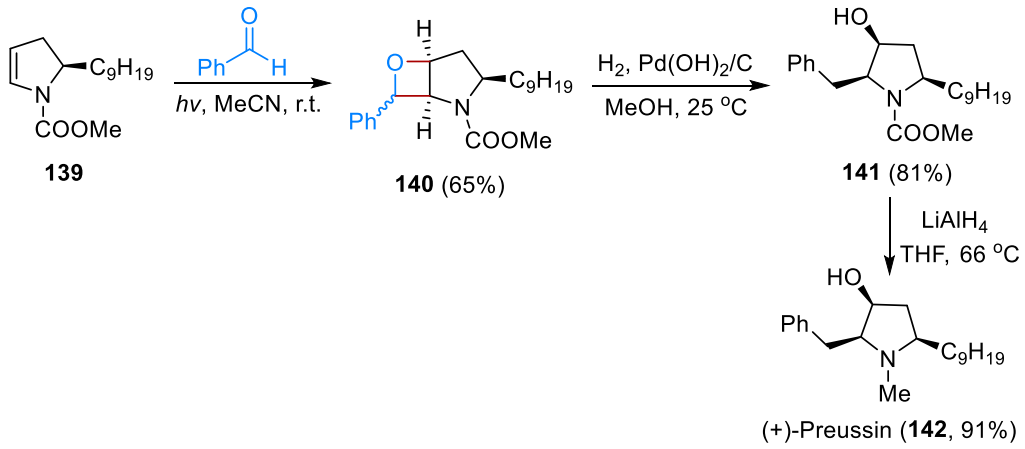

Scheme 40: Paternò-Büchi reaction for the synthesis of (+)-Preussin (**142**).[85]

With the use of the Paternò-Büchi reaction as a key step, Just *et al.* reported a short and efficient synthesis of naturally occurring HIV nucleoside oxetanocin (**146**) via the bicyclic oxetane **145** as key intermediate (**Scheme 41**).[86]

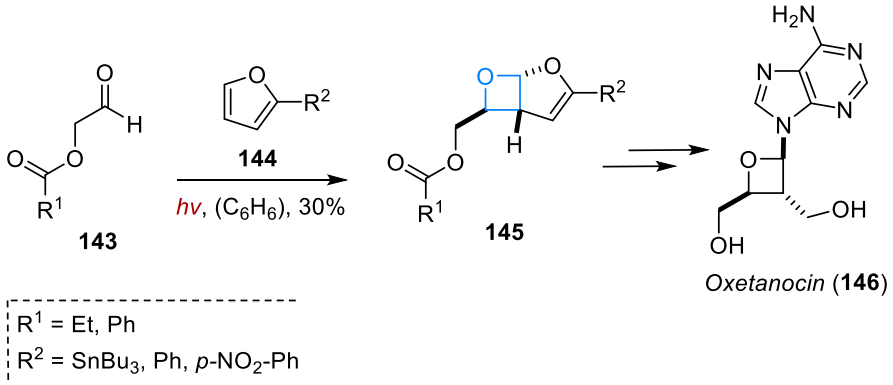

Scheme 41: Paternò-Büchi reaction for the synthesis of oxetanocin intermediate **145** by Just *et al*.[86]

Recent advances in visible light-enabled Paternò-Büchi reactions have led to the synthesis of new and structurally complex oxetanes.[87-90] Schindler and co-workers reported a highly efficient visible light-mediated triplet sensitized Paternò-Büchi reaction using an Iridium(III)-based photosensitizer (**Scheme 42**).[88] In contrast to the traditional Paternò-Büchi reaction, where a carbonyl substrates excited to its triplet state via UV irradiation, this approach relies on the triplet energy transfer from photosensitizer to carbonyl substrates to deliver the oxetanes. By employing aryl glyoxylates **147** in combination with various alkenes **148**, several complex oxetane scaffolds **149** could be synthesised with remarkable efficiency, achieving up to 99% yield.

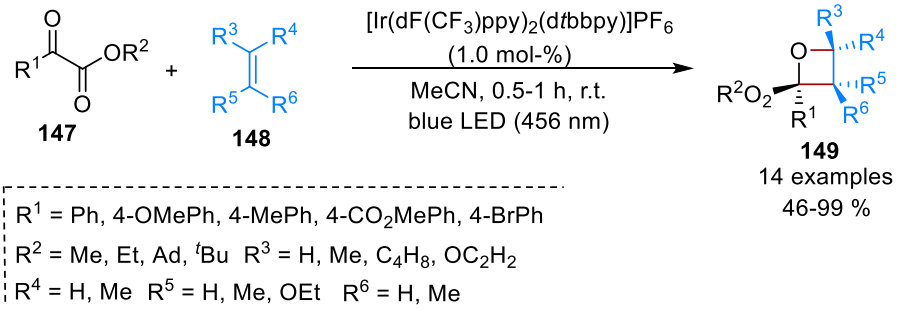

Scheme 42: Visible light energy transfer-mediated Paternò-Büchi reaction of aryl glyoxylates with alkenes [88]

In 2020, the Yoon group also reported an efficient sensitized Paternò-Büchi reaction employing an Iridium (III) sensitizer under visible light-irradiation (**Scheme 43**).[90] In their method, triplet-excited benzoylformate esters **150** undergo the Paternò-Büchi cycloaddition with alkenes **151** to afford functionalized oxetanes **152**.

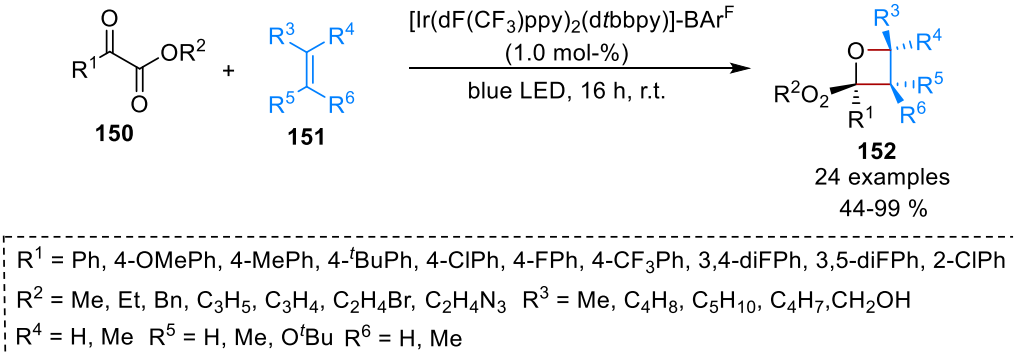

Scheme 43: Visible light-mediated intermolecular Paternò-Büchi reaction of benzoylformate esters [90]

1.2.3 The Aza-Paternò-Büchi reaction

Analogous to the Paternò-Büchi reaction, the Aza Paternò-Büchi reaction emerged as a direct and efficient strategy to access four-membered nitrogen-containing azetidines **155** via a photochemical reaction between an imine **153** and an alkene **154** (**Scheme 44**).[91] The Aza Paternò-Büchi reaction thus complements traditional methods for the synthesis of azetidines which involve a nucleophilic substitution reaction using nitrogen as a nucleophile[92], ring opening of strained azabicyclobutenes[92,93] or reduction of β-lactams.[92] Moreover, the aforementioned conventional approaches for the synthesis of azetidines require multi-step sequences along with pre-functionalised starting materials. Similar to oxetanes, azetidines

also exist in numerous natural products (*e.g.* **157**)[94] and pharmaceuticals (*e.g.* **156**)[95] (**Scheme 45a**).

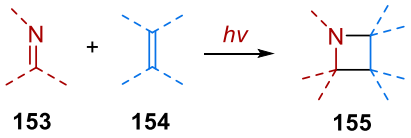

Scheme 44: Schematic representation of Aza Paternò-Büchi reaction.

In 1968, Tsuge and co-workers were the first to report the Aza Paternò-Büchi reaction between 1,3,4-oxadiazole **159** and indene (**158**) to access azetidine **160** under ultraviolet light irradiation (**Scheme 45b**).[96] Subsequently, several research groups demonstrated to access a variety of azetidine derivatives with different new reagent system under UV-light excitation, and the majority of these reactions reported were intermolecular [2+2]-photocycloadditions between imine and alkene.[91,97-100]

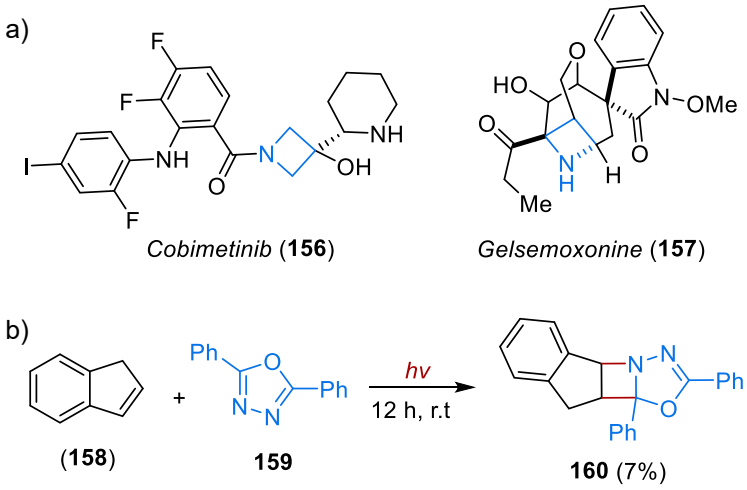

Scheme 45: a) Azetidine containing natural product and pharmaceutical[94,95] b) First example of Aza Paternò-Büchi reaction between Indene (**158**) and 1,3,4-oxadiazole **159** for the synthesis of azetidine **160**.[96]

Utilizing the advancements in photocatalysis, Schindler and co-workers reported a visible light-mediated intramolecular Aza Paternò-Büchi reaction between readily available imine- and alkene-containing precursors for the synthesis of highly functionalized azetidines (**Scheme 46**).[99] With simple and mild reaction conditions using an iridium(III)-based photosensitizer, several azetidines derivatives **162** could be synthesised from alkene and oxime moiety **161** with a yield up to 99%. Moreover, in contrast to energy transfer from excited photosensitizer to imine, this reaction proceeds via triplet energy transfer from excited photosensitizer to alkene.

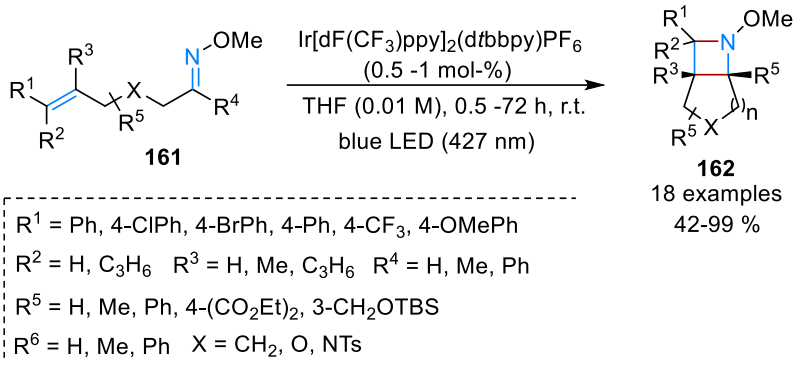

Scheme 46: Visible light-mediated intramolecular Aza Paternò-Büchi reaction by Schindler *et al.*[99]

In 2020, the same group developed an example of triplet sensitized intermolecular Aza Paternò-Büchi reaction again using an iridium (III) photosensitizer under visible light irradiation (**Scheme 47**).[98]. Here, the reaction of 2-isoxazoline-3-carboxylates **163** proceeds via triplet energy transfer from the excited photosensitizer to the oxime substrate followed by [2+2] cycloaddition to yield functionalized azetidines **165**.

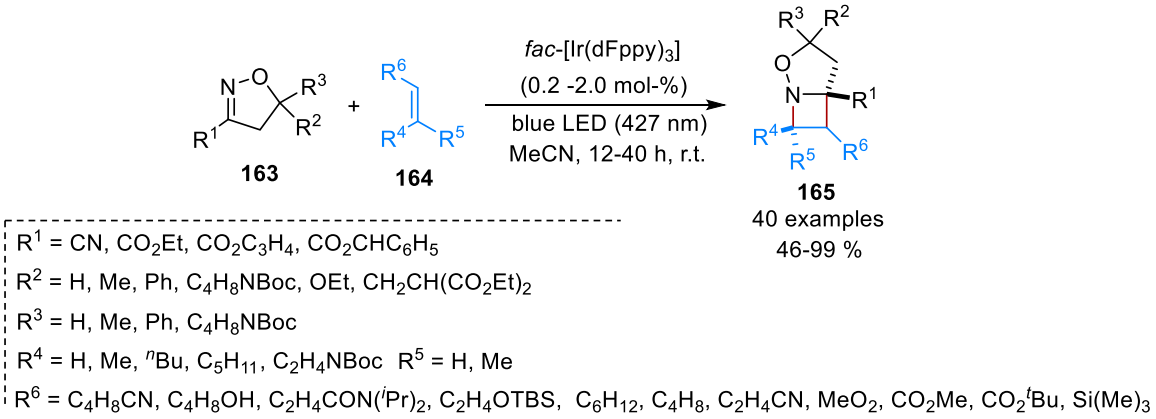

Scheme 47: Intermolecular Aza Paternò-Büchi reaction by Schindler *et al.*[98]

Bach and co-workers reported an enantioselective synthesis of azacyclobutane derivatives by visible light-mediated sensitized Aza Paternò-Büchi reactions (**Scheme 48**).[101] The [2+2]-cycloaddition reaction between 3-substituted quinoxalinones **166** and different substituted styrenes **167** was accomplished through the use of a chiral thioxanthone photosensitizer **115**, to afford the corresponding azetidines **168** with excellent enantioselectivity. The two-point hydrogen bonding interaction between the sensitizer and the substrate favours the formation of a 1:1 complex. Enhanced hydrogen bonding between catalyst and substrate was achieved by performing the reactions at lower temperature (−25°C or −35°C).

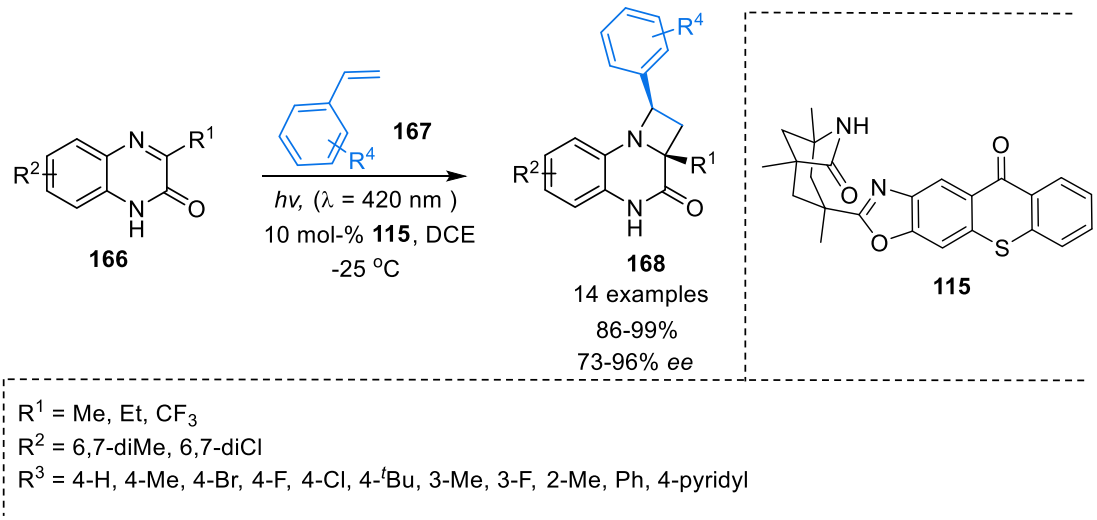

Scheme 48: Enantioselective Aza Paternò-Büchi reaction of quinoxaline-2-(1*H*)-ones.[101]

1.2.4 Dehydrogenative cycloaddition reactions

Over the past few years, dehydrogenative cycloaddition reactions of saturated compounds have emerged as potentially more step economic alternative to the conventional cycloadditions between unsaturated reactants. These reactions proceed via *in-situ* dehydrogenation of the saturated precursors followed by cycloaddition (**Scheme 49**). In this context, dehydrogenative Povarov [4+2]-cycloadditions have been extensively studied and carried out by employing metals catalysts such as Cu(I)- and Cu(II)- salts or Fe(II), Au(I), and Au(II) complexes along with stoichiometric amounts of oxidising agents such as DDQ, organic peroxides or dioxygen.[102-107]

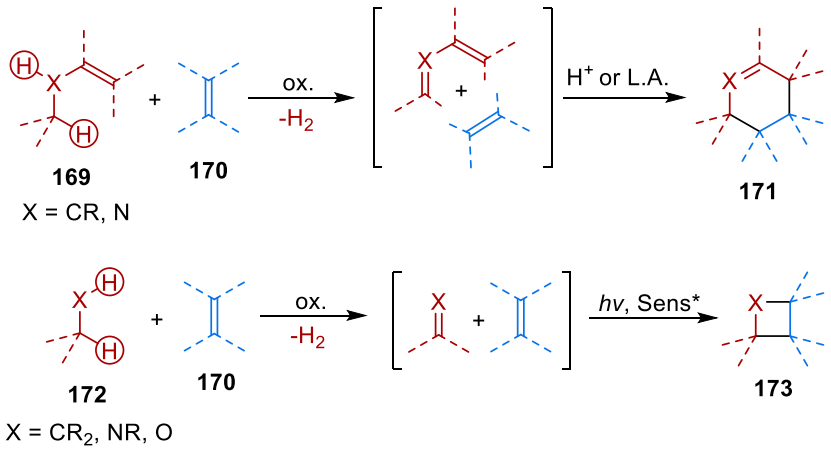

Scheme 49: Concept of dehydrogenative [4+2]-and [2+2]-cycloadditions.

Macheño and Richeter were the first to report a thermal one-pot oxidative Povarov/aromatization tandem reaction of substituted glycine derivatives **174** with electron-rich alkenes **175** (**Scheme 50**).[106] Using iron(III) chloride as a catalyst in combination with mild, nontoxic TEMPO oxoammonium salt as formal hydrogen acceptor, substituted quinolones **176** were synthesised with high yields.

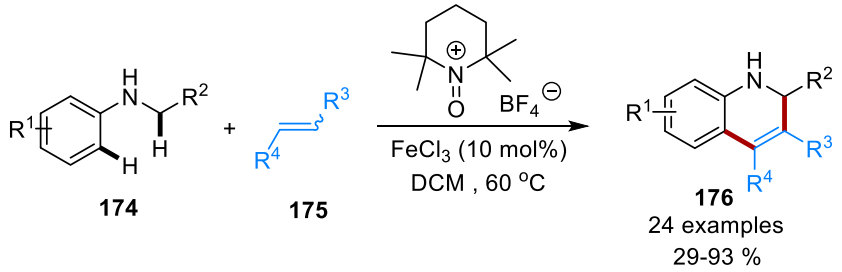

R^1 = 4-MePh, 2-MePh, 3-MePh, 3,5-diMePh, 4-MeOPh, 4-ClPh, 4-Br, 4-COMePh,
R^2 = Ph, Me, COOEt, COPh, $PO(OEt)_2$
R^3 = Ph, OMePh, 4-^{t}BuPh, *n*-hex, $PhCHCH_2$, OBu, OEt, 4-ClPh, 2-ClPh
R^4 = H, Et, Ph

Scheme 50: $FeCl_3$ and TEMPO oxoammonium salt-mediated dehydrogenative Povarov reactions.[106]

In 2021, Zeng *et al*. reported an example of a dual-catalysed dehydrogenative Aza [4+2]-cycloaddition of amines with 1,3-dienes (**Scheme 51**).[107] Utilizing copper(I) bromide as a catalyst along with N-methylmorpholine (NMM) as a co-catalyst, an oxidative dehydrogenation and consecutive Aza [4+2]-cycloaddition between *N*-aryl glycine esters **177** and 2,3-dimethyl-1,3-butadiene **178** was carried out at 80 °C and 1 atm of air for the synthesis of 1,2,3,6-tetrahydropyridines **179**.

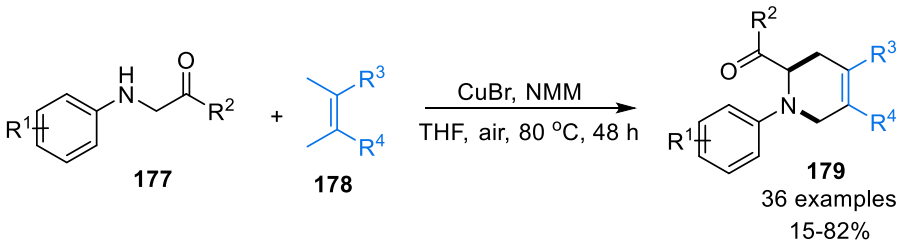

R^1 = 4-Br, 4-F, 4-Cl, 4-CF_3, 4-OMe, 5-Br, 3,5-diMe, 2-I-4-Br, OCH_2O, Naphtyl
R^2 = OMe, OEt, ^{i}Pr, ^{t}Bu, CH_2CF_3, N-$[(CH_2)_4]_2$, N-$(Et)_2$, N-$[(CH_2)_2O(CH_2)_2]_2$, Peptide
R^3 = Me, OMe, $CH_2CO_2C_2H_5$, Ph, 4-MePh, 4-FPh, 4-ClPh, 4-BrPh, biPh, 3-MePh, 5-OMenaph
R^4 = H, Me, OMe, $CH_2CO_2C_2H_5$

Scheme 51: Dual catalysed dehydrogenative [4+2]-cycloaddition of *N*-aryl glycine esters.[107]

In addition to the single dehydrogenative reaction, a thermal double dehydrogenative Povarov cycloaddition reaction was also developed. In 2016, Huo *et al.,* reported a metal-free carbon

tetrabromide-mediated dual-oxidative dehydrogenative (DOD) cycloaddition between *N*-arylglycine esters **180** and 1,4-dioxane (**181**) to access complex quinolone scaffolds **182** (**Scheme 52**).[108]

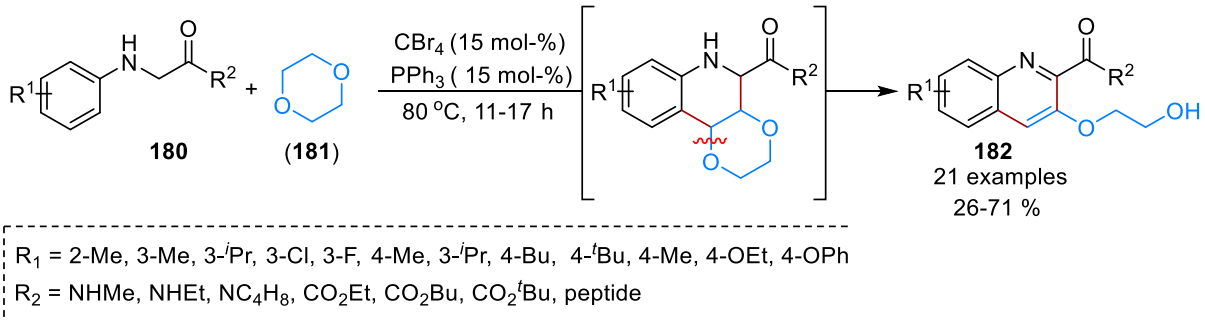

Scheme 52: Metal-free double oxidative dehydrogenative Povarov reaction.[108]

Our group has recently developed an iodine and visible light-mediated dehydrogenative Povarov [4+2]-cycloaddition of glycine esters with indoles and 1,1-disubstituted alkenes under aerobic conditions. As shown in **Scheme 53 (left)**, an initial dehydrogenation of *N*-aryl glycine esters **183** followed by cycloaddition with indoles **184** and aromatization led to the synthesis of tetracyclic indolo[3,2-*c*]quinoline products **185**.[109] On the other hand, **Scheme 53, (right)** shows the dehydrogenative Povarov cycloaddition and C_{sp3}-H oxygenation reaction between *N*-aryl glycines **183** and 1,1-disubstituted alkenes **186** to afford the cycloadducts **187**.[110]

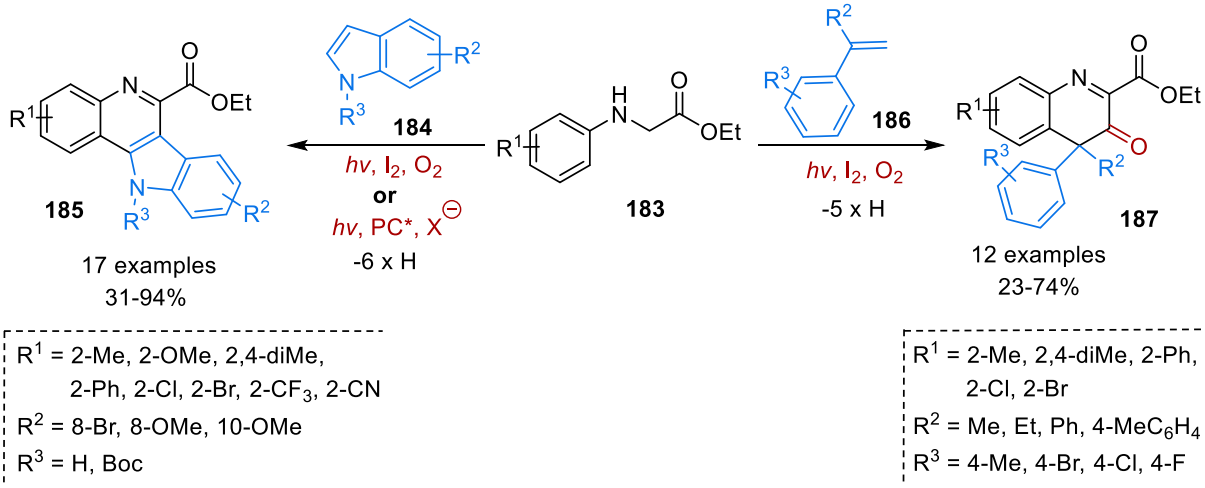

Scheme 53: Dehydrogenative Povarov reactions of *N*-aryl glycine esters.[109,110]

In addition to dehydrogenative [4+2]-cycloadditions, Wu and co-workers developed a Pd/C-catalysed dehydrogenative [3+2]-cycloaddition, which includes a thermal metal-catalysed dehydrogenation of phenylalanine derivatives **188** for the generation of azomethine ylides and

subsequent [3+2]-cycloaddition with *trans*-β-nitrostyrenes **189**, to access structurally complex benzo-fused tropane scaffolds **190** with high diastereoselectivity (**Scheme 54**).[111]

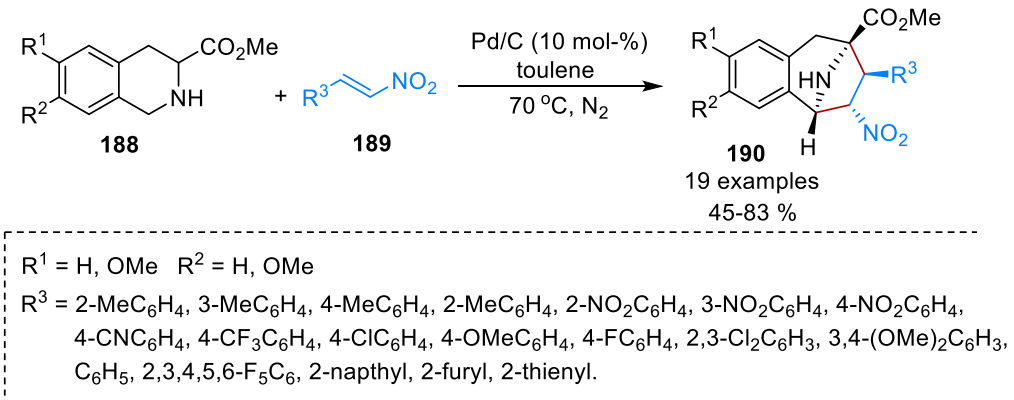

Scheme 54: Dehydrogenative [3+2] cycloaddition for the synthesis of functionalised tropanes.[111]

Furthermore, Singh *et al*. reported a highly selective Pd-catalysed dehydrogenative [2+2+2]-cycloaddition of quinones **191** with fulvenes **192**, enabling efficient synthesis of polyarylquinones **193** (**Scheme 55**).[112] By employing this novel ligand-assisted, $Pd(OAc)_2$-catalyzed approach, a number of fulvene and quinone fused polyarylquinones **193** could be readily synthesized. More importantly the obtained polyarylquinone derivatives exhibited a high cytotoxic activity against human osteosarcoma cells (MG-63) due to their excellent redox properties.

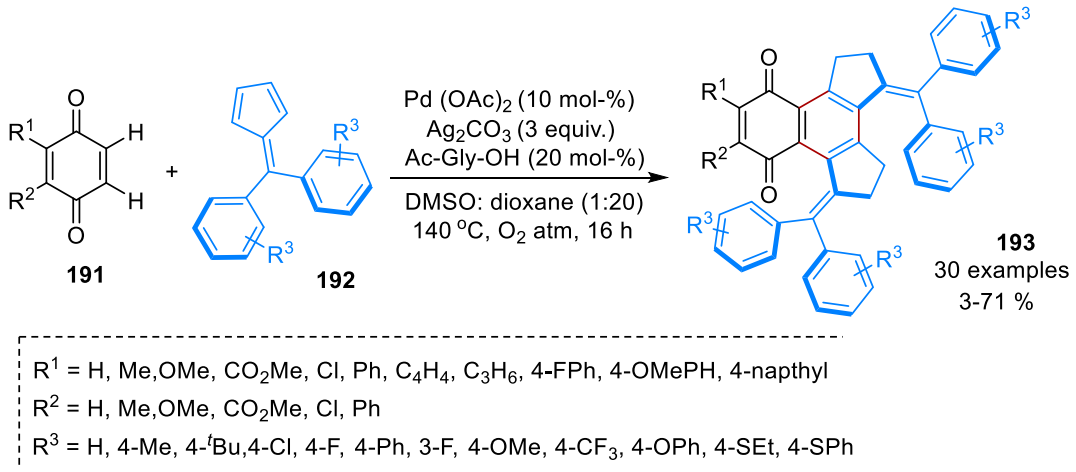

Scheme 55: Dehydrogenative [2+2+2] cycloaddition for the synthesis of polyarylquinones **193**.[112]

2. Objective of this work

The development of simple and environmentally benign methodologies for the construction of carbon-carbon or carbon-heteroatom bonds is a primary interest in organic synthesis. In this regard, we aimed to develop efficient thermal and photoinduced catalytic processes for the formation of C-C or C-X bonds through the generation of carbon-centered radicals and their subsequent addition reactions to alkenes and sensitized cycloadditions.

Our initial focus was the radical functionalization of biomass-derived 5-chloromethylfurfural (CMF) by way of its utilization in radical addition and ATRA-type reactions to access value-added products from this furanic platform chemical.

Secondly, we focused on developing visible light-induced sensitized photocycloaddition reactions of 2-cyanochrome with alkenes for the synthesis of the respective cycloadducts as an alternative method for the direct UV-induced cycloadditions of 2-cyanochrome.

In a third project, we attempted to develop an *in situ*-dehydrogenative aza [2+2] cycloaddition reaction of dihydroquinoxaline-2-(1*H*)-ones with alkenes for the straightforward access to polyfunctional azetidine derivatives directly from reduced and readily accessible heterocyclic precursors.

3. Summary of Published Results

3.1 Value-added chemicals from biomass-derived furans: radical functionalisation of 5-chloromethylfurfural (CMF) by metal-free ATRA reactions

For more than two centuries, fossil fuels have been the foremost and pivotal source of chemicals, fuels, and energy for mankind. In light of the eventual depletion of fossil fuels and the increasing negative environmental impact of their use, the utilization of biomass as a promising substitute has been investigated for some time. Biomass is considered as the most attractive alternative feedstock due to its widespread availability as a carbon source apart from oil and coal and it comprises several molecular components like carbohydrates, lignin, lipids, proteins, fatty acids and others. The valorisation of renewable resources, especially biomass to produce value-added chemicals in a more efficient, economical and sustainable manner continues to be an important goal of chemical research.[113-118] 5-Hydroxymethylfurfural (**HMF, 194**) is a dehydration product of biomass-derived carbohydrates and exhibits significant potential for the production of high-value renewable chemicals, polymers and biofuels. [119]

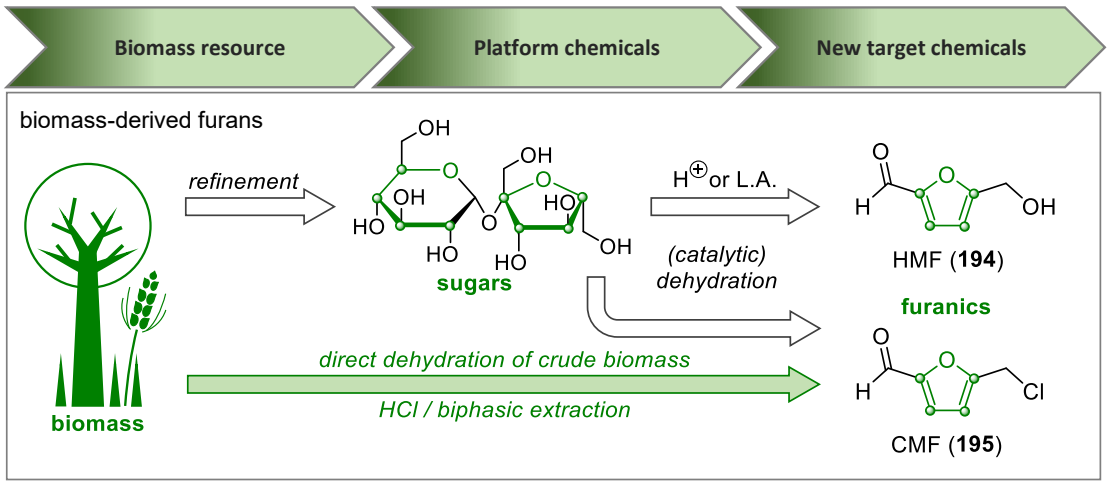

Scheme 56: Conversion of biomass in to furans HMF (**194**) and CMF (**195**).

HMF can be easily obtained from hexoses such as sucrose, glucose or fructose by thermal, Lewis- or Brønsted acid-mediated dehydration. The efficient conversion of raw biomass into HMF still remains a challenge as HMF undergoes an acid catalysed decomposition to humine and polyfuranic resin. The chlorinated compound, 5-chloromethylfurfural (**CMF, 195**), a considerably more lipophilic analogue of HMF, can be obtained in high yield directly from crude biomass.[120] In 2008, Mascal and Nikitin reported an efficient way for the direct synthesis of CMF form biomass by using aqueous hydrochloric acid treatment in combination with biphasic extraction techniques and isolated yields are greater than 71%.[121] Subsequently, Brasholz *et al.* established a highly efficient biphasic continuous flow method for the synthesis of CMF and

other furanic derivatives from D-fructose and sucrose on a gram-scale.[122] Under optimised conditions, 10 g of D-fructose can be readily converted into almost 6.5 g of CMF in only 20 min of reaction time at 100 °C using dichloromethane (DCM) as a solvent. In the same way, 10 g of sucrose can be easily converted in to 5.23 g (61%) of CMF at 130 °C. Both HMF and CMF can be transformed into important simple chemicals such as furan-2,5-dicarboxylic acid, 2,5- dimethylfuran, levulinic acid and others on a large scale. **Figure 3** represents the useful transformation of HMF and CMF into value-added products.[119,120]

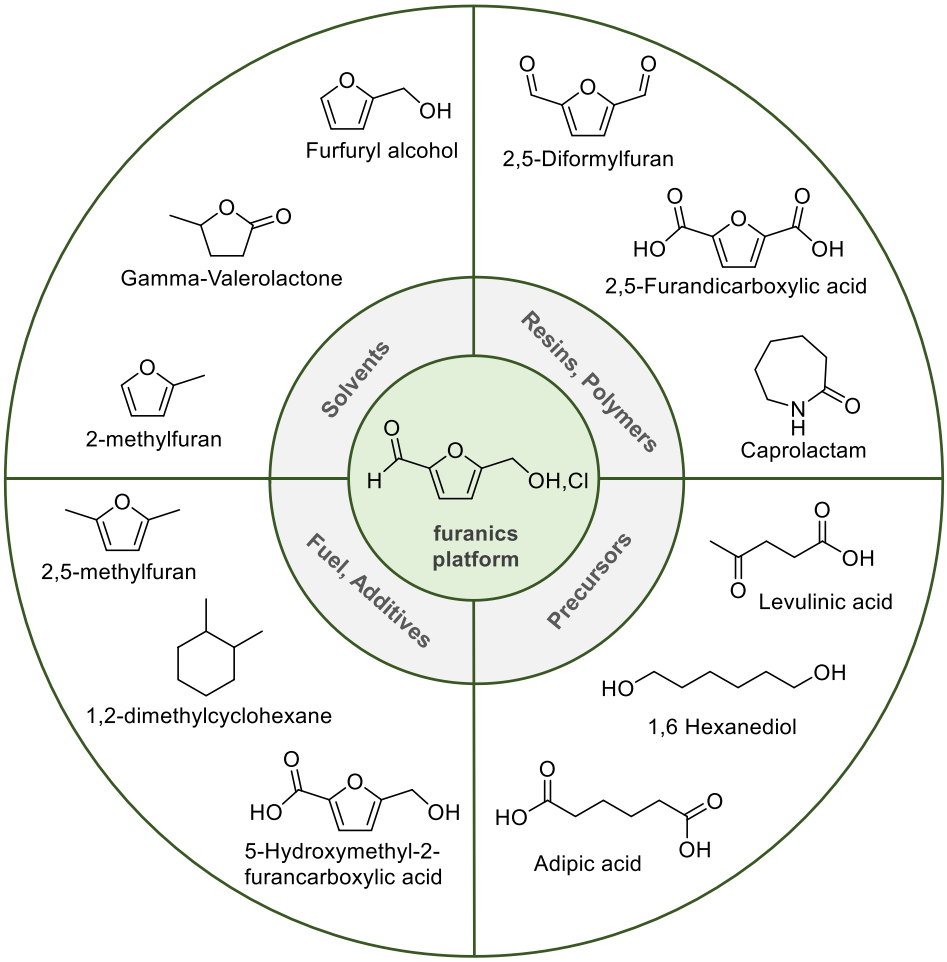

Figure 3: Value-added products derived from both HMF (**194**) and CMF (**195**).[119,120]

So far different catalytic reactions such as oxidations, hydrogenations, aminations and hydrodeoxygenations are performed to valorize HMF (**194**) and CMF (**195**) into their respective derivatives.[123] However, to the best of our knowledge, the radical functionalisation of HMF (**194**) or CMF (**195**) has not been explored so far. Therefore, we reasoned to investigate the radical functionalisation of CMF (**195**) by way of a homolytic C-Cl bond cleavage that would lead to the corresponding (2-formyl-5-furanyl)methyl radical **196** as a reactive intermediate. If the key radical **196** could be generated and reacted with alkenes, value added products like alkyl or arylmethylfurfurals could be expected (**Scheme 57**).

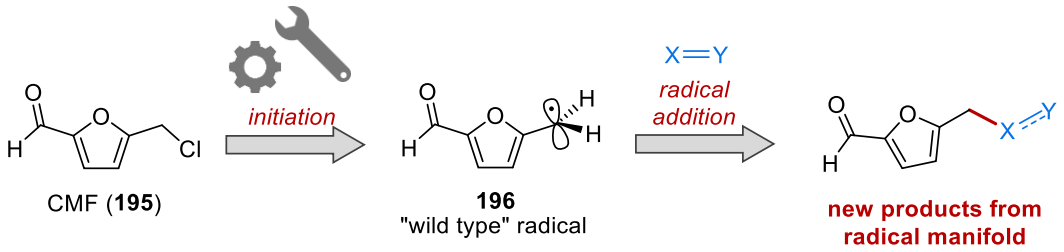

Scheme 57: The idea of radical functionalisation of CMF (**195**) and subsequent addition of (2-formyl-5-furanyl)methyl radical **196** to alkenes.

We subsequently succeeded in engaging CMF (**195**) in metal-free ATRA reactions with styrenes **197** as the alkenes that would lead to the chain-elongated products **198** through the utilization of of the metal-free Et_3B/O_2 initiator system**.** Furthermore, computational studies on the key intermediate, 2-formyl-5-furfurylradical **196** derived from CMF (**195**) were performed in cooperation with the group of Prof. Dr. Julia Rehbein at the University of Regensburg, in order to elucidate its electronic structure and radical addition behavior by using NBO[124] population analysis in combination with post-HF methods (MP2)[125] and density functional theory (DFT) calculations.

Our investigations began initially with considering a reductive photoredox-induced C-Cl bond cleavage of CMF (**195**),[126] however, these attempts failed even after extensive experimentation. As an alternative to photoredox induced C-Cl bond cleavage, we opted for the triethylborane/O_2 reagent system[15] to activate CMF (**195**). The reaction of CMF (**195**) with styrene (**197a**) and triethylborane under atmospheric air (3 X 5ml) at 60 °C resulted in the formation of secondary benzylic chloride **198a** and the dimeric product **199** in in small quantities (**Scheme 58**).

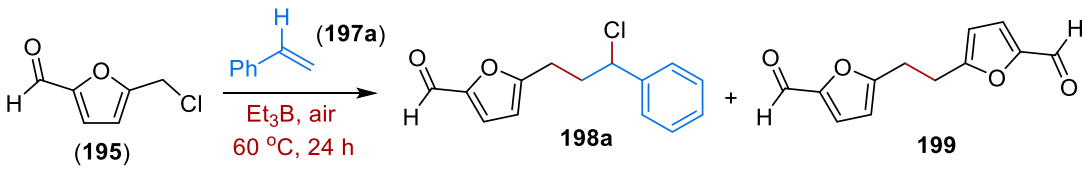

Scheme 58: Atom transfer radical addition reaction of CMF (**195**) using triethylborane/oxygen.

Subsequently, our objective was to systematically optimize the reaction conditions (**Table 1**). In the initial phase of the experiments, CMF (**195**) and styrene (**197a**) were treated with 2 equivalents of Et_3B in MeCN, under atmospheric air at a temperature of 60 °C. After 24h of reaction time, approximately 29-30% conversion of CMF (**195**) was observed with a mixture of yet uncharacterized products (entry 1). Significantly, in the presence of 1 equivalent of tetrabutyl ammonium idodie (TBAI) an 87% conversion of CMF (**195**) with 23% of ATRA

product **198a** formed and 10% of furanic dimer **199** was observed. Variation of the molar equivalents of TBAI further improved the conversion of CMF (**195**) with better yields of ATRA product **198a**. When the quantity of TBAI was reduced from 1 equivalent to 0.5 equivalents, a decrease in the conversion of CMF (**195**) and the yield of ATRA product **198a** was observed. On the other hand, 2 equivalents of TBAI showed comparably analogous results to those obtained from the use of 1 equivalent. However, when the reaction condition changed to 4 equivalents of TBAI, the yield of ATRA product **198a** was further improved from 23% to 40% and variation of the equimolar amounts of the TBAI was found to have a direct impact on the reaction outcome.

Table 1: Optimization and control experiments for ATRA reaction of CMF (**195**).

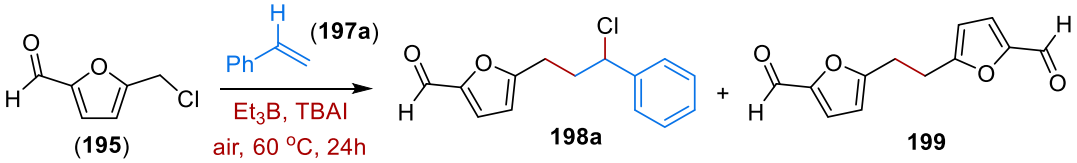

#	Et_3B	TBAI	197a (equiv.)	solvent	conv. 195 [%][a]	yield. 198a [%][a]	yield 199 [%][a]
1	2	0	15	MeCN	29	0	0
2	2	1	15	MeCN	87	23	10
3[b]	2	1	15	MeCN	0	0	0
4	2	0.5	8	MeCN	100	16	2
5	2	2	8	MeCN	100	31	3
6	2	4	8	MeCN	100	40	3
7	2	4	4	MeCN	95	30	2
8	2	4	10	MeCN	100	42	3
9	2	4	20	MeCN	100	30	2
10	0.25	4	10	MeCN	91	38	3
11	0.5	4	10	MeCN	96	74	3
12	1	4	10	MeCN	98	51	5
13	0.5	4	10	THF	74	50	2
14	0.5	4	10	DMF	63	28	2
15	**0.5**	**4**	**10**	**Acetone**	**97**	**75 (78)**[c]	**3**

Reactions were performed on a 0.3 mmol scale of (**195**) [a] Determined by ^{1}H-NMR analysis using CH_2Br_2 as the internal standard. [b] Reaction in the absence of oxygen. [c] Yield of the isolated product after chromatography.

Systematic variation of different parameters, that included the molar equivalents of Et_3B, styrene (**197a**), oxygen concentration[127] and the solvent resulted in a significant further enhancement of the yield of ATRA product **198a**. Utilization of 0.5 equivalents of Et_3B showed a better outcome in comparison to using 0.25 and 1 equivalents of Et_3B correspondingly (entries 10-12). Importantly, we did not find any differences in the conversion of CMF (**195**) and yield of ATRA product **198a** when 15 and 10 equivalents of styrene (**197a**) was used, respectively. With the aim of developing a sustainable procedure in mind, we decided to restrict the styrene (**197a**) to 10 equivalents. Piercing the reaction vial septum with a cannula throughout the reaction showed better results compared to injecting air with a syringe at an interval of three times. Moreover, variation in the reaction temperature did not show any favorable results, and the outcome of all conducted reactions indicated that a temperature of 60°C is optimal to achieve complete conversion of CMF (**195**) within 24 h of reaction time.

At the end of the optimization studies, impact of different solvents on the yield of ATRA product **198a** as well as the conversion of CMF (**195**) was evaluated (entries 13-15). No further improvement in the conversion of CMF (**195**) was observed when the reaction was conducted in DMF and THF. On the contrary, the yield of ATRA product was diminished. Employing acetone as a reaction solvent showed better conversion of CMF (**195**) with a favorable yield of ATRA product **198a**. On the other hand, when the reaction was performed only for 12h, a notable large incomplete conversion of CMF (**195**) was observed. Ultimately, the reaction was optimised with the conditions of 4 equivalents of TBAI, 0.5 equivalents of Et_3B, 10 equivalents styrene (**197a**) in acetone, under air at 60 °C for 24 h to obtain ATRA product **198a** with the excellent isolated yield of 78% after chromatography and the undesired dimer **199** being observed in only 3%. As a control experiment, no conversion of CMF (**195**) has been observed in the absence of oxygen.

We also wished to perform *in-silico* theoretical calculations to evaluate factors that potentially would influence the desired radical functionalisation of CMF (**195**). We anticipated that spin delocalisation around the molecule would render the (2-formyl-5-furanyl)methyl radical **196** only moderately nucleophilic as typical for benzylic radicals.[128] In addition, 2-furylmethyl radicals **196** are known to lead to multiple secondary fragmentation products by ring opening (**Scheme 59a**).[129] Following careful consideration of all these factors, we initiated DFT calculations with our cooperation partner Prof. Dr. Julia Rehbein and co-workers to elucidate the electronic structure of **196** and its reactivity towards alkenes.

In this study, Natural Bond Orbital [NBO, uMP2/6-311+G**][124,125] approach was used to investigate the spin density distribution, singly occupied molecular orbital (SOMO) energy ε of radical **196**, and a comparative analysis was performed with the closely related 2-furylmethyl

radical **200**, 4-formyltolyl radical **201** and tolyl radical **202**. The calculations indicated that in case of radical **196** spin density is situated primarily at the benzylic methyl carbon along with a notable presence at the C-2 position. In all other cases (**200, 201 and 202**) the highest spin density is located only at the benzylic methyl carbon (**Scheme 59b**) and it revealed radical **196** showed the lowest SOMO energy ε (-9.168 eV) whereas the highest SOMO energy ε was shown by radical **200** (-8.167 eV). The order SOMO energies ε follows as **201** < **196** – **202** < **200**. Subsequently, computed SOMO energies of radials **196, 200-202** were correlated with the highest occupied molecular orbital (HOMO) and lowest unoccupied molecular orbital (LUMO) energies of diverse alkenes to evaluate potential reaction partners. These correlations showed that, particularly, styrene derivates **197** have an energy gap of SOMO to LUMO which is considerably higher than that of SOMO to HOMO. Therefore, the interaction between the SOMO of radical **196** and the HOMO of styrene derivates **197** is much more favorable.

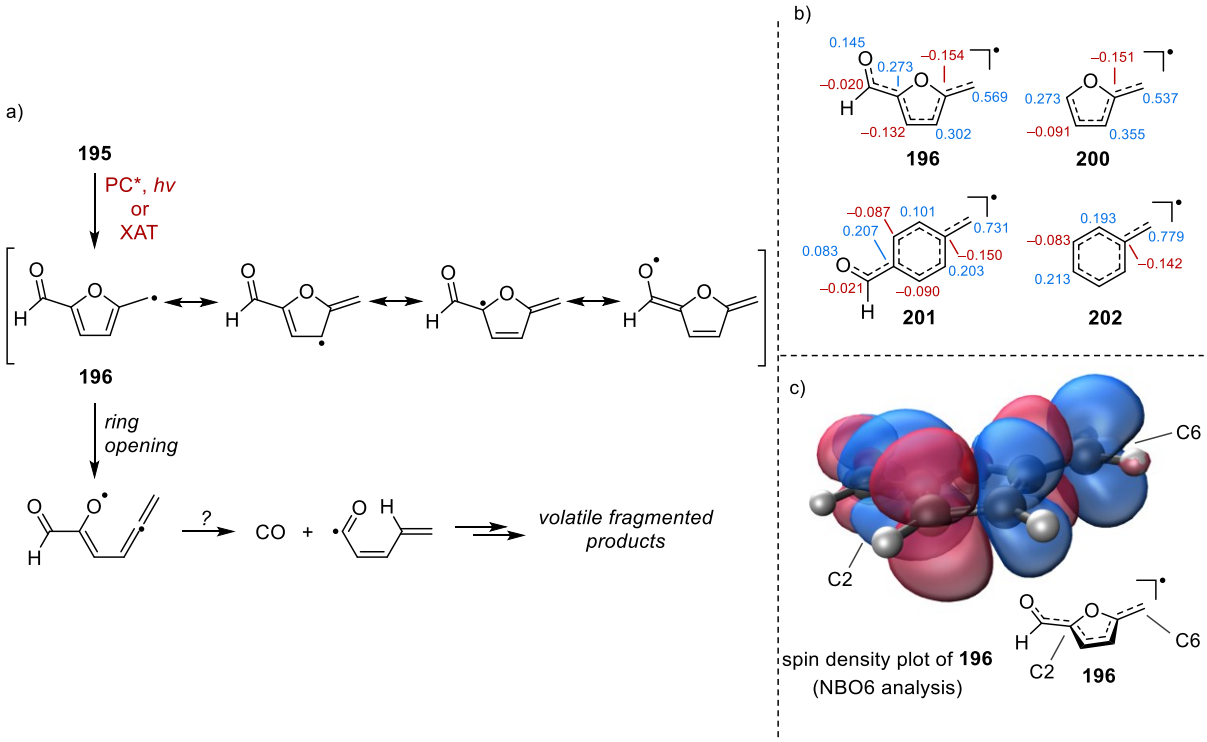

Scheme 59: Methods of radical intermediate **196** generation and subsequent ring opening. (b) Comparison of spin densities of radical **196** with closely related radicals **200, 201** and **202** (c) Spin density plot of radical **196**: blue shades designate high spin density.

Different energy gaps between radicals **196, 200-202** and the HOMO of styrene derivates **197** are shown in **Table 2**. As evident, a potentially much faster reaction between radical **196** and electron-withdrawing styrenes (4-cyano **197g** and 4-fluorostyrenes, **197f**) is expected based on the low $\Delta\varepsilon$ (FMO) of 0.169 eV. In contrast, the reaction rate is expected to be comparatively

slow in the case of electron-donor substituted styrenes (4-methoxystyrene **197n)** with the largest SOMO-HOMO gap Δε (FMO) of 0.894. The calculations indicated similar trends for 4-formyltolyl radical **201**. The smallest energy gap observed with the HOMO of the acceptor-substituted 4-cyano styrene **197g** (Δε 0.171 eV), while the largest value was obtained for donor-substituted 4-methoxy styrene **197n** (Δε = 1.234 eV).

Table 2: SOMO energies of radicals **196, 200-202**, HOMO energies of 4-substituted styrenes **197** and energy gaps Δε (eV) calculated using NBOs at the uMP2/6-311+G** level of theory.[124,125]

Radicals	SOMO (eV)	**196** **-8.828**	**200** **-8.167**	**201** **-9.168**	**202** **-8.771**
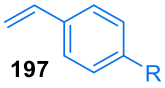 **197**	HOMO (eV)	Δε (eV)	Δε (eV)	Δε (eV)	Δε (eV)
R = H	-8.399	0.429	-0.232	0.769	0.372
R = Me	-8.136	0.692	0.031	1.032	0.635
R = OMe	-7.934	0.894	0. 233	1.234	0.837
R = F	-8.550	0.278	0.383	0.618	0.221
R = CN	-8.997	0.169	0.83	0.171	-0.226

As shown in **Scheme 60,** a number of ATRA products (**198a-198r**) employing electron-rich and electron-deficient radical acceptors as a reaction partner could be prepared using the optimised conditions with yields ranging from 25 to 84%. In case of *m*-methoxy-derivate **198j**, we obtained 73% yield, however, in the case of *o*-methoxy **197k** and *p*-ethoxystyrene **197i**, surprisingly eliminated products **198k** and **198i** were obtained with yields of 41% and 31%, respectively. While the 2,6-dichloro derivative **198h** was accessible only in 35% of yield, this was likely attributed to the presence of steric hindrance. Upon utilization of α-methylstyrene (**197n-197q**) as a reaction partner, reaction efficacy was significantly reduced and we observed incomplete conversion of CMF after 24 h of reaction time. We were able to access only isomeric C2-C3 and C3-C4 alkene derivatives **198n-198q** with yields from 25-33%. Employing 1,1-diphenylethylene **197m** also led to a substantial reduction in yield and obtained a trisubstituted alkene derivative **198m** with a yield of 29%. Structurally diverse electron-rich and deficient alkenes were also evaluated. However, they did not furnish any ATRA product under standard conditions. Experimental results presented in **Scheme 60** strongly correlated with the calculated respective FMO energy gaps Δε (**Table 2**) and clearly reflected the influence of SOMO/HOMO energy gaps of reaction partners in the respective product formation. As shown in Scheme 29, the reaction between CMF (**195**) and 4-cyano styrene

197g gave derivative **198g** in a significantly higher isolated yield (59%) compared to the reaction between 1-methoxy **198k** (41%), 4-ethoxy derivates **198i** (30%).

The consistency of the synthetic experiments and the *in-silico* results encouraged us to perform a DFT calculation (uM06-2X/6- 311+G** basis set)[125,130] to assess energy profiles of the addition reaction of (2-formyl-5-furanyl)methyl radical **196** with 4-cyano- **197g** and 4-methoxystyrene **197n**. The results demonstrated that radical addition occurs at relatively low energy barriers, approximately 11 kcal mol^{-1} in both cases (**Scheme 61**). Furthermore, we observed that the energy of adduct generated by the reaction with 4-cyanostyrene **197g** is about 2 kcal mol^{-1} lower than that of adduct formed by the reaction with 4-methoxystyrene **197n**.

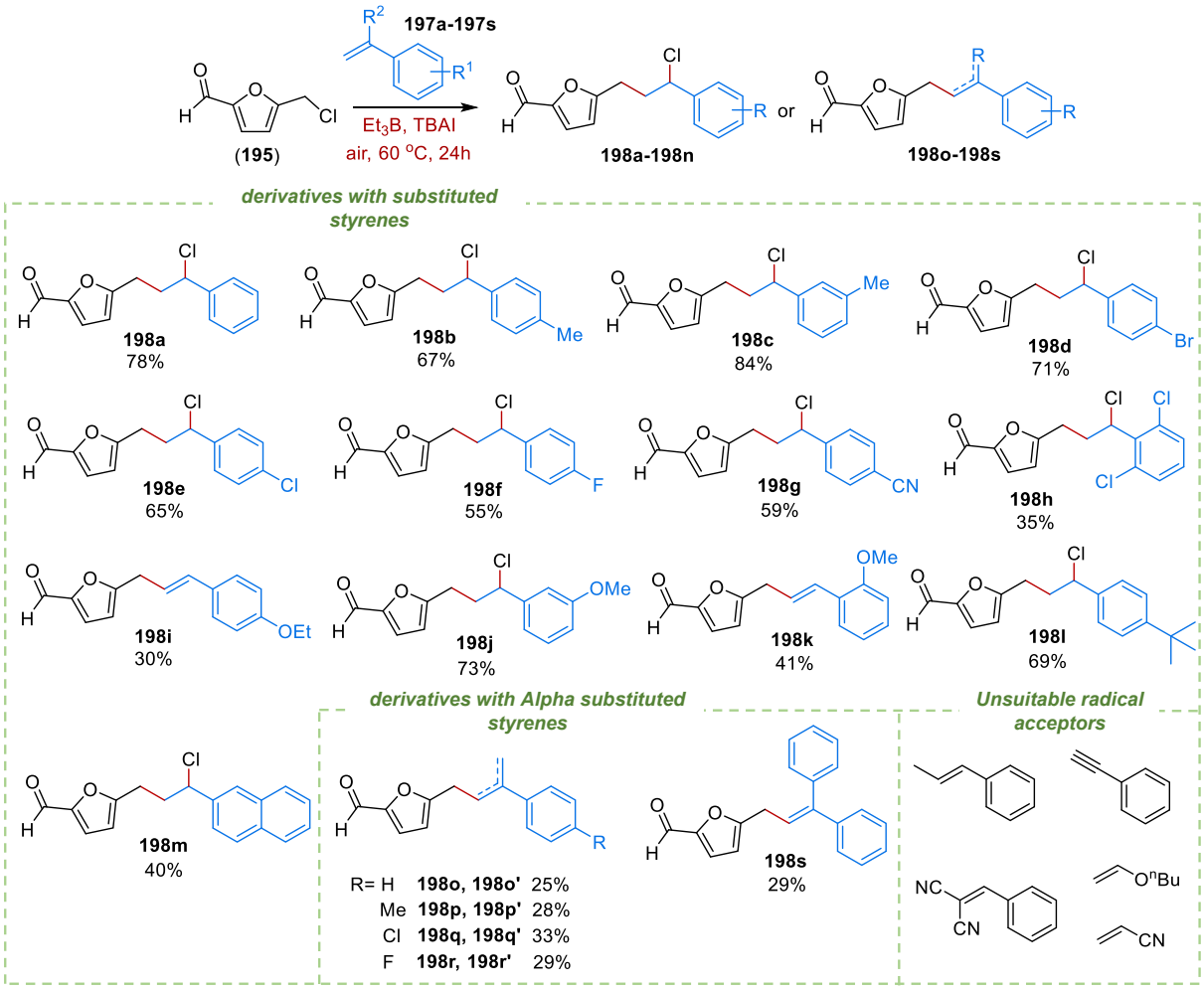

Scheme 60: Triethylborane/oxygen-mediated ATRA reaction of CMF (**195**) for the preparation of ATRA products **198.**

The proposed mechanism for the atom transfer radical addiction reaction between CMF (**195**) and styrene (**197**) mediated by Et_3B/O_2 depicted in **Scheme 62**. The aerobic oxidation of Et_3B results in the formation of reactive ethyl radicals,[7] which involve in iodine atom abstraction

from iodomethylfurfural (IMF, **203**) which is generated *in-situ* by the reaction between CMF (**195**) and iodide anion, to give (2-formyl-5-furanyl)methyl radical **196**. Subsequently, radical **196** reacts with styrene **197** leading to the well stabilised benzylic radical adduct **204**. Adduct **204** reacts with IMF **203** via abstraction of atomic iodine from IMF **203** in a chain propagation step to give reactive secondary benzylic iodides **205**, which further undergo nucleophilic substitution with chloride anion to deliver the more stable secondary benzylic chlorides **198**.

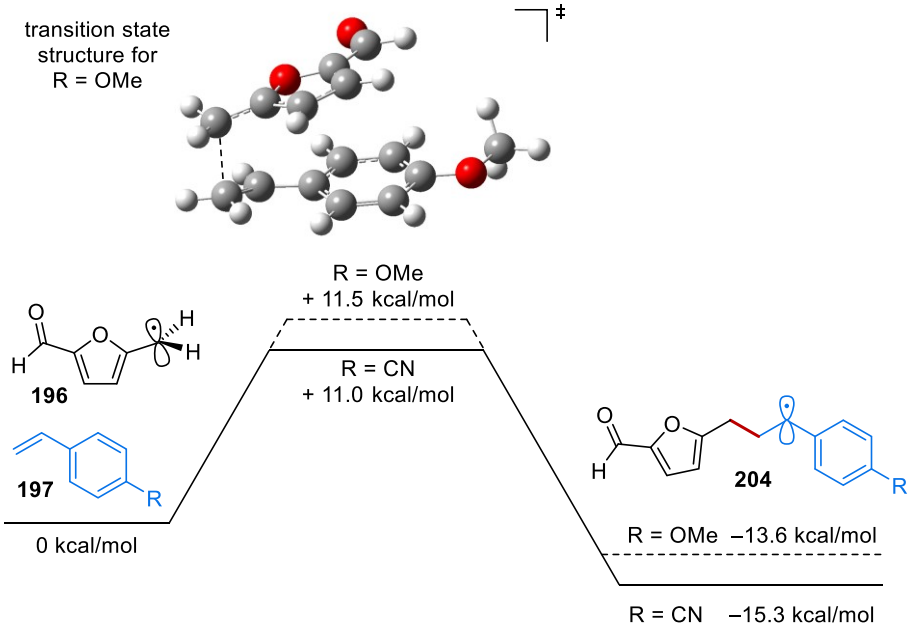

Scheme 61: Calculated energy profiles and the transition state structure for radical **196** and 4-sustituted styrenes **197**.

Further evidence for the radical intermediates **196** and **204** was gained by control experiments in the presence of the radical scavenger TEMPO and mass spectrometric analysis of the reaction mixture for their adducts **206**, **207**. Moreover, adduct **206** was isolated in yield of 44% when CMF (**195**) was alone reacted with the TEMPO and Et_3B/O_2.

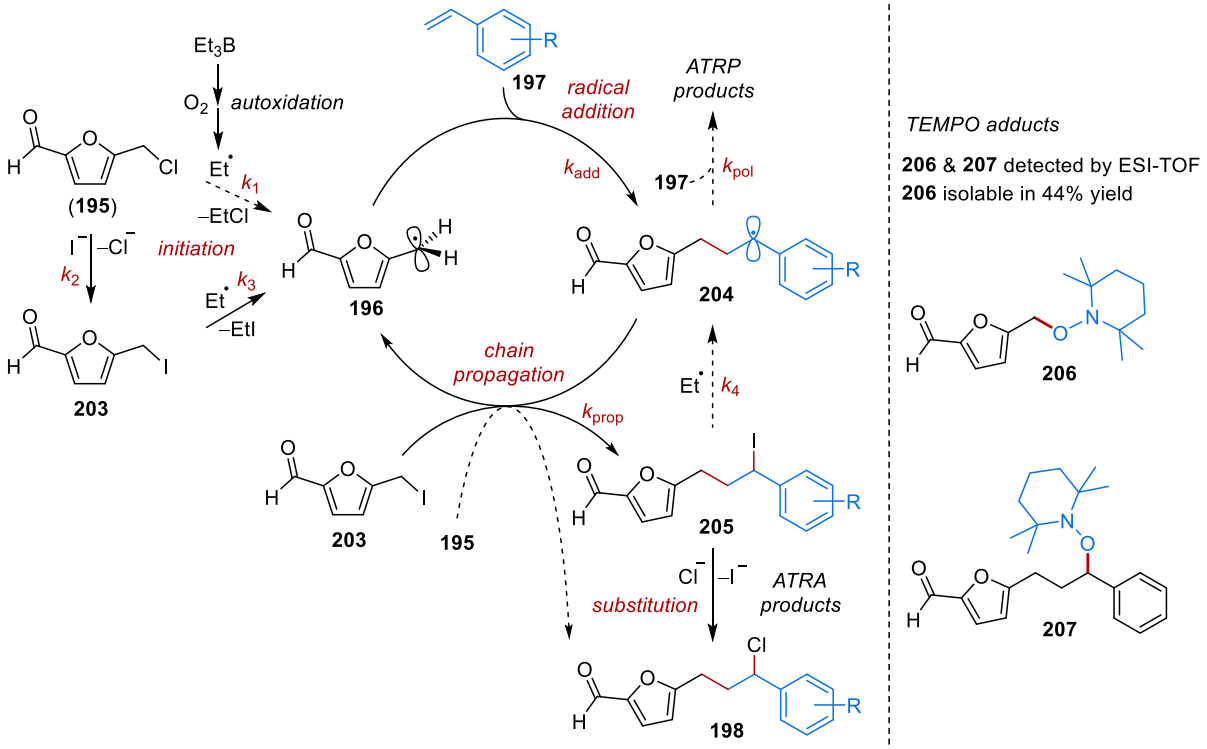

Scheme 62: Proposed reaction mechanism for the ATRA reaction of CMF (**195**) with styrene (**197a**).

In summary, we successfully enabled atom transfer radical addition reaction between biomass-derived 5-chloromethylfurfural (**195**) and styrene (**197a**) using a sustainable and metal-free Et_3B/O_2 system for the first time. Additionally, through the application of *in-silico* methods, in-depth investigations were conducted on radical **196** and its behavior in radical addition reactions. The calculated molecular and reaction parameters showed a strong correlation with the experimental outcomes of our synthetic experiments. This novel methodology shows a broad substrate scope and provides access to a number of derivatives with electron-donating and electron-withdrawing styrenes.

3.2. Visible light-induced Iridium (III)-sensitized [2+2] and [3+2] photocycloadditions of 2-cyanochromone with alkenes

Photocycloaddition reactions have been recognized as a powerful tool for the rapid construction of molecular complexity (*cf.* Chapter 1.2). Over the years, visible light photocatalysis[23,24] emerged as a promising alternative for direct UV-induced cycloaddition reactions. Notably, recent advancements in visible light photocatalysis led to increased attention towards triplet energy transfer (EnT) cycloaddition reactions.[28-30,61-68,131] Energy transfer-induced reactions rely on the relative triplet energies of the photocatalyst and substrate rather than the redox potentials of the photocatalyst and substrates. So far, numerous organophotosensitizers have been developed and demonstrated their versatile applications in EnT photocatalysis.[132] However, polyheteroaryl complexes of ruthenium (II) and iridium (III) are the most commonly employed photosensitizers due to their specific and tunable photophysical properties.[133]

Cyano-substituted enones, enoates and eneamides expose interesting behaviour in their cycloaddition reactions with alkenes as they deliver structurally diverse cycloaddition products. These reactions have well been investigated under direct UV excitation as well as through the use of acetone or aryl ketones as photosensitizers along with long-wave irradiation, in a limited number of examples.[134,135]

Saito and co-workers reported an intermolecular photocycloaddition reaction of cyano-substituted cyclic enones to alkenes under direct UV excitation (**Scheme 63**).[135b] Irradiation of cyclic enone **208** in the presence of excess 2-methyl-2-butene (**209**) led to [2+2] and [3+2] products **210** and **211** in an equal ratio. Additionally, photocycloaddition of **208** with alkenes using acetophenone or benzophenone as a sensitizer was performed and similar results were observed in comparison to direct excitation. Employing further alkenes gave the respective [2+2] and [3+2] products in almost equal ratios, while reaction of **208** with 1-cyclohexene and 1-cyclcopetene as an alkene at room temperature gave only [2+2] cycloadducts. Importantly, a temperature dependent [2+2] and [3+2] product formation was observed when 1-methylcyclohexene used as reaction partner.

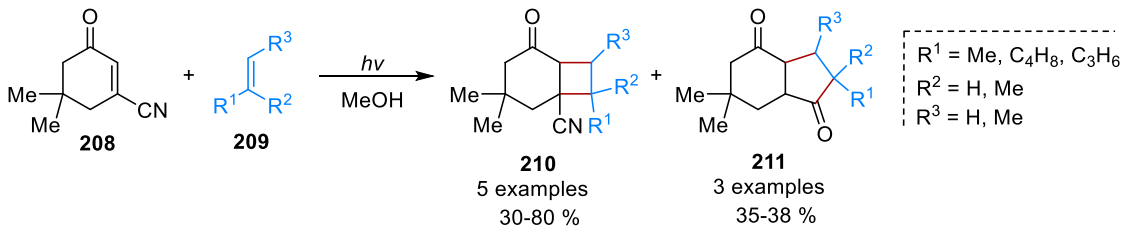

Scheme 63: Photocycloaddition of cyano-substituted enones under UV irradiation by Saito *et al*.[135b]

Margaretha *et al.* demonstrated an acetone-sensitised photocycloaddition of cyano-substituted enoate **212** with alkenes (**Scheme 64**).[135f] The photocycloaddition reaction of α-cyano enoate **212** with 2,3-dimethylbut-2-ene (**213**) in the presence of acetone as a sensitizer under UV irradiation resulted in the formation of corresponding [2+2] and [3+2] cycloadducts. Furthermore, when thioxanthone was used as a photosensitizer, only [2+2] cycloaddition product was obtained.

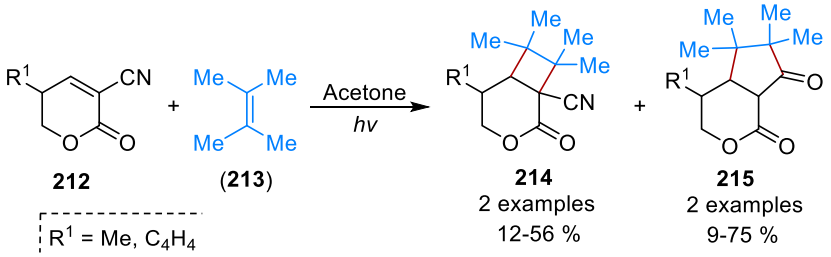

Scheme 64: Acetone-sensitised photocycloaddition of cyano-substituted enones **212** by Margaretha *et al*.[135f]

Scheme 65 depicts the expected behavior of a general β-cyanoenone **216** with alkenes **217** in photocycloadditions. The reaction between triplet excited β-cyanoenone **216** and alkene **217** initially results in the formation of cyano-substituted triplet 1,4-biradical intermediate **218**,[136] which subsequently undergoes intersystem crossing and ring-close to deliver cyanocyclobutane **219.** Alternatively, a cyclic triplet nitrene intermediate **220** can be generated through a competing 1,5-cyclization of the triplet biradical intermediate **218**. Subsequently, a cyclopentenylimine **221** is formed by transfer of hydrogen to the nitrene nitrogen atom and a hydrogen abstraction that re-installs the conjugated double bond. Upon aqueous workup, cyclopentenylimine **221** is hydrolysed to give cyclopentenone **222** as a final [3+2]-product. The structure of the reactants plays a significant a role in the ratios of [2+2]- and [3+2]-products, although certain cases interestingly displayed a temperature-dependent product ratio during the formation of [2+2]- and [3+2]-products.[134, 135b]

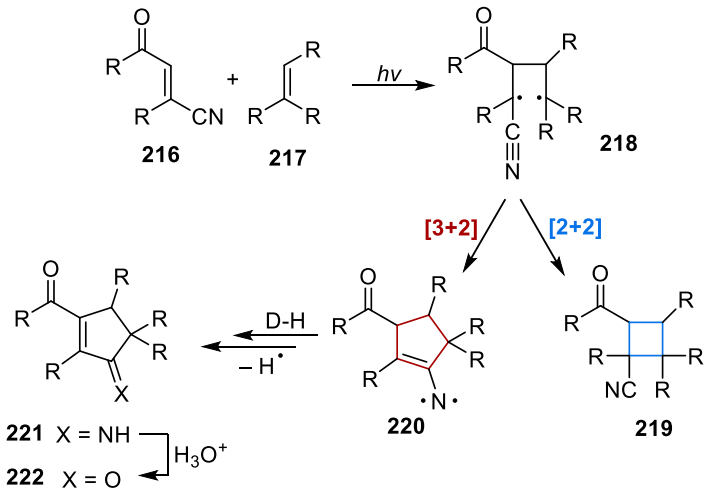

Scheme 65: Schematic representation of β-cyanoenone **216** photocycloadditions.

Earlier, Saito *et al*. reported a temperature dependent photocycloaddition of 2-cyanochromone (**223**) with alkenes **224** under direct UV excitation, to afford cycloadducts **225** and **226** with moderate yield and low selectivity in the [2+2]- versus [3+2]-cycloaddition (**Scheme 66**).[134] Aiming to improve existing reaction conditions and selectivity, we decided to apply visible light photocatalysis in the development of new efficient catalytic system for the cycloadditions of 2-cyanochromone.

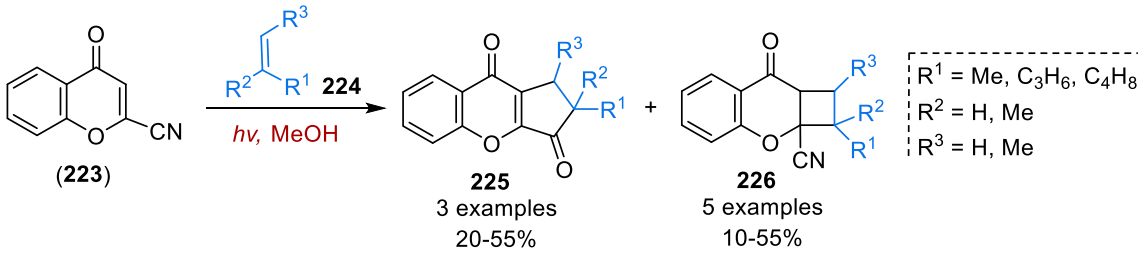

Scheme 66: [3+2]-and [2+2]-photocycloaddition of 2-cyanochromone by Saito *et al*.[134]

We began our investigation by screening various photocatalysts to enable the cycloaddition of cyanochromone (**223**) with styrene (**227**) (**Table 3**). We observed that all of the utilized photosensitizers except Eosin Y and Rose Bengal could promote the cycloaddition reaction to give *exo*-[2+2]-cycloadduct **228** as a major product and its regioisomer **229** as a minor product. In the class of organosensitizers, thioxanthone was most effective for the cycloaddition reaction between cyanochromone (**223**) and styrene (**227**) with 70% conversion of (**223**), along with the yields of 42% and 8% of **228** and **229**, respectively (entries 1-2). However, among the employed Iridium (III) metal-based complexes, $(Ir[dF(CF_3)ppy]_2[dtbpy])PF_6$ showed a better outcome with catalyst loading of 2 mol-% (entries 6-8) and observed optimum efficiency could be attained with catalyst loading of 3 mol-% (entries 9-11). Further, variations

in the amount of styrene (**227**) and reaction time demonstrated that 10 equivalents of **227** with 36 h of reaction time was optimal for almost complete conversion of chromone (**223**), to give cycloadducts **228** and **229** in yields of 72% and 14%, respectively (entries 12-14) and with almost entire diastereocontrol. However, variation of the reaction solvent did not show any further improvements in comparison to MeCN (entries 15-17). Performing the reaction without photosensitizer or irradiation resulted in no product formation (entries 16).

Table 3: Optimization and control experiments for photocycloaddition of 2-cyanochrome (**223**).

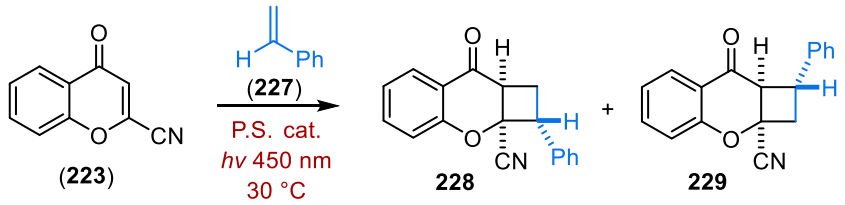

#	P.S.	mol-%	time	(227) (equiv.)	solvent	conv. (223) [%][a]	yield 228 [%][a]	yield 229 [%][a]
1	1,5-AAQ	10	24	20	MeCN	10	3	1
2	thioxanthone	10	24	20	MeCN	70	42	8
3	Eosin Y[b]	2	24	10	MeCN	18	0	0
4	Rose Bengal[b]	2	24	10	MeCN	32	0	0
5	4CzIPN	2	24	20	MeCN	40	17	5
6	$Ir(ppy)_3$	2	24	20	MeCN	35	0	0
7	$[Ir(ppy)_2(dtbpy)^+$	2	24	20	MeCN	55	13	5
8	$(Ir[dF(CF_3)ppy]_2(dtbpy))^+$	2	24	20	MeCN	70	43	12
9	$(Ir[dF(CF_3)ppy]_2(dtbpy))^+$	1	24	20	MeCN	50	32	10
10	$(Ir[dF(CF_3)ppy]_2(dtbpy))^+$	3	24	20	MeCN	79	58	11
11	$(Ir[dF(CF_3)ppy]_2(dtbpy))^+$	4	24	20	MeCN	70	41	10
12	$(Ir[dF(CF_3)ppy]_2(dtbpy))^+$	3	36	20	MeCN	93	64	13
13	**$(Ir[dF(CF_3)ppy]_2(dtbpy))^+$**	**3**	**36**	**10**	**MeCN**	**96**	**72 (71)[c]**	**14**
14	$(Ir[dF(CF_3)ppy]_2(dtbpy))^+$	3	36	5	MeCN	87	64	14
15	$(Ir[dF(CF_3)ppy]_2(dtbpy))^+$	3	36	10	Acetone	85	48	13
16	$(Ir[dF(CF_3)ppy]_2(dtbpy))^+$	3	36	10	DCM	89	43	15
17	$(Ir[dF(CF_3)ppy]_2(dtbpy))^+$	3	36	10	DMF	67	30	9
18	No P.S. / no light	0/3	36	10	MeCN	4/2	0/0	0/0

Reactions were performed on a 0.1 mmol scale of (**223**). [a] Determined by ^{1}H-NMR analysis using CH_2Br_2 as the internal standard. [b] 530 nm LED (30W) used. [c] Yield of the isolated product after chromatography.

As shown in **Scheme 67**, a series of cycloadducts **228a-228t** were synthesised using different alkenes **227a-227t** as a reaction partner under established reaction conditions (entry 11). Cyclobutanes **228a-228i**were synthesised with yields ranging from 58-76% through the use of

monosubstituted styrenes **227a-227i**, while in the case of 2,6-diclorostyrene **227j** cycloadduct **228j** was obtained in a moderate yield of 28%.

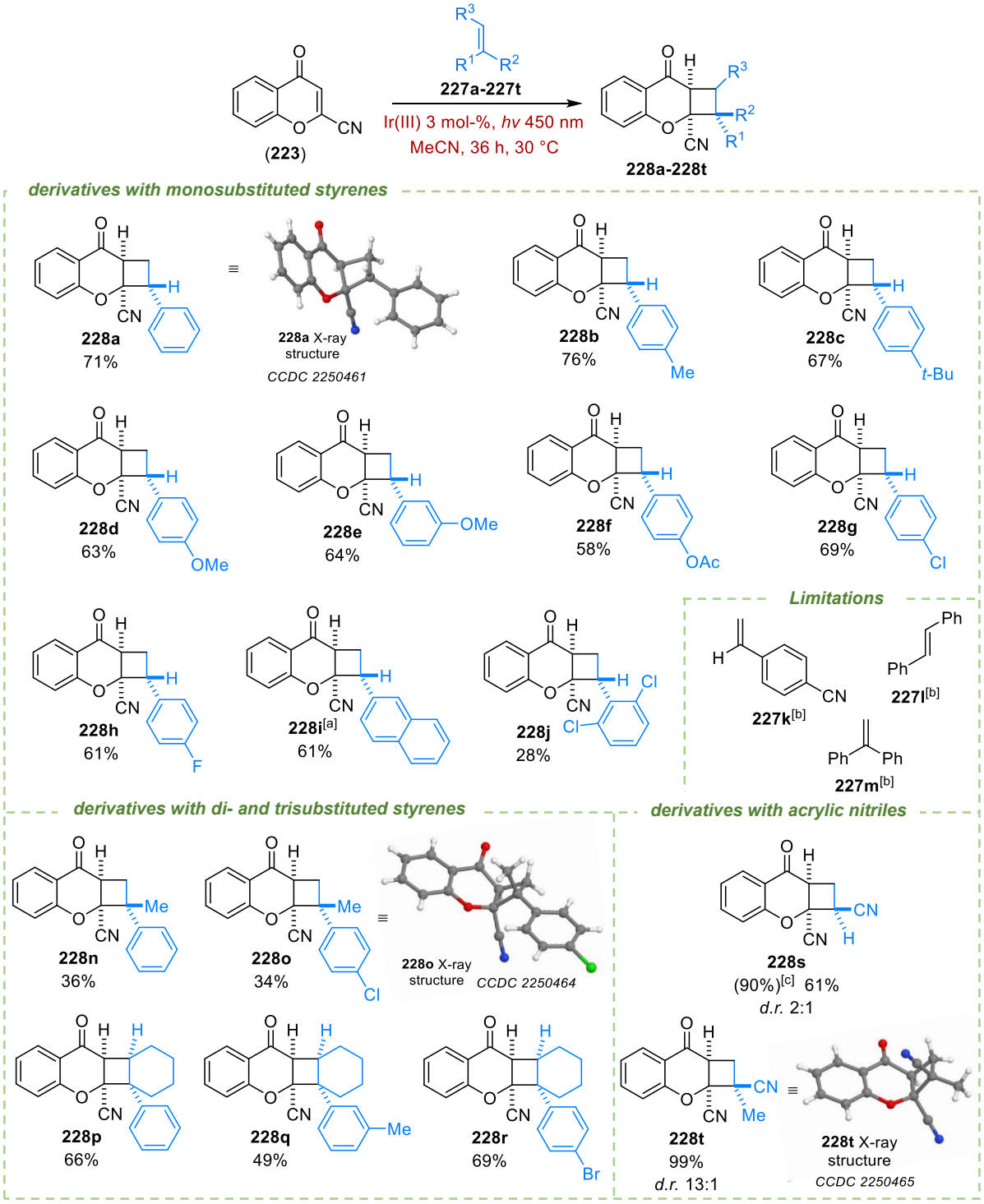

Scheme 67: Scope of visible light-medicate Ir(III)-sensitized photocycloadditions of 2-cyanochrome (**223**) with different alkenes. [a] Isolated as a 5:1 mixture of regioisomers. [b] Yield determined by ^{1}H-NMR analysis using CH_2Br_2 as the internal standard. [c] Combined yield of both isomers determined by ^{1}H NMR analysis.

In all reactions with monosubstituted styrenes, a corresponding regioisomer was observed, with the regioselectivity ranging from 3.5:1 for compound **228c** to 14:1 in the case of compound **228h**. Using α-methyl styrenes **227n** and **227o** as reaction partners, cyclobutanes **228n** and **228o** were synthesised with *r.r* of 6:1 in both cases. On the other hand, 1-arylcyclohexenones **227p-227r** and acrylonitriles **227s** and **227t** delivered only single regio- and diastereoisomers **228p-228t** with 49-99% of yield. In case of 4-cyanostyrene **227k**, the corresponding [2+2]-cycloadducts observed in crude NMR analysis as a mixture with the yield of 26%, while *trans*-stilbene **227i** and 1,1-diphenylethyele **227m** were found as unsuitable reaction partners with the yield of 0% and 9%, respectively. In all above mentioned cases, none of the corresponding possible [3+2]-cycloadducts were detected after careful NMR analysis of crude reaction products.

Table 4: Visible light-mediated Ir(III)-sensitized [2+2]- and [3+2]-cycloadditions of 2-cyanochrome (**223**) with di- and trisubstituted alkenes.

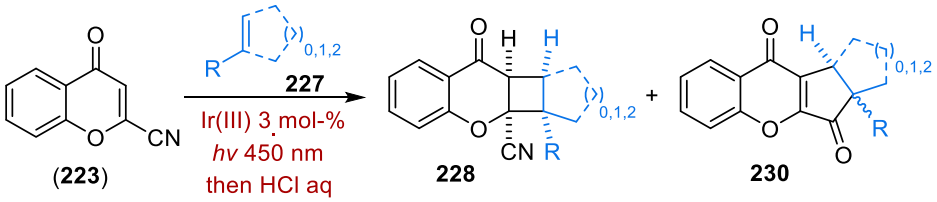

#	alkene	T (°C)	ratio 228:230[a]		yield of 228 (%)[b]	yield of 230 (%)[b]
1	**227u**	30	**228u:230u**	1:1.6	18	28
		65[c]	**228u:230u**	1:1.6	12[d]	19[d]
2	**227v**	30	**228v:230v**	0:1	0	44
		-10[c]	**228v:230v**	0:1	0[d]	24[d,e]
3	**227w**	30	**228w:230w**	1:2.8	8	24
		65[c]	**228w:230w**	1:2.8	8[d]	26[d]
4	**227x**	30	**228x:230x**	1:3.7	11[d]	41
5	**227p**	30	**228p:230p**	1:0	66	0
		65[c]	**228p:230p**	1:0	65[d]	0[d]

Reactions conditions: [a] 0.1 mmol scale of **223,** alkene **227** (10 equiv.), (Ir[dF(CF_3)ppy]$_2$[dtbpy])PF_6 3 mol-%, MeCN, 450 nm LED (30 W), 30 °C, 48 h or 450 nm LED (10 W), 65 °C, 48 h, then HCl aq., acetone, r.t.,16 h. [a] Determined by ^{1}H-NMR-analysis. [b] Yield of the isolated product after chromatography. [c] 10 W 450 nm LED used. [d] Determined by ^{1}H-NMR analysis using CH_2Br_2 as the internal standard. [e] Yields based on 76% conversion of (**223**).

Saito and co-workers[134] previously demonstrated the formation of the [2+2] and [3+2] cycloaddition products when cyanochromone (**223**) irradiated under direct UV along with 1-methylcyclopentene (**227u**) or 1-methylcyclohexane (**227v**) as a reaction partner. A temperature dependent [2+2] and [3+2] product formation was observed and increased selectivity towards the [3+2] cycloadduct formation was noticed when 1-methylcyclohexane is used. Subsequently, in our studies, we employed 1-methylcyclopentene (**227u**), 1-methylcyclohexane (**227v**), 2-methyl-2-butene (**227w**) and 2,3-dimethyl-2-butene (**227x**) as reaction partners under the established reaction conditions (**Table 4**). The reaction with 1-methylcyclopentene (**227u**) gave both [2+2]- and [3+2]-cycloadducts **228u** and **230u** in a ratio of 1:1.6 with an isolated yield of 18% and 28%, respectively. In case of 1-methylcyclohexene (**227v**), only [3+2]-adduct **230v** was obtained as a pure single *cis*-diastereomer with 44% of isolated yield. On the other hand, products **228w** (a mixture of regioisomers) and **230w** in a ratio of 1:2.8 with the combined yield of 32% were obtained. Using 2,3-dimethyl-2-butene (**227x**) as a reaction partner showed improved selectivity towards [3+2]-cycloadduct formation compared to [2+2]-cycloadduct with the ratio of 3.7:1.

Although we obtained overall moderate yield of cycloadducts, a slight improvement of product selectivity towards the [3+2]-cycloadducts **230v** and **230w** was observed with the new reaction conditions in comparison with the direct UV-induced reactions.[134] However altering the reaction temperatures from 30 °C to 65 °C or from 30 °C to -10 °C, did not show in any change in the respective [2+2]- and [3+2]-product ratios (**Table 4**). Similarly, no temperature effects on the product selectivity was observed when 1-phenylcyclohexene (**227p**), styrene (**227a**) used and only corresponding [2+2]-products **228p, 228a** and **229a** were obtained. These findings clearly demonstrated that [3+2]-cyclization of aryl-substituted biradicals **321** are impeded probably due to their short triplet lifetime compared to alkyl cyano 1,4-biradicals.

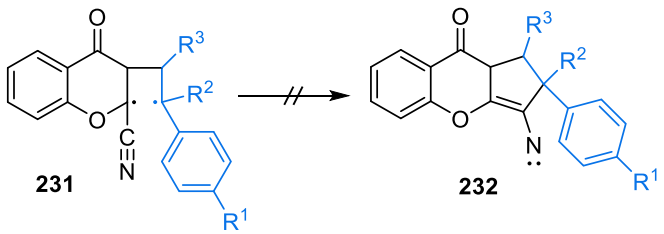

Scheme 68: Infeasible [3+2]-cycloaddition reaction of aryl substituted 1,4-biradicals **231**.

In conclusion, visible light-induced cycloadditions of 2-cyanochrome (**223**) with diverse alkenes using $(Ir[dF(CF_3)ppy]_2[dtbpy])PF_6$ as a photosensitizer were developed to synthesise respective [2+2]-cycloadducts in high yield. By utilizing new reaction conditions, cyclobutane derivatives **228** of mono-, di- and trisubstituted styrenes and acrylonitriles could be accessed

with good regiocontrol and high diastereoselectivity. Additionally, in the case of tri-alkyl-substituted alkenes, the [3+2]-cycloaddition products, cyclopentenone-fused chromones **230** can also be synthesised. However, performing the reactions at different temperatures did not result in any significant shift towards selective [2+2]- or [3+2]- product formation.

3.3. Photocatalytic azetidine synthesis by aerobic dehydrogenative [2+2]-cycloadditions of amines with alkenes

In addition to conventional cycloaddition reactions of unsaturated reactants, dehydrogenative cycloadditions lately gained significant attention. These processes involve an *in situ* dehydrogenation of saturated reactants prior to the cycloaddition event. While thermal dehydrogenative cycloadditions are well-established and elegant examples of [4+2]-, [3+2]-, and [2+2+2]-cycloadditions have been reported,[102-108, 111,112] photochemical variants of such processed remain rare thus far.

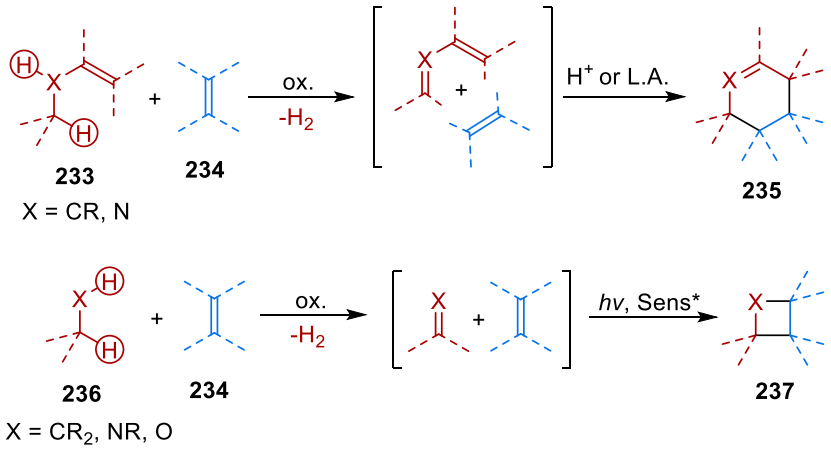

Scheme 69: Concept of dehydrogenative [4+2]-and [2+2]-cycloadditions.

The thermal one-pot oxidative Povarov/aromatization tandem reaction of substituted glycine derivatives **238** with electron-rich alkenes **239** was first reported by Macheño and Richeter (**Scheme 70**).[106] Substituted quinolones **240** were synthesised using iron(III) chloride as a catalyst in combination with mild, non-toxic TEMPO oxoammonium salt as a formal hydrogen acceptor.

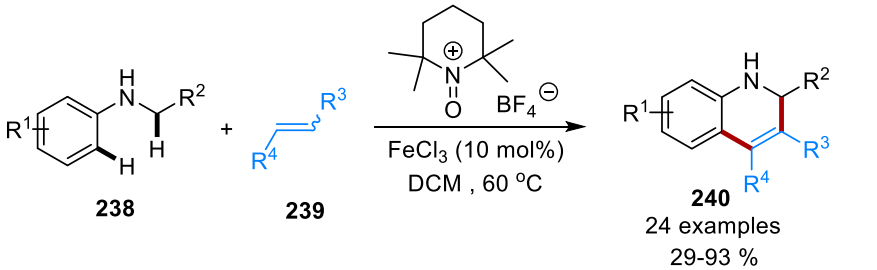

R^1 = 4-MePh, 2-MePh, 3-MePh, 3,5-diMePh, 4-MeOPh, 4-ClPh, 4-Br, 4-COMePh,
R^2 = Ph, Me, COOEt, COPh, $PO(OEt)_2$
R^3 = Ph, OMePh, 4-^{t}BuPh, *n*-hex, $PhCHCH_2$, OBu, OEt, 4-ClPh, 2-ClPh
R^4 = H, Et, Ph

Scheme 70: $FeCl_3$ and TEMPO oxoammonium salt-mediated dehydrogenative [4+2] cycloadditions.[106]

Another variant of dehydrogenative cycloaddition, a thermal double dehydrogenative Povarov cycloaddition reaction was developed by Huo *et al.*[108] This method provided an access to synthesise complex quinolone scaffolds **243** from readily available inexpensive *N*-arylglycine esters **241** and 1,4-dioxane (**242**) using carbon tetrabromide-mediated dual-oxidative dehydrogenative (DOD) cycloaddition approach. (**Scheme 71**).

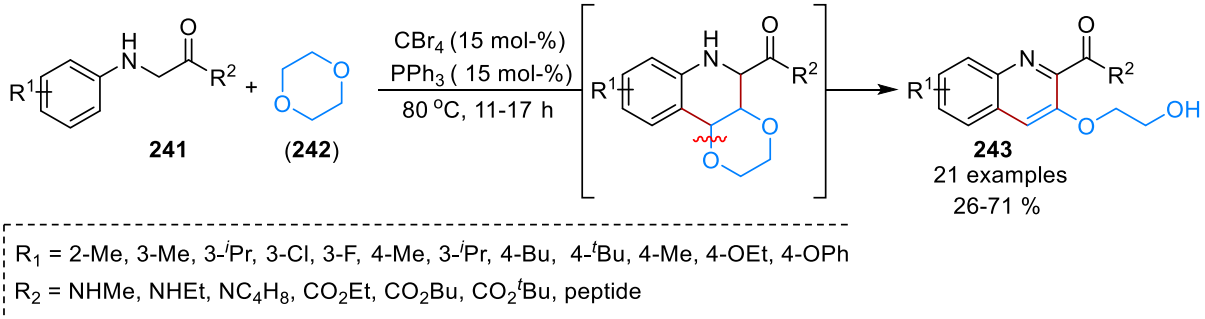

Scheme 71: Metal-free double oxidative dehydrogenative Povarov reaction.[108]

As one further example, our laboratory recently developed an iodine and visible light-mediated dehydrogenative Povarov reaction of glycine esters **244** with indoles **245** and 1,1-disubstituted alkenes **247**, to efficiently synthesise corresponding cycloadducts **246** and **248** in a single step (**Scheme 72**).[109,110]

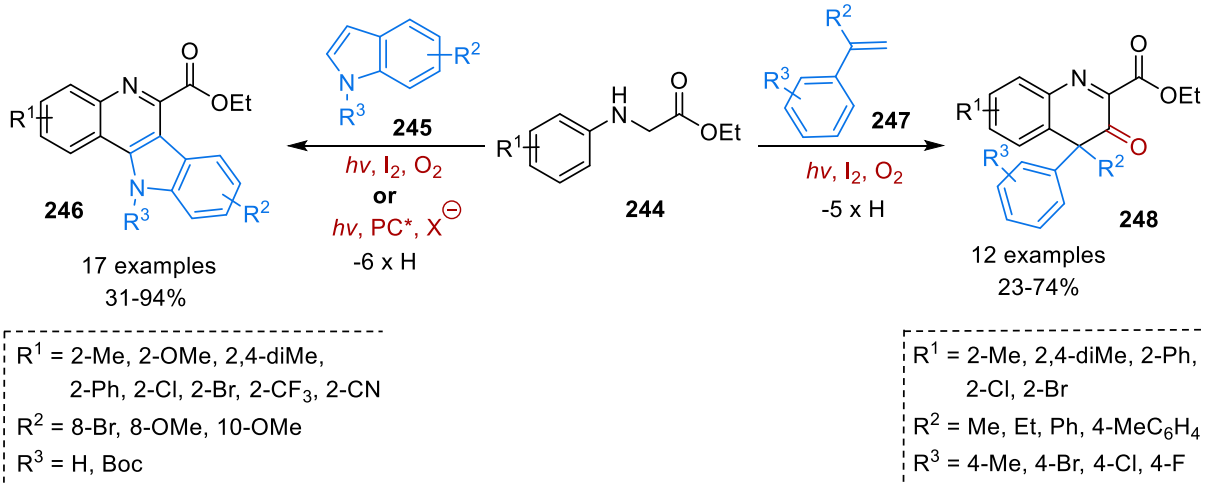

Scheme 72: Dehydrogenative Povarov reactions of *N*-aryl glycine esters.[109,110]

Although dehydrogenative cycloadditions offer numerous advantages, such as high atom economy and construction of multiple bonds in a single step, most of the reactions still require the use of stoichiometric amounts of oxidants and high reaction temperatures. Furthermore, these approaches have been extensively applied only in the case of dehydrogenative [4+2] and [3+2] cycloadditions and the potential of dehydrogenative [2+2] cycloadditions remains largely unexplored. Therefore, there is a strong need to develop sustainable methods for the

dehydrogenative cycloadditions especially, for the dehydrogenative [2+2] cycloadditions. Hence, we reasoned to develop green and efficient catalytic method for the dehydrogenative [2+2] cycloadditions.

The dehydrogenative aza [2+2] cycloaddition of amines **249** with simple alkanes **250** is considered to be highly attractive process for the synthesis of functionalized azetidines **251** (**Scheme 73**). Furthermore, the oxidative generation of imines followed by cycloaddition with alkenes eliminates the need for multi-step reactions process and purification of intermediates.

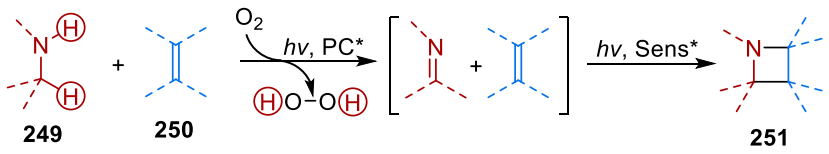

Scheme 73: The idea of dehydrogenative aza-[2+2]-cycloadditions.

In 1984, Nishio and co-workers reported an Aza Paternò-Büchi reaction of quinoxaline-2-(1*H*)-ones **252** with olefins **253** under UV irradiation to afford azetidines **254** (**Scheme 74, left**).[137,138] The reaction displayed good regioselectivity while the diastereoselectivity was influenced by the steric properties of both the imine and alkene. Employing aryl-substituted alkenes as olefins provided the respective azetidine products as a single regio- and diastereomers.

In addition to the Nishio group, recently, Bach and co-workers reported an enantioselective Aza Paternò-Büchi reaction of 3-substituted quinoxalinones **252** with styrenes **255** utilizing chiral thioxanthone **115** as a triplet sensitizer, to synthesise a variety of functionalised azetidine derivatives **256** with high enantioselectivity (**Scheme 74, right**).[101]

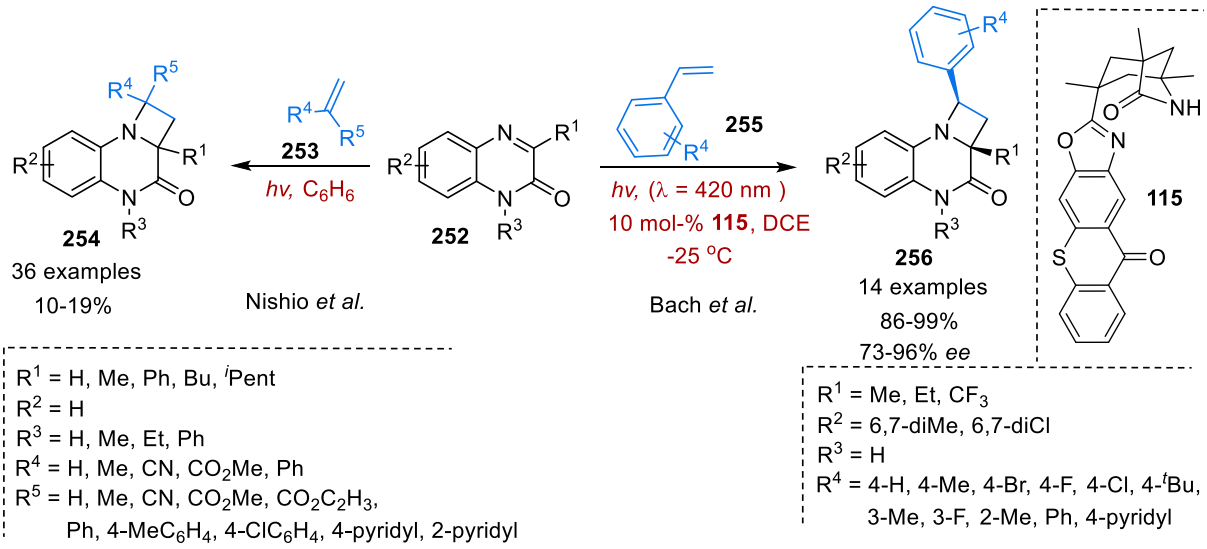

Scheme 74: Aza [2+2]-photocycloadditions of quinoxaline-2-(1*H*)-ones **252** with alkenes. [137,138,101]

Utilizing the known ability of quinoxalinones **260** to undergo the Aza Paternò-Büchi reaction, we aimed to develop a dehydrogenative variant of this reaction. In this context, dihydroquinoxalinones **259** would serve as imine precursors, and they could readily be made from α-amino acids **258** and ortho-bromo aniline (**257**) by a simple copper-mediated coupling reaction (**Scheme 75**).[139,140]

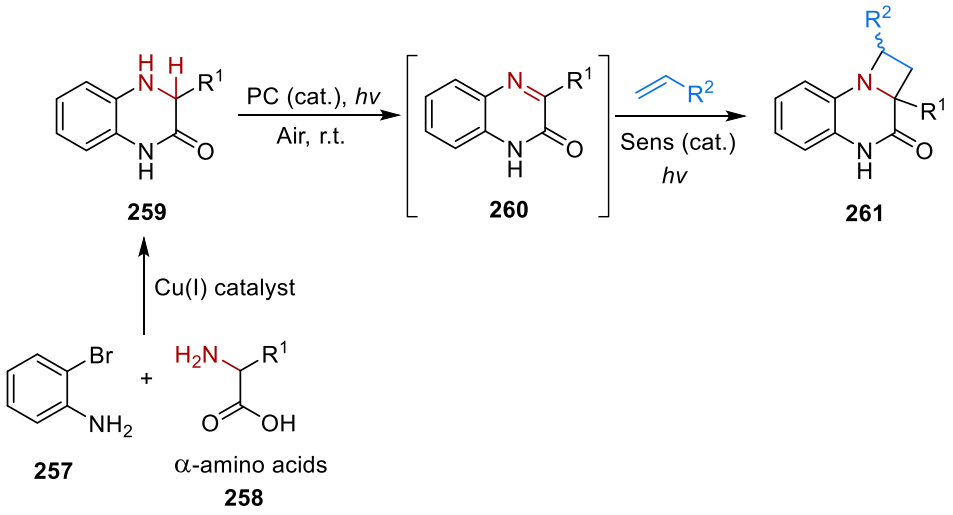

Scheme 75: The idea of synthesis of amino acid-derived dihydroquinoxalinones **259** and their dehydrogenative aza [2+2]-photocycloadditions with alkenes.

We started our investigation to find a potential catalytic system for each individual step, that is, the dehydrogenation of **262** to **263** and the subsequent [2+2]-cycloaddition between quinoxalinone **263** and styrene (**264a**), as well as for the one-pot dehydrogenative [2+2]-cycloaddition (**Scheme 76**).

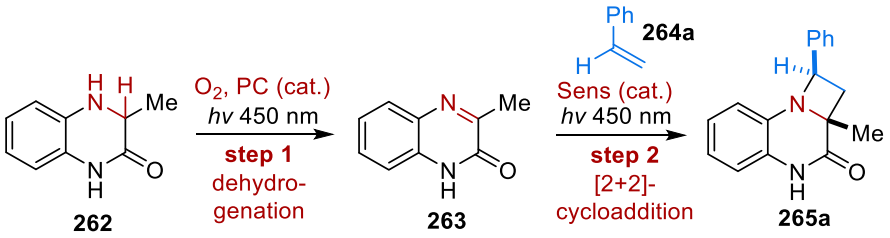

Scheme 76: Dehydrogenation and [2+2]-photocycloaddition of quinoxaline-2-(1*H*)-ones.

At the outset of the study, several anthraquinone dyes, potent organic photooxidants, thioxanthone and several iridium (III) complexes were evaluated to determine their efficacy in catalyzing the dehydrogenation of **262** → **263** (step 1). Substituted anthraquinones and thioxanthone were found very effective in promoting the intended oxidation of **262** → **263** with high yields (**Table 5**, entries 1-5). Gratifyingly, both $Ir[dF(CF_3)ppy]_2(dtbpy)^+$ and $Ir(ppy)_3$ as well exhibited excellent efficacy as a photocatalyst for the oxidation of **262** → **263** (entries 7,8). Furthermore, utilization of Rose Bengal[141] (2 mol-%) under 530 nm green LED irradiation also

showed a high degree of efficacy in catalyzing the dehydrogenation of **262** (entry 6). On the other hand, autooxidation of compound **262** in the absence of a photocatalyst showed only 15% of conversion after 3 h of irradiation under air, whereas no reaction occurred in the dark (entries 10-13).

Table 5: Investigation of the photocatalytic dehydrogenation of **262** to **263.**

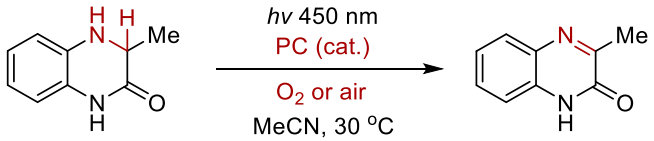

262 **263**

#	PC (cat.)	PC (mol-%)	O_2	time	conv. 262 [%][a]	yield. 263 [%][a]
1	1,5-diaminoanthraquinone	10	balloon	1 h	100	96
2	1,8-dihydroxyanthraquinone	10	balloon	1 h	100	97
3	2-chloroanthraquinone	10	balloon	1 h	100	96
4	1,5-dichloroanthraquinone	10	balloon	1 h	100	97
5	thioxanthone	10	balloon	1 h	100	98
6	rose bengal [b]	2	balloon	1 h	87	87
7	$Ir[dF(CF_3)ppy]_2(dtbpy)PF_6$	2	balloon	1 h	100	89
8	$Ir(ppy)_3$	2	balloon	1 h	100	99
9	**$Ir(ppy)_3$**	**2**	**air**	**3 h**	**100**	**98**
10	without PC	-/-	balloon	1 h	20	15
11	without PC	-/-	air	3 h	15	12
12	$Ir(ppy)_3$	2	argon	3 h	0	0
13	$Ir(ppy)_3$ [c]	2	balloon	3 h	0	0

Reactions were performed on a 0.10 mmol scale of **262** at 30 °C. [a] Determined by ^{1}H-NMR-analysis using CH_2Br_2 as the internal standard. [b] Light sources: 530 nm green LED, 10 W. [c] Without irradiation. AQ = anthraquinone.

Following the initial studies, all photocatalysts evaluated for step 1 were screened in the Aza Paternò-Büchi reaction between quinoxalinone **263** and styrene (**264a**) (step 2). We observed that anthraquinone and thioxanthone showed minimal efficacy in promoting the second step, whereas both $Ir[dF(CF_3)ppy]_2(dtbpy)+$ and $Ir(ppy)_3$ gave high yields of the Aza [2+2] product (**Table 6**). The photocycloaddition reaction between **263** and **264a** with $Ir(ppy)_3$ was found to be slightly superior then $Ir[dF(CF_3)ppy]_2(dtbpy)^+$. Utilizing 2 mol-% of $Ir(ppy)_3$ with 20 equivalents of styrene (**264a**) in acetonitrile under 450 nm blue LED irradiation for 24 h, azetidine **265a** was isolated in a high yield of 89%. Different solvents were evaluated for photocycloaddition however, none of them showed outcomes compared superior to

acetonitrile (entries 10-12). 1,5-Dichloroanthraquinone and thioxanthone were found moderately effective in promoting the reaction between **263** and **264a** when CFL lamps were used instead of 450 nm LEDs (entries 6,7). Moreover, a slow degradation of **265a** was observed when the $Ir(ppy)_3$-mediated reaction was performed under an O_2 atmosphere, and no reaction was observed between **263** and **264a** in the absence of light or photosensitizer (entries 13,14).

Table 6: Investigation of photosensitized [2+2]-cycloaddition between quinoxalinone **263** and styrene (**264a**).

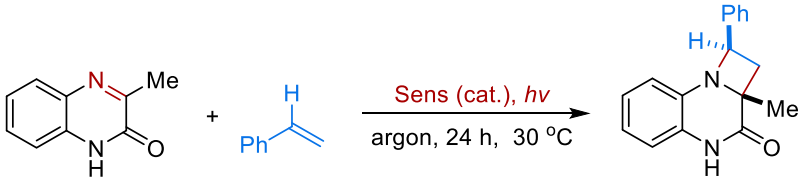

263 (**264a**) **265a** *d.r.* > 19:1

#	Sens. (cat.)	Sens (mol-%)	solvent	light source [a]	conv. 263 [%][b]	yield. 265a [%][b]
1	1,5-diaminoanthraquinone	10	MeCN	LED 450 nm	0	0
2	1,8-dihydroxyanthraquinone	10	MeCN	LED 450 nm	0	0
3	2-chloroanthraquinone	10	MeCN	LED 450 nm	0	0
4	1,5-dichloroanthraquinone	10	MeCN	LED 450 nm	0	0
5	thioxanthone	10	MeCN	LED 450 nm	0	0
6	1,5-dichloroanthraquinone	10	MeCN	CFL 450 ± 50nm	66	11
7	thioxanthone	10	MeCN	CFL 370 ± 50nm	90	60
8	$Ir[dF(CF_3)ppy]_2(dtbpy)PF_6$	2	MeCN	LED 450 nm	93	84
9	**$Ir(ppy)_3$**	**2**	**MeCN**	**LED 450 nm**	**99**	**90 (89)[c]**
10	$Ir(ppy)_3$	2	DCM	LED 450 nm	92	80
11	$Ir(ppy)_3$	2	DMF	LED 450 nm	90	75
12	$Ir(ppy)_3$	2	MeOH	LED 450 nm	19	0
13	No Sens./ no light	0/2	MeCN	LED 450 nm	0/0	0/0
14	$Ir(ppy)_3$ [d]	2	MeCN	LED 450 nm	95	56

Reactions were performed on a 0.10 mmol scale of **263** at 30 °C and under an argon atmosphere. [a] Light sources: 450 nm blue LED, 30 W / 450 ± 50 nm CFL, 2 × 18W / 370 ± 20 nm CFL, 2 × 18 W. [b] Determined by ^{1}H-NMR-analysis using CH_2Br_2 as the internal standard. [c] Isolated yield. [d] Under oxygen atmosphere

Once it was established that $Ir[dF(CF_3)ppy]_2(dtbpy)^+$ and $Ir(ppy)_3$ both can serve as efficient photosensitizers for catalyzing dehydrogenation reaction **262** → **263** (step 1) as well as

photocycloaddition reaction between **263** and **264a** (step 2), we initiated our investigations to explore the possibility of performing the one-pot dehydrogenative cycloaddition reaction. We observed that both catalysts were efficient in promoting it and $Ir(ppy)_3$ showed a slightly superior outcome. Several experiments were performed to establish the optimum reaction conditions and we found that styrene (**264a**) could be added to the reaction mixture from the very beginning (**Table 7**). Additionally, it was observed that the reaction requires an exposure to ambient atmosphere only for 3 h by using a cannula for gas exchange. After 3 h, the cannula was removed and irradiation was continued in the sealed vessel for a further 21 h. Hence, it was not necessary to replace air with an inert gas after the complete consumption of substrate **262**. Utilizing the optimized conditions, azetidine **265a** could be obtained with an isolated yield of 75%. Further, a series of control experiments was performed and it was verified that azetidine **265a** was sufficiently stable to the photooxidative reaction conditions with only very marginal degradation.

Table 7: Optimization of the photocatalytic dehydrogenative [2+2] cycloaddition between dihydroquinox -alinone **262** and styrene (**264a**).

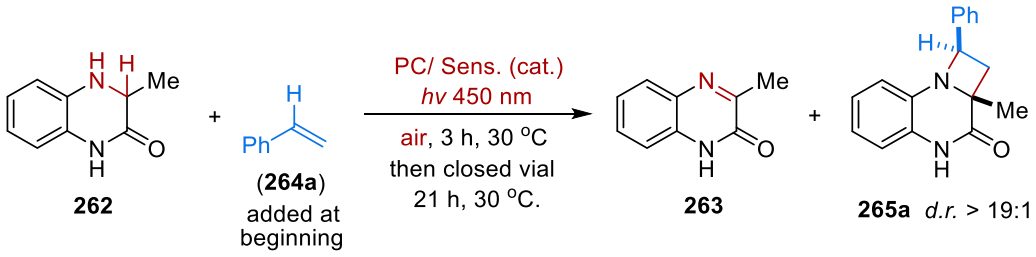

#	PC / Sens. (cat.)	PC / Sens. (mol-%)	264a (eq.)	solvent	conv. 262 [%][a]	yield. 263 [%][a]	yield. 265a [%][a]
1	$Ir[dF(CF_3)ppy]_2(dtbpy)PF_6$	2	20	MeCN	94	8	62
2	$Ir(ppy)_3$	2	20	MeCN	100	8	74
3	$Ir(ppy)_3$	2	10	MeCN	100	4	76
4	**$Ir(ppy)_3$**	**2**	**5**	**MeCN**	**100**	**9**	**76 (74)[b]**
5	$Ir(ppy)_3$	4	5	MeCN	100	6	77
6	$Ir(ppy)_3$	2	5	DCM	97	19	54
7	$Ir(ppy)_3$	2	5	DMF	100	15	53
8	without PC / Sens.	-/-	5	MeCN	13	11	0
9	$Ir(ppy)_3$[c]	2	20	MeCN	0	0	0
10	$Ir(ppy)_3$[d]	2	20	MeCN	100	3	51
11	$Ir(ppy)_3$[e]	2	20	MeCN	0	0	0

Reactions were performed on a 0.10 mmol scale of **262** at 30 °C and the septum was pierced with a cannula for 3 h, then the cannula was removed. [a] Determined by ^{1}H-NMR-analysis using CH_2Br_2 as the internal standard. [b] Isolated yield. [c] Without irradiation. [d] Completely under oxygen atmosphere. [e] Completely under argon atmosphere

As depicted in **Scheme 78**, a series of azetidine derivatives **265a-265t** were synthesised under the optimized reaction conditions with excellent yields ranging from 59-74%. Various racemic azetidine products **265a-265h** could be readily prepared as single regio- and diastereoisomers (*d.r.* > 19:1) starting from dihydroquinoxaline **262** in combination with different *para*- and *meta*-substituted styrenes **264a-264h** as a reaction partner. Moreover, 1,3-dichloro-2-vinylbenzene derivative **265i** could be obtained in a good yield (69%) despite its notable steric hindrance. *α*-Methyl styrenes **264j-264l** were also employed as reaction partners to access azetidine derivatives **265j-265l** with yields of 60-71%. On the other hand, utilization of *β*-methyl styrene **264m** led to cycloadduct **265m** in 52% yield (*d.r.* > 19:1). In addition, acrylic nitriles were used to access further azetidine derivates. Using methacrylonitrile, a single diastereomer **265n** was generated with a yield of 78%, whereas, a 1:1 mixture of diastereomers **265o** was obtained when acrylonitrile (**264o)** was used.

The amino acid-derived heterocyclic substrates **262b-262f** were synthesized by a coupling reaction between ortho-bromoaniline (**254**) and α-amino acids such as phenylalanine, valine and leucine using copper (I) as catalyst according to the reported protocols.[140] Further the synthesised amino acid-derived quinoxalinones were employed in dehydrogenative [2+2] cycloaddition reaction.

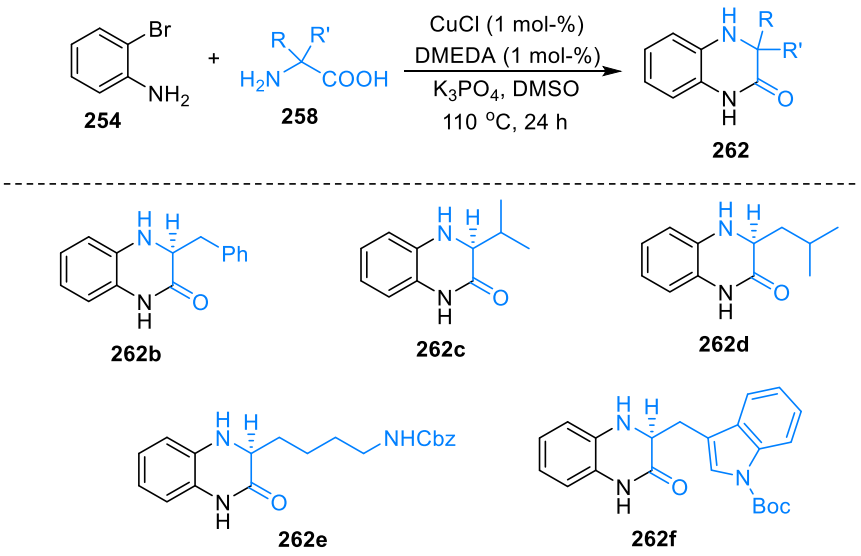

Scheme 77: Synthesis of amino acid-derived quinoxalinones.[140]

Scheme 78c shows that various cycloadducts **265p-265t** were successfully synthesised using different amino acid-derived dihydroquinoxalinones **262b-262f** along with styrene (**264a**)

under the optimized reaction conditions. In all cases (**265p, 265q, 265s and 265t**), except leucine-derived dihydroquinoxalinone compound (**265r**), a single regio- and diastereoisomers was observed. In the case of compound **265r**, a 2:1 mixture of diastereomers was observed. Several additional alkenes as reaction partners for one-pot dehydrogenative cycloaddition reactions were evaluated, however, none of them were found to be suitable (**Scheme 78d**).

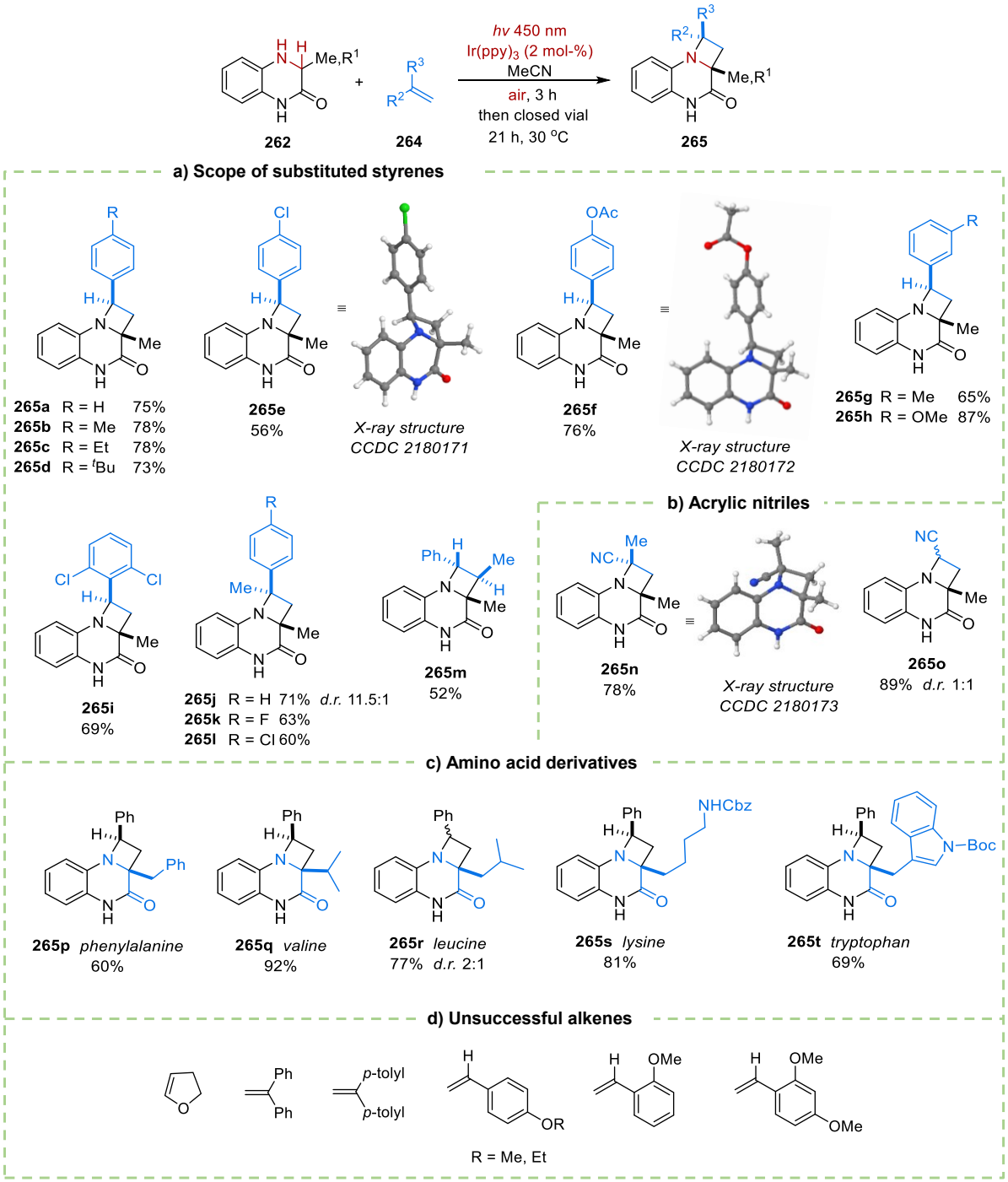

Scheme 78: Scope of the visible light-mediated dehydrogenative aza [2+2] cycloaddition of dihydroquinoxalinones with different alkenes.

With regard to the study of the reaction mechanism, several experiments for reactive oxygen species (ROS) detection, reaction quenching and radical trapping were performed for each individual step as well as for one-pot dehydrogenative cycloaddition reaction. To determine whether singlet oxygen was generated during dehydrogenation of **262** → **263,** 2 equivalents of 2-methyl-2-butene (**266**) were used as an additive along with **262** under the standard reaction conditions (**Scheme 79**). After 3 h of reaction time, quinoxalinone **263** was formed in a 73% yield. Notably, the absence of Schenck-Ene products **268** and **269** indicated that singlet oxygen ($^1O_2$) was not present.

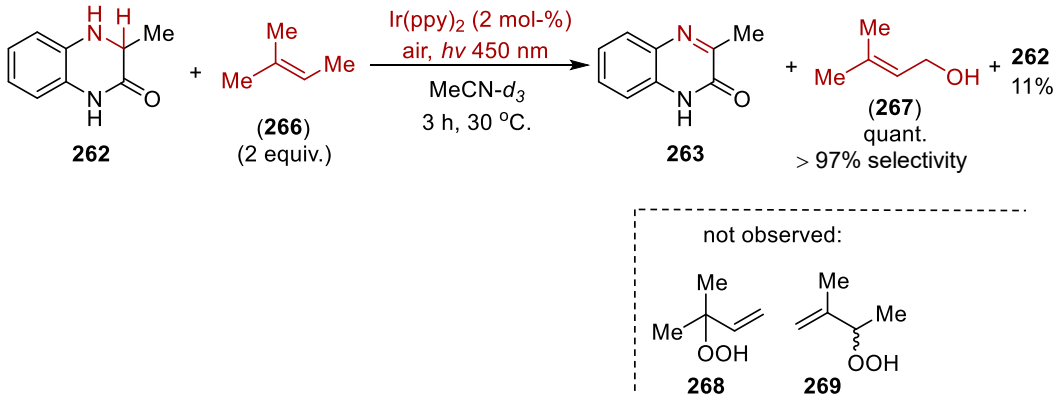

Scheme 79: Control experiment for the detection of $^1O_2$ in the reaction **262** to **263.**

Instead, the observed transformation of 2-methyl-2-butene (**266**) into prenol (**267**) evidently showed the presence of radical species, which resulted from the initial generation of superoxide radical anion $O_2^{\bullet-}$ by the photocatalyst. To support the aforementioned observations, the dehydrogenation reaction of **262** → **263** was performed along with the $^1O_2$-quencher DABCO[142] and almost no effect on the conversion of substrate **262** was detected (**Table 8**). Therefore, a nitro-blue tetrazolium (NBT) assay[143] was performed on the $Ir(ppy)_3$-catalyzed oxidation **262** → **263** in order to probe for the presence of superoxide. Using UV-Vis monitoring, we determined a rapid conversion of NBT into its monoformazan with an absorption band at 520 nm (**Figure 4**).[143b]

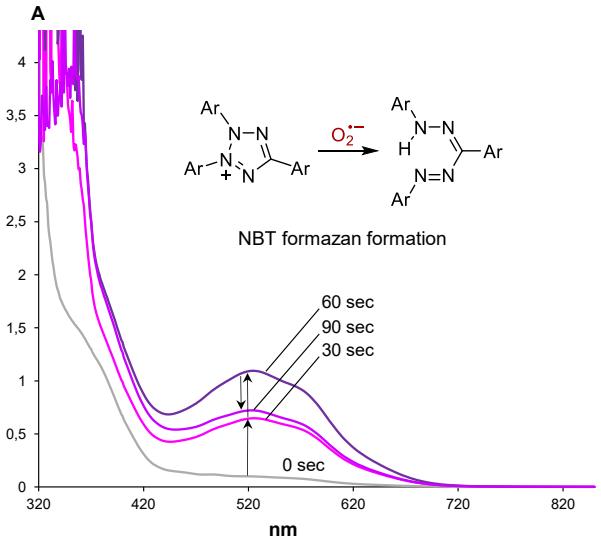

Figure 4: UV-Vis spectra of irradiated reaction solution of **262** (1.67 µmol), with $Ir(ppy)_3$ (0.03 µmol) and nitro-blue tetrazolium chloride (NBT) (0.31 µmol) in DMF (3.00 mL).

Subsequently, diverse ROS and radical scavenging agents were employed to observe the influence on each individual step and one-pot reaction. As by the results represented in **Table 8,** superoxide scavengers Tiron·H_2O (sodium 4,5-dihydroxybenzene-1,3-disulfonate)[144] and butylated hydroxytoluene (BHT)[145] strongly inhibited the dehydrogenation **262** → **263**, and led to a marked reduction in the conversion of **262**. Followed by above observations, free-radical quenchers Trolox (6-hydroxy-2,5,7,8-tetramethylchroman-2-carboxylic acid)[146] and TEMPO[147] also showed moderate inhibition of the reaction **262** → **263**. However, none of these radical quenching agents showed any effect on the sensitized [2+2]-photocycloaddition **263** + **264a** → **265a**. In contrast to reaction **263** + **264a** → **265a**, the one-pot dehydrogenative reaction **262** + **264a** → **265a** was significantly inhibited by Trolox, TEMPO and gave **263** and **265a** in relative ratios of 42:58 and 57:43 respectively. Moderate inhibition of the reaction **262** + **264a** → **265a** was observed with Tiron·H_2O and BHT, while the presence of DABCO showed a very marginal impact.

Table 8: Influence of ROS quenching and scavenging agents on the $Ir(ppy)_3$-catalyzed reactions **262** → **26**, **263** + **264a** → **265a** and **262** + **264a** → **265a**.

	Additive (2 equiv.)				
Ir(ppy)3-catalyzed reaction	**DABCO**	**Tiron·H_2O**	**BHT**	**Trolox**	**TEMPO**
262 → **263** standard cond., 24 h	ratio **262: 263** 11: 89	ratio **262: 263** 25: 75	ratio **262: 263** 60: 40	ratio **262: 263** 25: 75	ratio **262: 263** 13: 87
263+ **264** → **265** standard cond., 24 h	ratio **263: 265** 9: 91	ratio **263: 265** 1: 99	ratio **263: 265** 2: 98	ratio **263: 265** 3: 97	ratio **263: 265** 1: 99

262 + **264** → **265** standard cond., 24 h	ratio **262: 263 : 265** 0: 7: 93	ratio **262: 263 : 265** 40: 12: 48	ratio **262: 263 : 265** 40: 16: 44	ratio **262: 263 : 265** 0: 42: 58	ratio **262: 263 : 265** 0: 57: 43
	ratio **263 : 265** 7: 93	ratio **263 : 265** 20: 80	ratio **263: 265** 27: 73	ratio **263: 265** 42: 58	ratio **263: 265** 57: 43

All reactions were performed on 0.10 mmol scale under standard conditions in MeCN-d_3, followed by ^{1}H-NMR analysis.

In addition to the radical quenching experiments, the cyclic voltammogram of dihydroquinoxalinone **262** was recorded to obtain the redox potentials of the dihydroquinoxalinone substrate. The potentials were determined in MeCN using 0.1 M Bu_4NPF_6 as an electrolyte on a glassy carbon working electrode against an ANE_2 (Ag+/Ag) reference electrode, and a Pt counter electrode with ferrocene as a standard at a scan rate of 100 mV s^{-1}. The measured reduction potentials were calibrated relative to the saturated calomel electrode (SCE) for a direct comparison.

Redox potential conversion:[148]

$$E_{ox} = +0.460 \text{ V vs. Fc+/Fc} \rightarrow E_{ox} = (0.460 + 0.380) \text{ V} = +0.840 \text{ V vs. SCE.}$$

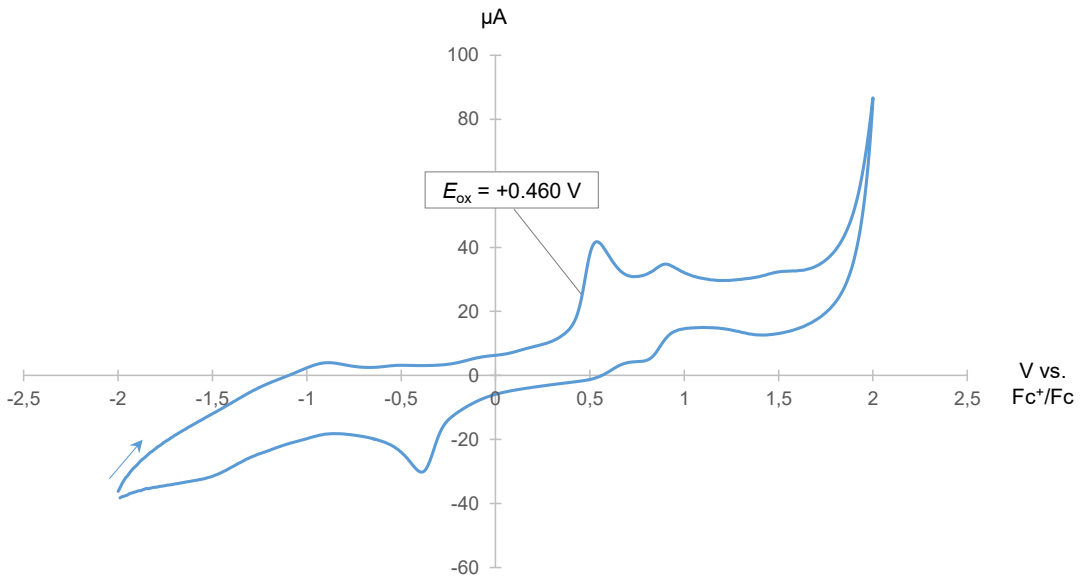

Figure 5: Cyclic voltammogram of dihydroquinoxalinone **262**.

In addition, a time/conversion profile was recorded with the use NMR spectroscopic analysis to verify whether **263** is an intermediate in the dehydrogenative reaction **262** + **264a** → **265a** (**Figure 6**). It was observed that complete consumption of dihydroquinoxalinone **262** achieved within 120 min, and parallel formation of quinoxalinone **263** and cycloadduct **265a** was also observed. Besides this, an increased formation of product **265a** was observed from **263** and **264a** after **262** is fully converted. These observations indicated that two pathways contributed

to the formation of **265a**, where the first pathway proceeds through a consecutive reaction via intermediate **263** and the second pathway led to the direct conversion of substrate **262** into azetidine **265a**.

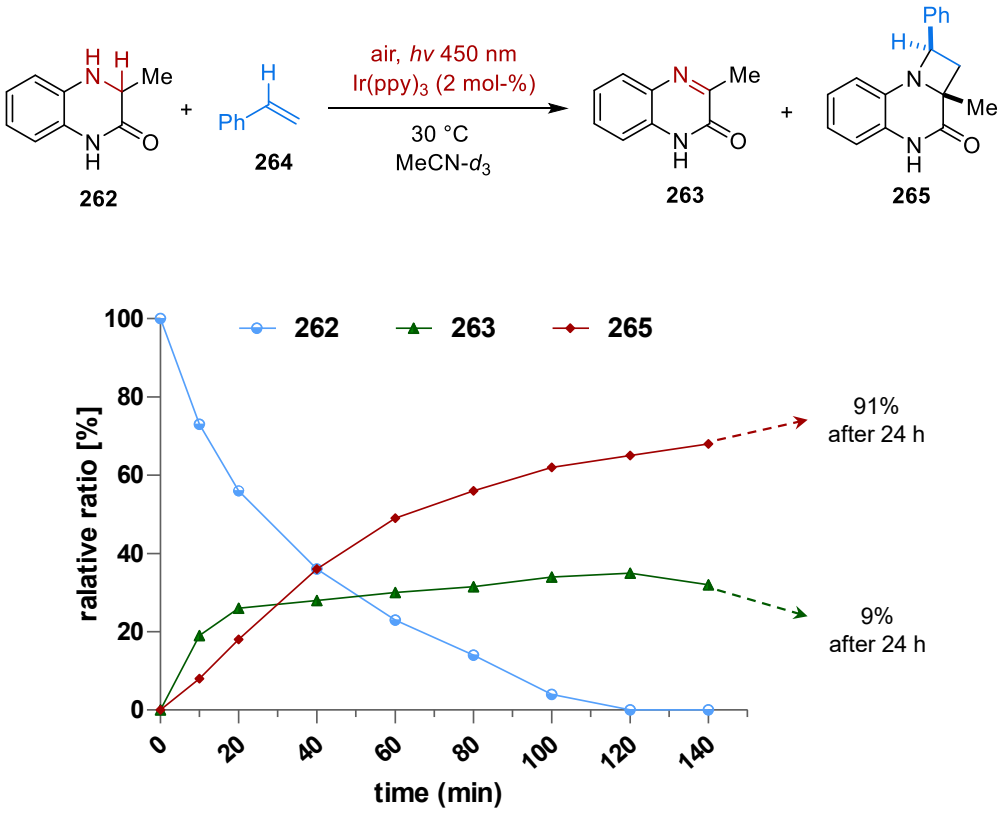

Figure 6. Time/conversion profile for the Ir(ppy)$_3$ catalyzed reaction **262** + **264** → **265**

Consistent with the above observations, a proposed mechanism for Ir(ppy)$_3$-catalyzed photocatalytic dehydrogenative [2+2]-cycloaddition between dihydroquinoxalinones **262** and styrene (**264a**) was proposed that is shown in **Scheme 80**. The reaction proceeds via an initial excitation of Ir(ppy)$_3$ to its triplet state under blue (450 nm) light irradiation with the excited state reduction potential E^*_{red} of +0.31 V vs. SCE,[149] while, experimentally determined oxidation potential E_{ox} of dihydroquinoxalinone **262** was +0.84 V vs. SCE, which rules out one-electron oxidation of compounds **262** by Ir(ppy)$_3$*. Instead, the generation of superoxide radical anion $O_2^{\bullet-}$ takes place through the oxidative quench of Ir(ppy)$_3$* (E^*_{ox} = -1.73 V vs. SCE)[149] by O_2 (E_{red} O_2/ $O_2^{\bullet-}$ ≈ -1.00 V vs. SCE).[143a] The resulting superoxide radical anion $O_2^{\bullet-}$ subsequently undergoes a reaction with substrate **262** via hydrogen abstraction, leading to the formation of well-stabilized α-amino radical **270** and HOO^-.The formed radical intermediate **270** will lead to azetidine **265** via two product-forming pathways as long as continues to be generated of **263** from dihydro compound **262**.

Pathway I involves single electron transfer (SET) oxidation of radical **270** by the Ir (IV) species (E_{red} = +0.77 V vs. SCE)[149] leading to the corresponding iminium ion. Subsequent deprotonation of the iminium ion gives quinoxalinone **263** and H_2O_2. Once quinoxalinone **263** is generated, it undergoes sensitized [2+2]-cycloaddition with styrene (**264a**) by ring closure via triplet biradical intermediate. Only in the final stage of reaction, by-product 1,3-diarylcyclobutanes **273** were observed. This observation proves that the photocycloadditions between quinoxalinones **263** and styrenes (**264a**) proceed via selective sensitization of the heterocycles **263**. On the other hand, in pathway II, radical **270** will undergo radical addition with styrene (**264a**) to give adduct **271**, followed by SET oxidation by Ir (IV) which leads to the benzylic cation **272**, which further undergoes a cationic cyclization to give azetidine **265**.

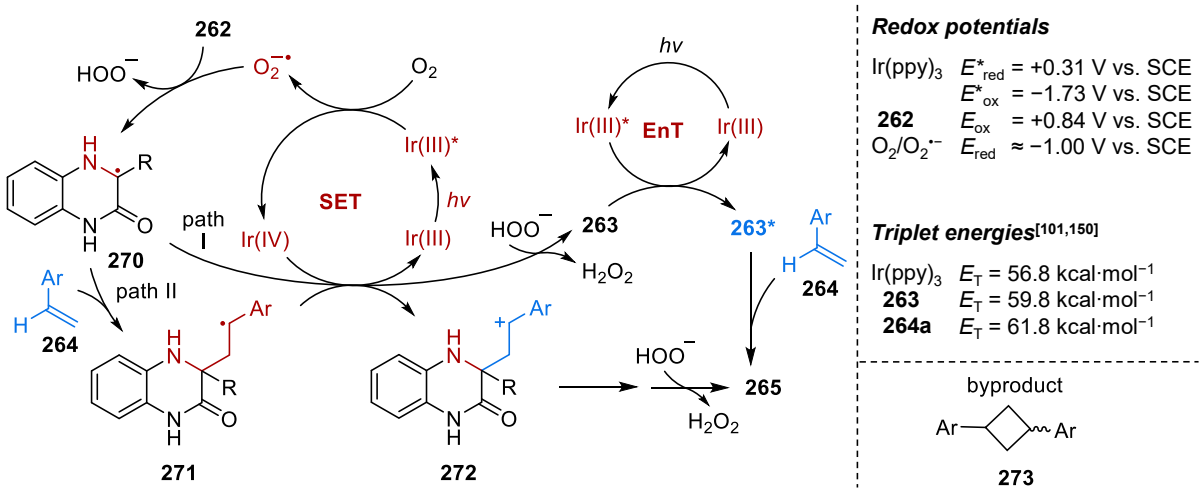

Scheme 80: Proposed reaction mechanism of visible light-mediated $Ir(ppy)_3$ catalyzed dehydrogenative aza- Paternò-Büchi reaction of quinoxalinone **262** with styrene (**264a**).

In conclusion, $Ir(ppy)_3$-catalyzed one-pot dehydrogenative aza [2+2] cycloadditions between amines and alkenes were developed, to furnish the corresponding azetidines with high yield and stereoselectivity. Additionally, amino acid-derived azetidines are also readily accessible with high yields using diverse amino acid derived dihydroquinoxalinones.

4. References

[1] a) D. P. Curran, *Synthesis* **1988**, *6*, 417-439; b) D. P. Curran, *Synthesis* **1988**, *7*, 489-513; c) H. Togo, *Advanced Free Radical Reactions for Organic Synthesis*, *Elsevier*, 2003; d) P. Renaud, M. P. Sibi, ed. *Radicals in Organic Synthesis*, 1st ed. Wiley-VCH, Weinheim, 2001; e) M. Yan, J. C. Lo, J. T. Edwards, P. S. Baran, *J. Am. Chem. Soc*. **2016**, *138*, 12692-12714; f) R. W. Hoffmann, *Chem. Soc. Rev.* **2016**, *45*, 577-583.

[2] a) B. Giese, *Angew. Chem. Int. Ed*. **1983,** *22*, 753-764; b) S. P. Pitre, N. A. Weires, L. E. Overman, *J. Am. Chem. Soc.* **2019**, *141*, 2800-2813; c) L. Liu, R. M. Ward, J. M. Schomaker, *Chem. Rev.* **2019**, *119*, 12422-12490.

[3] a) A. G. Davies, *Organotin Chemistry*, John Wiley & Sons, **2006**; b) H. G. Kuivila, *Acc. Chem. Res.* **1968**, *1*, 299-305; c) H. Jasch, M. R. Heinrich, In *Encyclopedia of Radicals in Chemistry, Biology and Materials*, ed. C. Chatgilialoglu, A. Studer, John Wiley & Sons, Ltd. New York, **2012**, *2*, 529-560.

[4] a) M. Lehnig, W. P. Neumann, P. Seifert, *J. Organomet. Chem.* **1978**, *162*, 145-159; b) D. P. Curran, D. Kim, *Tetrahedron Lett.* **1986**, *27*, 5821-5824.

[5] P. A. Baguley, J. C. Walton, *Angew. Chem. Int. Ed.* **1998**, *37*, 3072-3082.

[6] a) V. Darmency, P. Renaud, *Top. Curr. Chem*. **2006**, *263*, 71-106; b) C. Ollivier, P. Renaud. *Chem. Rev.* **2001**, *101*, 3415-3434; c) T. Perchyonok, *Streamlining free radical green chemistry*. Royal Society of Chemistry, **2012** d) C. Chatgilialoglu, *Organosilanes in radical chemistry*. John Wiley & Sons, **2004**; e) C. Chatgilialoglu, C. Ferreri, Y. Landais, V. I. Timokhin. *Chem. Rev.* **2018**, *118*, 6516-6572.

[7] R. Uematsu, C. Saka, Y. Sumiya, T. Ichino, T. Taketsugu, S. Maeda, *Chem. Commun*. **2017**, *53*, 7302-7305.

[8] K. Miura, Y. Ichinose, K. Nozaki, K. Fugami, K. Oshima, K. Utimoto, *Bull. Chem. Soc. Jpn,* **1989***, 62*, 143-147.

[9] B. Giese, S. Lachhein, *Angew. Chem. Int. Ed.* **1981**, *20*, 967.

[10] a) M. S. Kharasch, H. Engelmann, F. R. Mayo, *J. Org. Chem.* **1937**, *2*, 288; b) M. S. Kharasch, E. V. Jensen, W. H. Urry, *Science* **1945**, *102*, 128; c) M. S. Kharasch, E. V. Jensen, W. H. Urry, *J. Am. Chem. Soc.* **1945**, *67*, 1626.

[11] T. Pintauer, K. Matyjaszewski, *Chem. Soc. Rev*. **2008**, *37*, 1087-1097.

[12] K. Severin, *Curr. Org. Synth.* **2006**, *10*, 217-224.

[13] D. P. Curran, D. Kim, C. Ziegler. *Tetrahedron,* **1991***,* 47, 6189-6196.

[14] D. P. Curran, C. T. Chang, *Tetrahedron Lett.* **1987**, *28*, 2477.

[15] H. Yorimitsu, H. Shinokubo, S. Matsubara, K. Oshima, K. Omoto, H. Fujimoto, *J. Org. Chem.* **2001***, 66*, 7776-7785.

[16] H. Yorimitsu, T. Nakamura, H. Shinokubo, K. Oshima, K. Omoto, H. Fujimoto. *J. Am. Chem. Soc.* **2000**, *122*, 11041-11047.

[17] T. Nakamura, H. Yorimitsu, H. Shinokubo, K. Oshima, *Synlett*. **1998,** *12*, 1351-1352.

[18] C. L. Mero, N. A. Porter, *J. Am. Chem. Soc.* **1999**, *121*, 5155-5160.

[19] a) M. Asscher, D. Vofsi, *J. Chem. Soc.* **1963**, 1887; b) M. Asscher, D. Vofsi, *J. Chem. Soc.* **1963**, 3921.

[20] a) Z.Y. Yang, D. J. Burton, *J. Org. Chem.* **1991**, *56*, 5125; b) J. O. Metzger, R. Mahler, *Angew. Chem. Int. Ed.* **1995**, *34*, 902; c) J. M. Munoz-Molina, A. Caballero, M. M. Diaz-Requejo, S. Trofimenko, T. R. Belderrain, P. J. Perez, *Inorg. Chem.* **2007**, *46*, 7725; d) A. J. Clark, *Eur. J. Org. Chem*. **2016**, 2231-2243

[21] a) L. Forti, F. Ghelfi, E. Libertini, U. M. Pagnoni, E. Soragni, *Tetrahedron,* **1997**, *53*, 17761; b) Z. Liu, J. Wang, Y. Zhao, B. Zhuo, *Adv. Synth. Catal.* **2009**, *351*, 371.

[22] H. Matsumoto, T. Nakano, Y. Nagai, *Tetrahedron Lett.* **1973**, *14*, 5147; b) L. Delaude, A. Demonceau, A. F. Noels, *Top. Organomet. Chem.* **2004**, *11*, 155.

[23] a) C. Stephenson, T. Yoon, D. W. C. MacMillan, *Visible light photocatalysis in organic chemistry*, Wiley-VCH Verlag GmbH & Co. Weinheim, Germany, **2018**; b) L. Marzo, S. K. Pagire, O. Reiser, B. König, *Angew. Chem. Int. Ed.* **2018,** *57*, 10034-10072; c) S. Crespi, M. Fagnoni. *Chem. Rev*. **2020**, *120*, 9790-9833; d) J. Xuan, W.-J. Xiao, *Angew. Chem.Int. Ed.* **2012**, *51*, 6828-6838.

[24] B. König, *Chemical Photocatalysis*, De Gruyter, Berlin, **2013**.

[25] N. A. Romero, D. A. Nicewicz, *Chem. Rev.* **2016**, *116*, 10075-10166.

[26] L. Capaldo, D. Ravelli, *Eur. J. Org. Chem.* **2017**, *15*, 2056-2071.

[27] J. W. Verhoeven, *Pure Appl. Chem.* **1996**, *68*, 2223-2286.

[28] F. Strieth-Kalthoff, M. J. James, M. Teders, L. Pitzer, F. Glorius, *Chem. Soc. Rev.* **2018**, *47*, 7190-7202.

[29] J. Großkopf, T. Kratz, T. Rigotti, T. Bach, *Chem. Rev.* **2022**, *122*, 1626-1653.

[30] Q.-Q. Zhou, Y.-Q. Zou, L.-Q. Lu, W.-J. Xiao, *Angew. Chem. Int. Ed.* **2019**, *58*, 1586-1604.

[31] D. L. Dexter, *J. Chem. Phys.* **1953**, *21*, 836.

[32] K. Singh, S. J. Staig, J. D. Weaver, *J. Am. Chem. Soc.* **2014**, *136*, 5275-5278.

[33] J. B. Metternich, R. Gilmour, *J. Am. Chem. Soc.* **2015**, *137*, 11254-11257.

[34] a) A. Córdova, H. Sundén, M. Engqvist, I. Ibrahem, J. Casas, *J. Am. Chem. Soc.* **2004**, *126*, 8914-8915; b) H. Sundén, M. Engqvist, J. Casas, I. Ibrahem, A. Córdova, *Angew. Chem. Int. Ed.* **2004**, *43*, 6532 -6535; c) D. J. Walaszek, K. Rybicka-Jasińska, S. Smoleń, M. Karczewski, D. Gryko, *Adv. Synth. Catal.* **2015**, *357*, 2061 – 2070.

[35] E. Brachet, T. Ghosh, I. Ghosh, B. König, *Chem. Sci.* **2015**, *6*, 987-992.

[36] E. P. Farney, T. P. Yoon, *Angew. Chem. Int. Ed.* **2014**, *53*, 793-797.

[37] M. Teders, C. Henkel, L. Anhäuser, F. Strieth-Kalthoff, A. Gómez-Suárez, R. Kleinmans, A. Kahnt, A. Rentmeister, D. Guldi, F. Glorius, *Nat. Chem.* **2018**, *10*, 981-988.

[38] H. E. Zimmerman, D. Armesto, *Chem. Rev.* **1996**, *96*, 3065-3112.

[39] a) N. Hoshi, Y. Furukawa, H. Hagiwara, H. Uda, K. Sato, *Chem. Lett.* **1980**, *9*, 47-50; b) M. M. Maturi, A. Pöthig, T. Bach, T. *Aust. J. Chem.* **2015**, *68*, 1682-1692.

[40] Y. Shen, M.-L. Shen, P.-S. Wang, *ACS Catal.* **2020**, *10*, 8247-8253.

[41] E. Arceo, E. Montroni, P. Melchiorre, *Angew. Chem. Int. Ed*. **2014**, *53*, 12064-12068.

[42] Q. Liu, F.-P. Zhu, X.-L. Jin, X.-J. Wang, H. Chen, L. -Z. Wu, *Chem. Eur. J.* **2015**, *21*, 10326-10329.

[43] K. L. Skubi, J. B. Kidd, H. Jung, I. A. Guzei, M.-H. Baik, T. P. Yoon, *J. Am. Chem. Soc*. **2017**, *139*, 17186-17192.

[44] J. Ma, F. Strieth-Kalthoff, T. Dalton, M. Freitag, J. L. Schwarz, K. Bergander, C. Daniliuc, F. Glorius, *Chem*, **2019**, *5*, 2854-2864.

[45] a) C. K. Prier, D. A. Rankic, D. W. C. MacMillan, *Chem. Rev.* **2013**, *113*, 5322-5363; b) J. M. R. Narayanam, C. R. J. Stephenson, *Chem. Soc. Rev.* **2011**, *40*, 102-113.

[46] T. Koike, M. Akita, *Inorg. Chem. Front.* **2014**, *1*, 562-576; b) K. Teegardin, J. I. Day, J. Chan, J. Weaver, *Org. Process Res. Dev.* **2016**, *20*, 1156-1163.

[47] E. H. Discekici, N. J. Treat, S. O. Poelma, K. M. Mattson, Z. M. Hudson, Y. Luo, C. J. Hawker, J. Read de Alaniz, *Chem. Commun.* **2015***, 51,* 11705-11708.

[48] F. Speck, D. Rombach, H.-A. Wagenknecht, *Beilstein J. Org. Chem.* **2019**, *15*, 52-59.

[49] D. A. Nicewicz, T. M. Nguyen, *ACS Catal.* **2014**, *4*, 355-360.

[50] M. A. Ischay, M. E. Anzovino, J. Du, T. P. Yoon, *J. Am. Chem. Soc.* **2008**, *130*, 12886-12887.

[51] J. Du, T. P. Yoon, *J. Am. Chem. Soc*. **2009**,*131*, 14604.

[52] S. Lin, M. A. Ischay, C. G. Fry, T. P. Yoon, *J. Am. Chem. Soc.* **2011**, *133*, 19350.

[53] J. Xuan, X.-D. Xia, T.-T. Zeng, Z.-J. Feng, J.-R. Chen, L.-Q. Lu, W.-J. Xiao, *Angew. Chem. Int. Ed.* **2014**, *53*, 5653-5656.

[54] T. Courant, G. Masson, *J. Org. Chem.* **2016**, *81*, 6945-6952.

[55] D. Bag, H. Kour and S. D. Sawant, *Org. Biomol. Chem.* **2020**, *18*, 8278-8293.

[56] O. Reiser, *Acc. Chem. Res.* **2016**, *49*, 1990-1996.

[57] D. H. Barton, M. A. Csiba J. C. Jaszberenyi, *Tetrahedron Lett.* **1994**, *35*, 2869.

[58] a) J. D. Nguyen, J. W. Tucker, M. D. Konieczynska, C. R. Stephenson, *J. Am. Chem. Soc.* **2011**, *133*, 4160; b) C. Wallentin, J. D. Nguyen, P. Finkbeiner, C. J. Stephenson, *J. Am. Chem. Soc*. **2012**, *134*, 8875-8884.

[59] M. Pirtsch, S. Paria, T. Matsuno, H. Isobe, O. Reiser, *Chem. Eur. J.* **2012**, *18*, 7336.

[60] S. Kobayashi, K. A. Jørgensen, Ed. *Cycloaddition Reactions in Organic Synthesis*, Wiley-VCH, Weinheim, **2001**; b) N. Nishikawa, Ed. *Methods and Applications of Cycloaddition Reactions in Organic Syntheses*, John Wiley & Sons, Hoboken, **2013**.

[61] J. Iriondo-Alberdi, M. F. Greaney. *Eur. J. Org. Chem.* **2007**, *29,* 4801-4815.

[62] M. Sicignano, R. I. Rodríguez, J. Alemán, *Eur. J. Org. Chem.* **2021**, 3303-3321.

[63] M. Zhu, X. Zhang, C. Zheng, S.-L. You, *Acc. Chem. Res.* **2022**, *55*, 2510-2525.

[64] N. Hoffmann, *Chem. Rev.* **2008**, *108*, 1052-1103.

[65] F. Mueller, J. Mattay, *Chem. Rev.* **1993**, *93*, 99-117.

[66] Z. Zhang, Y.-J. Zhou, X.-W. Liang, *Org. Biomol. Chem.* **2020***, 18*, 5558-5566.

[67] S. Poplata, A. Tröster, Y.-Q. Zou, T. Bach, *Chem. Rev.* **2016**, *116*, 9748-9815.

[68] D. Sarkar, N. Bera, S. Ghosh, *Eur. J. Org. Chem.* **2020**, 1310-1326.

[69] B. Gerard, S. Sangji, D. J. O'Leary, J. A. Porco Jr, *J. Am.Chem. Soc.* **2006**, *128*, 7754-7755.

[70] K. C. Nicolaou, D. L. F. Gray, *J. Am. Chem. Soc.* **2004**, *126*, 607-612.

[71] S. M. Sieburth, J. Chen, K. Ravindran, J.-l. Chen, *J. Am. Chem. Soc.* **1996**, *118*, 10803–10810; b) S. M. Sieburth, T. H. Ai-Tel, D. Rucando, *Tetrahedron Lett.* **1997**, *38*, 8433–8434; c) Y.-g. Lee, K. F. McGee Jr, J. Chen, D. Rucando, S. M. Sieburth, *J. Org. Chem.* **2000**, *65*, 6676–6681.

[72] K. S. Feldman, M. J. Wu, D. P. Rotella, *J. Am. Chem. Soc.* **1989**, *111*, 6457-6458; b) K. S. Feldman, M. J. Wu, D. P.Rotella, *J. Am. Chem. Soc.* **1990**, *112*, 8490-8496.

[73] P. Klán, J. Wirz. *Photochemistry of organic compounds: from concepts to practice*. John Wiley & Sons, **2009**.

[74] a) E. J. Corey, R. B. Mitra, H. Uda, *J. Am. Chem. Soc.* **1963**, *85*, 362-363; b) E. J. Corey, R. B. Mitra, H. Uda, *J. Am. Chem. Soc.* **1964**, *86*, 485-492.

[75] M. C. Pirrung, *J. Am. Chem. Soc.* **1981**, *103*, 82-87.

[76] G. O. Schenck, W. Hartmann, S. P. Mannsfeld, W. Metzner, C. H. Krauch, *Chem. Ber.* **1962**, *95,* 1642-1647.

[77] E.J. Corey, D. E. Cane, L. Libit, *J. Am. Chem. Soc*. **1971**, *93*, 7016-7021.

[78] C. Müller, A. Bauer, T. Bach, Angew. Chem. Int. Ed. **2009**, *48*, 6640-6642.

[79] Z. Lu, T. P. Yoon, *Angew. Chem. Int. Ed.* **2012**, *51*,10329-10332.

[80] J. Zhao, J. L. Brosmer, Q. Tang, Z. Yang, K. N. Houk, P. L. Diaconescu, O. Kwon, *J. Am. Chem. Soc.* **2017**, *139*, 9807-9810.

[81] A. Tröster, R. Alonso, A. Bauer, T. Bach, *J. Am. Chem. Soc.* **2016**, *138*, 7808-7811.

[82] a) M. D'. Auria, R. Racioppi, *Molecules,* **2013**, *18*, 11384-11428; b) M. Abe, *J. Chin. Chem. Soc.* **2008**, *55*, 479-486.

[83] a) S. L. Schreiber, K. Satake, *J. Am. Chem. Soc.* **1983**, *105*, 6723-6724; b) T. Bach, *Synlett*, **2000**, 1699-1707; c) Y. Zhang, J. Xue, Y. Gao, H.-K. Fun, J.-H. Xu, *J. Chem. Soc. Perkin Trans.* **2002***, 1*, 345-353.

[84] a) S. L. Schreiber, K. Satake, *J. Am. Chem. Soc*. **1983**, *105*, 6723; b) S. L. Schreiber, K. Satake, *J. Am. Chem. Soc.* **1984**, *106*, 4186; c) S. L. Schreiber, *Science*, **1985**, *227*, 857.

[85] T. Bach, H. Brummerhop, Angew. Chem. Int. Ed. 1998, 37, 3400-3402.

[86] R. Hambalek, G. Just, *Tetrahedron Lett.* **1990**, *31*, 5445-5448.

[87] D. Zhang, C. Wu, H. Zhou, Y. Ma, Y. Zhu, *Asian J. Org. Chem.* **2022**, *11*, No. e202200561.

[88] K. A. Rykaczewski, C. S. Schindler, *Org. Lett.* **2020**, *22*, 6516-6519.

[89] J. Mateos, A. Vega-Peñaloza, P. Franchesci, F. Rigodanza, P. Andreetta, X. Companyo, G. Pelosi, M. Bonchio, L. Dell'Amico, *Chem. Sci.* **2020**, *11*, 6532-6538.

[90] J. Zheng, X. Dong, T. P. Yoon, *Org. Lett.* **2020**, *22*, 6520-6525.

[91] A. D. Richardson, M. R. Becker, C. S. Schindler, *Chem. Sci.* **2020**, *11*, 7553-7561.

[92] a) A. Brandi, S. Cicchi, F. M. Cordero, *Chem. Rev.* **2008**, *108*, 3988-4035; b) D. Antermite, L. Degennaro, R. Luisi, *Org. Biomol. Chem.* **2017**, *15*, 34-50.

[93] R. Gianatassio, J. M. Lopchuk, J. Wang, C. M. Pan, L. R. Malins, L. Prieto, T. A. Brandt, M. R. Collins, G. M. Gallego, N. W. Sach, J. E. Spangler, H. Zhu, J. Zhu, P. S. Baran, *Science* **2016**, *351*, 241-246.

[94] H. Yoda, M. Takahashi, T. Sengoku, in *Heterocycles in Natural Product Synthesis*, ed. K. C. Majumdar and S. K. Chattopadhyay, Wiley-VCH, Weinheim, 1st ed. 2011; b) M. Kitajima, N. Kogure, K. Yamaguchi, H. Takayama, N. Aimi, *Org. Lett*. **2003**, *5*, 2075-2078.

[95] a) P. V. Fish, A. D. Brown, E. Evrard, L. R. Roberts, *Bioorg. Med. Chem. Lett.* **2009**, *19*, 1871-1875; b) A. Brown, T. B. Brown, A. Calabrese, D. Ellis, N. Puhalo, M. Ralph, L. Watson, *Bioorg. Med. Chem. Lett*. **2010**, *20*, 516-520.

[96] O. Tsuge, M. Tashiro, K. Oe, *Tetrahedron Lett.* **1968**, *9*, 3971-3974.

[97] D. E. Blackmun, S. A. Chamness, C.S. Schindler, *Org. Lett.* **2022***, 24*, 3053-3057.

[98] M.R Becker, E. R. Wearing, C. S. Schindler, *Nat. Chem.* **2020**, *12*, 898-905.

[99] M. R. Becker, A. D. Richardson, C. S. Schindler, *Nat. Commun.* **2019**, *10*, 5095.

[100] E. Kumarasamy, S. K. Kandappa, R. Raghunathan, S. Jockusch, J. Sivaguru, *Angew. Chem. Int. Ed*. **2017**, *56*, 7056-7061.

[101] X. Li, J. Großkopf, C. Jandl, T. Bach, *Angew. Chem. Int. Ed.* **2021**, *60*, 2684-2688.

[102] Z. Xie, J. Jia, X. Liu, L. Liu, *Adv. Synth. Catal.* **2016**, *358*, 919-925.

[103] M. Ni, Y. Zhang, T. Gong, B. Feng, *Adv. Synth. Catal.* **2017**, *359*, 824-831.

[104] C. Qi, H. Cong, K. J. Cahill, P. Müller, R. P. Johnson, J. A. Porco, Jr., *Angew. Chem. Int. Ed.* **2013**, *52*, 8345-8348.

[105] Y. Nakao, E. Morita, H. Idei, T. Hiyama, *J. Am. Chem. Soc.* **2011**, *133*, 3264-3267.

[106] Richter, O .G. Mancheño, *Org.Lett.* **2011**, *13*, 6066-6069.

[107] X. Chen, G. Zhang, R. Zeng, *Org. Lett.* **2021**, *23*, 7144-7149.

[108] C. Huo, H. Xie, F. Chen, J. Tang, Y. Wang, *Adv. Synth. Catal.* **2016**, *358*, 724-730.

[109] E. Schendera, L.-N. Unkel, P. P. H. Quyen, G. Salkewitz, F. Hoffmann, A. Villinger, M. Brasholz, *Chem. Eur. J.* **2020**, *26*, 269-274.

[110] E. Schendera, A. Villinger, M. Brasholz, *Org. Biomol. Chem.* **2020**, *18*, 6912-6915.

[111] H.-J. Wang, L. Guo, C.-F. Zhu, Y.-F. Luo, Y.-G. Li, X. Wu, *Eur. J. Org. Chem.* **2018**, 5456-5459.

[112] S. Hore, A. Singh, S. De, N. Singh, V. Gandon, R. P. Singh, *ACS Catal.* **2022**, *10*, 6227-6237.

[113] J. C. Serrano-Ruiz, R. M. West and J. A. Dumesic, *Annu. Rev. Chem. Biomol. Eng.* **2010**, *1*, 7-100.

[114] A. Corma, S. Iborra, A. Velty, *Chem. Rev.* **2007**, *107*, 24112502.

[115] J. A. Melero, J. Iglesias, A. Garcia, A. *Energy Environ. Sci.* **2012**, *5*, 7393-7420.

[116] V. G. Yadav, G. D. Yadav, S. C. Patankar, *Clean Technol. Environ. Policy,* **2020***, 22*,1757-1774.

[117] G. W. Huber, S. Iborra, A. Corma, *Chem. Rev.* **2006**, *106*, 4044-4098.

[118] a) S. Wang, A. Cheng, F. Liu, J. Zhang, T. Xia, X. Zeng, W. Fan, Y. Zhang, *Ind. Chem. Mater.* **2023**, *1*, 188-206; b) F. H. Isikgora, C. R. Becer, *Polym. Chem*. **2015**, *6*, 4497-4559.

[119] a) R.-J. van Putten, J. C. van der Waal, E. de Jong, C. B. Rasrendra, H. J. Heeres, J. G. de Vries, *Chem. Rev.* **2013**, *113*, 1499-1597; b) C. Thoma, J. Konnerth, W. Sailer-Kronlachner, P. Solt, T. Rosenau, H. W. G. van Herwijnen, *ChemSusChem*, **2020**, *13*, 3544-3564.

[120] a) M. Mascal, *ACS Sustainable Chem. Eng.* **2019***, 7*, 5588-5601; b) M. Mascal, *ChemSusChem*, **2015**, *8*, 3391-3395.

[121] M. Mascal, E. B. Nikitin, *ChemSusChem*, **2009**, *2*, 423-426.

[122] M. Brasholz, K. von Känel, C. H. Hornung, S. Saubern, J. Tsanaktsidis, *Green Chem.* **2011**, *13*, 1114-1117.

[123] a) F. Weigang, V. Charlie, Q. Yves and P. Florence, *Curr. Org. Synth.* **2019**, *16*, 583-614; b) Q.-S. Kong, X.-L. Li, H.-J. Xu, Y. Fu, *Fuel Process. Technol.* **2020**, *209*; c) D. Zhao, T. Su, Y. Wang, R. S. Varma, C. Len, *Mol. Catal*. **2020**, *495*; d) C. Thoma, J. Konnerth, W. Sailer-Kronlachner, T. Rosenau, A. Potthast, P. Solt, H. W. G. van Herwijnen, *ChemSusChem*, **2020**, *13*, 5408-5422; e) J. G. de Vries, *Adv. Heterocycl. Chem.* **2017**, *121*, 247-293; f) M. Mascal, S. Dutta, *Top. Curr. Chem*. **2014**, *353*, 41-83.

[124] E. D. Glendening, J. K. Badenhoop, A. E. Reed. *NBO 6.0,* Theoretical Chemistry Institute, University of Wisconsin, Madison, WI, 2013.

[125] a) A. J. H. Wachters, *J. Chem. Phys.* **1970**, *52*, 1033-1036; b) K. Raghavachari, G. W. Trucks, *J. Chem. Phys.* **1989**, *91*, 1062-1065; c) A. D. McLean, G. S. Chandler, *J. Chem. Phys.* **1980**, *72*, 5639-5648; d) M. P. McGrath, L. Radom, *J. Chem. Phys.* **1991**, *94*, 511-516; e) R. Krishnan, J. S. Binkley, R. Seeger, J. A. Pople, *Chem. Phys.* **1980**, *72*, 650-654; f) P. J. Hay, *J. Chem. Phys.* **1977**, *66*, 4377-4384; g) M. J. Frisch, J. A. Pople, J. S. Binkley, *J. Chem. Phys.* **1984**, *80*, 3265-3269; h) L. A. Curtiss, M. P. McGrath, J.-P Blaudeau, N. E . Davis, R. C. Binning, L. Radom, *J. Chem. Phys.* **1995**, *103*, 6104-6113; i) T. Clark, J. Chandrasekhar, G. W. Spitznagel, P. V. R. Schleyer, *J. Comput. Chem.* **1983**, *4*, 294-301; j) J.-P. Blaudeau, M. P. McGrath, L. A. Curtiss, L. Radom, *J. Chem. Phys.* **1997**, *107*, 5016-5021; k) R. C. Binning, L. A. Curtiss, *J. Comput. Chem.* **1990**, *11*, 1206-1216; l) S. Sæbø, Almlöf, *J. Chem. Phys. Lett.* **1989**, *154*, 83-89; m) M. Head-Gordon, J. A. Pople, M. Frisch, *J. Chem. Phys. Lett.* **1988**, *153*, 503-506; n) M. Head-Gordon, T. Head-Gordon, *Chem. Phys. Lett.* **1994**, *220*, 122-128; o) M. J. Frisch, M. Head-Gordon, J. A. Pople, *Chem. Phys. Lett*. **1990**, *166*, 281-289; p) M. J. Frisch, M. Head-Gordon, J. A. Pople, *Chem. Phys. Lett.* **1990**, *166*, 275-280.

[126] L. Gronbach, M. Brascholz, *Unpublished work.*

[127] D. P. Curran, T. R. McFadden, *J. Am. Chem. Soc*. **2016**, *138*, 7741-7752.

[128] a) H. Fischer, L. Radom, *Angew. Chem. Int. Ed.* **2001**, *40*, 1340-1371; b) K. Héberger, M. Walbiner, H. Fischer, *Angew. Chem. Int. Ed.* **1992**, *31*, 635-636.

[129] a) Y. Li, Y. Gan, C. Cao, *J. Comput. Chem*. **2019**, *40*, 1057-1065; b) C. Togbé, L.-S. Tran, D. Liu, D. Felsmann, P. Oßwald, P.-A. Glaude, B. Sirjean, R. Fournet, F. BattinLeclerc, K. Kohse-Höinghaus, *Combust. Flame,* **2014**, *161*, 780-797; c) L. D. Kispert, R. C. Quijano, C. U. Pittman, Jr., *J. Org. Chem*. **1971**, *36*, 3837-3838.

[130] Y. Zhao, D. G. Truhlar, *Theor. Chem. Account.* **2008**, *120*, 215-241.

[131] a) D. I. Schuster, G. Lem, N. A. Kaprinidis, *Chem. Rev.* **1993**, *93*, 3-22; b) M. T. Crimmins, *Chem. Rev.* **1988**, *88*, 1453-1473.

[132] a) A. Shiozuka, K. Sekine, Y. Kuninobu, *Synthesis*, **2022**, *54*, 2330-2339; b) N. F. Nikitas, P. L. Gkizis, C. G. Kokotos, *Org. Biomol. Chem.* **2021**, *19*, 5237-5253; c) J. Lu, B.

Pattengale, Q. Liu, S. Yang, W. Shi, S. Li, J. Hang, J. Zhang, *J. Am. Chem. Soc.* **2018**, *140*, 13719-13725; d) V. Mojr, E. Svobodá, K. Straková, T. Neveselý, J. Chudoba, H. Dvořáková, R. Cibulka, *Chem. Commun.* **2015**, *51*, 12036-12039.

[133] a) M. R. Schreier, X. Guo, B. Pfund, Y. Okamoto, T. R. Ward, C. Kerzig, O. S. Wenger, *Acc. Chem. Res.* **2022**, *55*, 1290-1300; b) Y. Wu, D. Kim, T. S. Teets, *Synlett*, **2022**, 1154-1179; c) L. Wang, *Catalysts* **2022***, 12*, 919; d) R. Bevernaegie, S. A. M. Wehlin, B. Elias, L. Troian-Gautier, *ChemPhotoChem* **2021**, *5*, 217-234; e) I. N. Mills, J. A. Porras, S. Bernhard, *Acc. Chem. Res.* **2018**, *51*, 352-364.

[134] I. Saito, K. Shimozono and T. Matsuura, *Tetrahedron Lett.* **1982**, *23*, 5439-5442.

[135] a) I. Saito, K. Shimozono, T. Matsuura, *J. Am. Chem. Soc.* **1980**, *102*, 3948-3950; b) I. Saito, K. Shimozono, T. Matsuura, *J. Org. Chem.* **1982**, *47*, 4356-4358; c) I. Saito, K. Shimozono, T. Matsuura, *J. Am. Chem. Soc.* **1983**, ***105***, 963-970; d) S. Andresen, P. Margaretha, *J. Chin. Chem. Soc.* **1995**, *42*, 991-993; e) S. Andresen, P. Margaretha, *J. Photochem. Photobiol. A, Chem.* **1998**, *112*, 135-138; f) D. Schwebel, J. Ziegenbalg, J. Kopf, P. Margaretha, *Helv. Chim. Acta*, **1999**, *82*, 177-181; g) D. Schwebel, M. Soltau, P. Margaretha, *Synthesis*, **2001**, 1111-1113; h) M. Soltau, M. Göwert, P. Margaretha, *Org. Lett.* **2005**, *23*, 5159-5161.

[136] W. C. Agosta, P. Margaretha, *Acc. Chem. Res.* **1996**, *29*, 179-182.

[137] T. Nishio, *J. Org. Chem.* **1984**, *49*, 827-832.

[138] T. Nishio, Y. Omote, *J. Chem. Soc. Perkin Trans. 1*, **1987**, 2611-2615.

[139] S. Kamila, E. R. Biehl, *Heterocycles,* **2006**, *68*, 1931-1939.

[140] S. Tanimori, H. Kashiwagi, T. Nishimura, M. Kirihata, *Adv. Synth. Catal.* **2010**, *352*, 2531-2537.

[141] M. K. Sahoo, G. Jaiswal, J. Rana, E. Balaraman, *Chem. Eur. J.* **2017**, *23*, 14167-14172.

[142] C. Ouannes, T. Wilson, *J. Am. Chem. Soc.* **1968**, *90*, 6527-6528.

[143] a) M. Hayyan, M. A. Hashim, I. M. AlNashef, *Chem. Rev*. **2016**, *116*, 3029-3085; b) R. Wang, R. Qu, C. Jing, Y. Zhai, Y. An, L. Shi, *RSC Adv*. **2017**, *7*, 10100-10107.

[144] S. O. Liubimovskii, L. Y. Ustynyuk, A. N. Tikhonov, *J. Mol. Liq.* **2021**, *333*, 115810.

[145] W. A. Yehye, N. A. Rahman, A. Ariffin, S. B. A. Hamid, A. A. Alhadi, F. A. Kadir, M. Yaeghoobi, *Eur. J. Med. Chem.* **2015**, *101*, 295-312.

[146] M. E. Alberto, N. Russo, A. Grand, A. Galano, *Phys. Chem. Chem. Phys.* **2013**, *15*, 4642-4650.

[147] a) A. L. J. Beckwith, V. W. Bowry, K. U. Ingold, *J. Am. Chem. Soc.* **1992**, *114*, 4983-4992; b) N. Kocherginky, H. M. Swartz, *Nitroxide Spin Labels, Reactions in Biology and Chemistry*, CRC Press: Boca Raton, **1995**.

[148] V. V. Pavlishchuk, A. W. Addison, *Inorg. Chim. Acta*, **2000**, *298*, 97-102.

[149] L. Flamigni, A. Barbieri, C. Sabatini, B. Ventura, F. Barigelletti, V. Balzani, S. Campagna, *Top. Curr. Chem.* **2007**, *281*, 143-204.

[150] T. Hofbeck, H. Yersin, *Inorg. Chem.* **2010**, *49*, 9290-9299; b) T. Ni, R. A. Caldwell, L. A. Melton, *J. Am. Chem. Soc.* **1989**, *111*, 457-464.

5. Contribution to the publications

In this chapter, sections 5.1 to 5.3 are selected publications for this thesis work. Further publications are available in section 5.4.

5.1. Value-added chemicals from biomass-derived furans: radical functionalisations of 5-chloromethylfurfural (CMF) by metal-free ATRA reactions

Rajesh Dasi, Daniel Schmidhuber, Lisa Marie Gronbach, Julia Rehbein*, Malte Brasholz*
Org. Biomol. Chem. **2021**, *19*, 1626-1631.
DOI: 10.1039/d1ob00013f

In this project, I performed the optimization of the reaction, investigation of the substrate scope, compound isolation, and characterization of all compounds. In addition, I performed all the control experiments and wrote supporting information for the manuscript. My contribution as the first author of this paper is approximately 75%.

Organic & Biomolecular Chemistry

ROYAL SOCIETY OF CHEMISTRY

PAPER

View Article Online
View Journal | View Issue

Cite this: *Org. Biomol. Chem.*, 2021, **19**, 1626

Value-added chemicals from biomass-derived furans: radical functionalisations of 5-chloromethylfurfural (CMF) by metal-free ATRA reactions†

Rajesh Dasi,[a] Daniel Schmidhuber,[b] Lisa Marie Gronbach,[a] Julia Rehbein *[b] and Malte Brasholz *[a]

Received 4th January 2021,
Accepted 28th January 2021

DOI: 10.1039/d1ob00013f

rsc.li/obc

Biomass-derived 5-chloromethylfurfural (CMF), a congener of the well-known carbohydrate-based platform chemical 5-hydroxymethylfurfural (HMF), can efficiently be functionalised by radical transformations of its benzylic chloromethyl group. We report here the first examples of these radical reactions by way of metal-free, triethylborane/oxygen-induced atom transfer radical addition (ATRA) reactions between CMF and styrenes, which proceed with high yield and selectivity. The key intermediate, the 2-formyl-5-furfuryl radical derived from CMF, and its radical addition reactions were studied with regard to its electronic structure, *i.e.* spin density distribution and frontier molecular orbitals based on the NBO ansatz and activation barriers of the addition step using DFT and post-HF methods.

Introduction

Decades ago, 5-hydroxymethylfurfural (HMF, **1**) was identified as an industrially viable renewable platform chemical for the production of fuel additives, polymers, C-6 diacids and diols, and numerous other strategically relevant high-volume chemical products. While HMF is available from the Lewis- or Brønsted-acid-mediated dehydration of several mono- and disaccharides, its efficient retrieval from cellulosic biomass is still challenging today as the attempt often results in low yields and selectivities.[1] By contrast to HMF, its chlorinated and consequently much more lipophilic congener 5-chloromethylfurfural (CMF, **2**) can be obtained in a high yield directly from crude biomass, by its simple treatment with aqueous hydrochloric acid in combination with biphasic extraction techniques (Scheme 1a).[2]

The derivative chemistry of HMF (**1**) and CMF (**2**) can be subdivided into a furanic and a levulinic manifold, and both have successfully been converted on a large scale into important bulk chemicals such as furan-2,5-dicarboxylic acid, 2,5-dimethyl-furan, levulinic acid, adipic acid and others, by conventional stoichiometric or more elaborate catalytic oxidation,

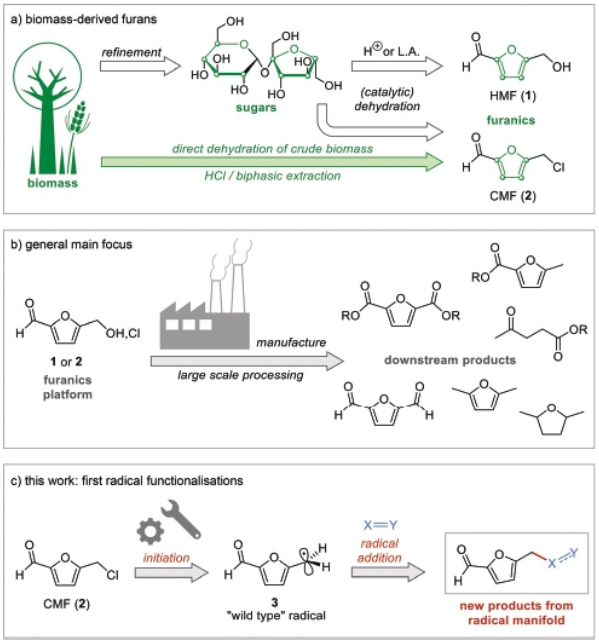

Scheme 1 (a) Furans HMF (**1**) and CMF (**2**) and their retrieval from biomass. (b) Industrial-scale conversion of **1** and **2** into value-added downstream bulk intermediates. (c) The idea of radical functionalizations of CMF (**2**) *via* the "wild type" (2-formyl-5-furanyl)methyl radical **3**.

[a]*University of Rostock, Institute of Chemistry, Albert-Einstein-Str. 3A, 18055 Rostock, Germany. E-mail: malte.brasholz@uni-rostock.de*
[b]*University of Regensburg, Institute of Organic Chemistry, Universitätsstr. 31, 93053 Regensburg, Germany. E-mail: julia.rehbein@chemie.uni-regensburg.de*

†Electronic supplementary information (ESI) available: Full experimental details and compound characterization data. See DOI: 10.1039/d1ob00013f

reduction and hydrolytic protocols (Scheme 1b).[3] On the other hand, to the best of our knowledge, the radical chemistry of HMF (**1**) or CMF (**2**) has not been explored thus far, despite CMF (**2**), with its benzylic chloromethyl group, obviously offering ample opportunities for transformations in the radical manifold (Scheme 1c).

We report here the first radical functionalisations of CMF (**2**) by way of highly efficient atom transfer radical addition (ATRA)[4] reactions with styrenes. Furthermore, we studied the properties and radical addition reactions of the key "wild-type" (2-formyl-5-furanyl)methyl radical **3** derived from CMF (**2**) by NBO population analysis in combination with post-HF methods (MP2) and density functional theory (DFT) calculations.

Results and discussion

During the reaction design, we anticipated that several factors would potentially impede the desired radical functionalisation of CMF (**2**). Irrespective of the chosen induction method, *e.g.*, a photoredox-catalysed reductive cleavage of the C–Cl bond or direct halogen atom transfer (XAT), complications could arise from the degree of spin delocalization in (2-formyl-5-furanyl) methyl radical **3**. In addition, **3** being a benzylic-like radical, a comparably slow rate of addition to alkenes would be expected.[5] Finally, 2-furylmethyl radicals are known to undergo ring-opening, leading to multiple secondary fragmentation products (Scheme 2a).[6] Therefore, we initiated a computational study to elucidate the electronic structure of radical **3** and to correlate it with its behavior in addition reactions with alkenes.

The spin density distribution in radical **3** was compared to those of the closely related 2-furylmethyl radical **4**, 4-formyltolyl radical **5** and tolyl radical **6** (NBO, uMP2/6-311+G**). In all radicals, the highest spin density is in fact located at the benzylic methylene carbon, but in radical **3**, to a considerable extent also at C-2 (Scheme 2b). The SOMO energies of species **3–6** were also calculated (NBO6, uMP2/6-311+G**). As shown in Table 1 (top row), the SOMO energies ε of the radicals can be ranked as follows: **5** < **3–6** < **4**, ranging from −9.168 eV to −8.167 eV. A correlation of the SOMO energies of radicals **3–6** with HOMO and LUMO energies of diverse alkenes as potential reaction partners showed that, in particular, styrene derivatives **7** possess HOMO energies close to the SOMO energies of **3–6** and therefore should be highly suitable radical acceptors. Based on the observed differences in $\Delta\varepsilon$ (FMO), one may (a) expect slight modulation in reactivity and (b) a change in the radicals' nucleophilic or electrophilic role in the addition reaction depending on the electron density of the styrene. As shown in Table 1, the combination of (2-formyl-5-furanyl) methyl radical **3** with electron-poor styrenes (R = CN, F) is expected to have the fastest reaction based on the low $\Delta\varepsilon$ (FMO) of 0.169 eV. For the much alike 4-formyltolyl radical **5**, the smallest energy gap is again that with the HOMO of the acceptor-substituted 4-cyanostyrene ($\Delta\varepsilon$ 0.171 eV), while the largest value for each was obtained for donor-substituted 4-methoxystyrene ($\Delta\varepsilon$ = 0.894 and 1.234 eV). The correlation of $\Delta\varepsilon$ (FMO) with activation barriers was later checked by calculating the actual addition barrier.

In our synthetic experiments, we initially aimed at developing photoredox-induced atom transfer radical addition (ATRA) reactions[7] between CMF (**2**) and styrene (**7a**). For this purpose, CMF (**2**) was first characterized by cyclic voltammetry, and a range of potential photocatalysts were subsequently evaluated in the reaction, both under oxidative and reductive quenching conditions. However, these experiments were only of limited success. After extensive experimentation, we found that only when using $Ir(dtbbpy)(ppy)_2^+$ as the photocatalyst, i-Pr_2NEt as the sacrificial electron donor, in combination with tetrabutylammonium iodide (TBAI), to convert CMF (**2**) *in situ* into the more easily reduced benzylic iodide, the ATRA product **8a** was

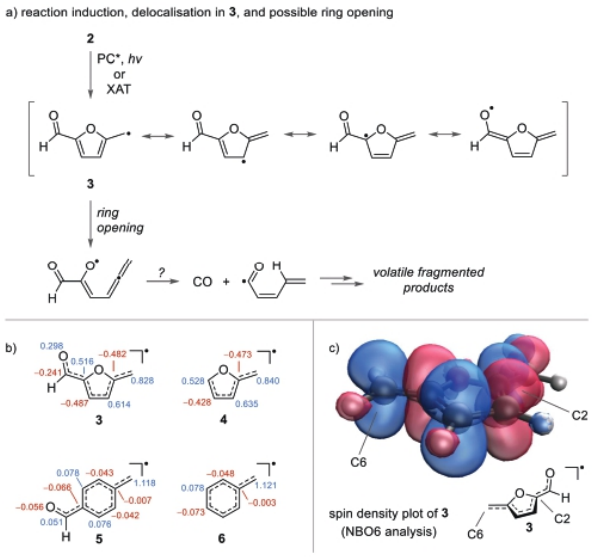

Scheme 2 (a) Methods for the generation of radical **3** and subsequent ring opening. (b) Comparison of spin densities (based on NBO analysis, uMP2/6-311+G**, the plot at an isovalue of 0.04) of radical **3** with those of the related radicals **4**, **5** and **6**. (c) Spin density plot of radical **3**: blue shades designate high spin density.

Table 1 SOMO energies of radicals **3–6**, HOMO energies of 4-substituted styrenes **7** and energy gaps $\Delta\varepsilon$ (in eV) calculated using NBOs at the uMP2/6-311+G** level of theory

Radicals	SOMO (eV)	**3** −8.828	**4** −8.167	**5** −9.168	**6** −8.771
7	HOMO (eV)	$\Delta\varepsilon$ (eV)	$\Delta\varepsilon$ (eV)	$\Delta\varepsilon$ (eV)	$\Delta\varepsilon$ (eV)
R = H	−8.399	0.429	−0.232	0.769	0.372
R = Me	−8.136	0.692	0.031	1.032	0.635
R = OMe	−7.934	0.894	0.233	1.234	0.837
R = F	−8.550	0.278	−0.383	0.618	0.221
R = CN	−8.997	0.169	−0.83	0.171	−0.226

produced in 32% yield, and this result could not be further improved.

As an alternative to photoredox-induction of the radical reaction, CMF (**2**) could also be activated by direct halogen atom abstraction, and as we attempted triethylborane/O_2 as a reagent system,[8] we could indeed realise the desired ATRA transformations in synthetically useful yields. The Et_3B/O_2-induced reaction was carefully optimized as shown in Table 2 (see also Table 1 of the ESI†). When CMF (**2**) and styrene (**7a**) were treated with 2 equivalents of Et_3B in MeCN, under air and at 60 °C, the conversion of **2** was 29% within 24 hours, yet, a mixture of undefined products was formed (entry 1). However, upon addition of 1 equivalent of TBAI, the conversion improved to 87%, and 23% of secondary benzylic chloride **8a** was obtained, along with 10% of furanic dimer **9**, as determined by quantitative ^{1}H-NMR analysis (entry 2). Subsequently, the influence of the molar equivalents of TBAI, Et_3B and styrene (**7a**), the oxygen concentration and the solvent was systematically studied (entries 3–16). Ultimately, using 0.5 equiv. of Et_3B, 4 equiv. of TBAI and a 10-fold excess of styrene (**7a**) in acetone, under air and at 60 °C for 24 h, the secondary benzylic chloride **8a** was provided in an excellent 78% isolated yield after chromatography, and the undesired dimer **9** was formed in only 3% yield. Shortening of the reaction time to 12 h led to largely incomplete conversion of CMF (**2**). Notably, in none of the reactions could any trace of the secondary benzylic iodide corresponding to **8a** be detected.

Under the optimized conditions, a series of ATRA products **8a–8k** could readily be synthesized (Scheme 3a). The yields ranged from 40 to 84%, while the 2,6-dichlorophenyl derivative **8h** formed in just 35% yield, probably as a result of steric hindrance of the double bond in parent styrene **7h**. While the *m*-methoxy derivative **8k** was accessible in 73% yield, the *o*-methoxy and *p*-ethoxy derivatives **8l** and **8m** were obtained exclusively as eliminated products, in moderate yields of 41% and 30%, respectively.

Small changes in the structure of the alkene partner exerted pronounced effects on the reaction efficiency. Utilizing α-methylstyrenes **10a–d**, the conversion of CMF (**2**) remained partially incomplete even after 24 h of reaction time, and isomeric C2–C3 and C3–C4 alkenes **11** were isolated in moderate yields of 25–33% (Scheme 3b). Consistently, when employing 1,1-diphenylethylene (**12**), trisubstituted alkene **13** was obtained in 29% yield. A number of alternative electron-rich and electron-deficient radical acceptors were evaluated (Scheme 3c); however, they were unsuitable reaction partners for (2-formyl-5-furanyl)methyl radical **3**, which mostly underwent unimolecular decomposition in their presence.

The experimental results in Scheme 3 reflect the influence of the SOMO/HOMO energy gaps of the reaction partners. While compound **8j** from the reaction between CMF (**2**) and 4-cyanostyrene was isolated in 59% yield, the eliminated 1-methoxy and 4-ethoxy derivatives **8l** and **8m** were obtained in significantly reduced yields of 41% and 30%, respectively, which correlates well with the calculated respective FMO energy gaps $\Delta\varepsilon$ (Table 1). A DFT calculation (uM06-2X/6-311+G** basis set) of the energy profiles for the addition reactions of (2-formyl-5-furanyl)methyl radical **3** with 4-cyano- and 4-methoxystyrene revealed that in both cases, the radical addition occurs with equally very low energy barriers of around 11 kcal mol^{-1}, the energy barrier of the latter reaction being marginally higher (Scheme 4). Both reactions are exothermic, while the adduct radical **14** from 4-cyanostyrene is *ca.* 2 kcal mol^{-1} lower in energy than the adduct formed by the

Table 2 Reaction optimization (summary)

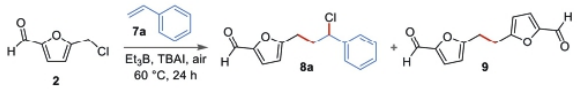

Entry	Et_3B (eq.)	TBAI (eq.)	**7a** (eq.)	Solvent	Conv. **2** [a] [%]	Yield **8a** [a] [%]	Yield **9** [a] [%]
1	2.0	0	15	MeCN	29	0	0
2	2.0	1	15	MeCN	87	23	10
3[b]	2.0	1	15	MeCN	0	0	0
4	2.0	0.5	8	MeCN	100	16	2
5	2.0	1	8	MeCN	100	30	2
6	2.0	2	8	MeCN	100	31	3
7	2.0	4	8	MeCN	100	40	3
8	2.0	4	4	MeCN	95	30	2
9	2.0	4	10	MeCN	100	42	3
10	2.0	4	20	MeCN	100	30	2
11	0.25	4	10	MeCN	91	38	3
12	**0.5**	**4**	**10**	**MeCN**	**96**	**74**	**3**
13	1.0	4	10	MeCN	98	51	5
14	0.5	4	10	THF	74	50	2
15	0.5	4	10	DMF	63	28	2
16	**0.5**	**4**	**10**	**Acetone**	**97**	**75 (78)**[c]	**3**

Reactions were performed on a 0.30 mmol scale of **2**. [a] Determined by ^{1}H-NMR spectroscopy against CH_2Br_2 as an internal standard. [b] Reaction in the absence of O_2. [c] Yield of the isolated product after chromatography.

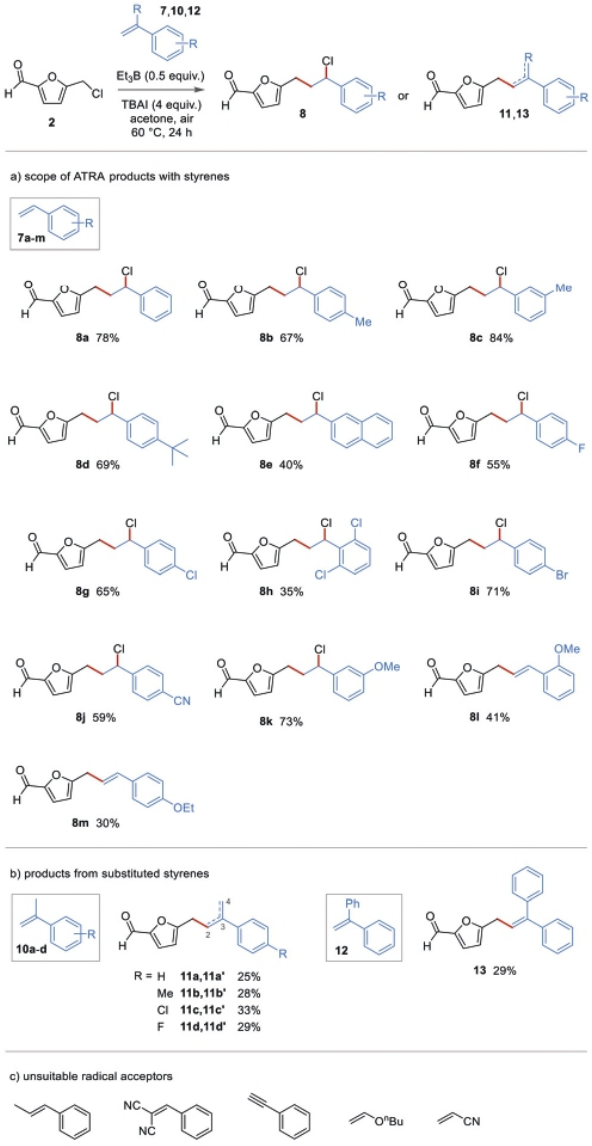

Scheme 3 Reactions were performed on a 0.30 mmol scale of **2**, under the conditions of entry 16 in Table 2.

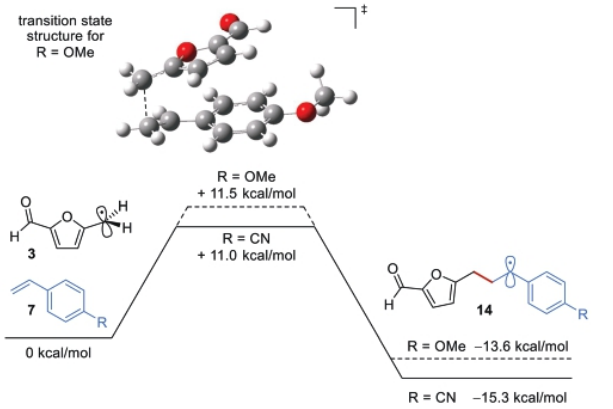

Scheme 4 Calculated energy profiles and the transition state structure for radical **3** and 4-methoxystyrene.

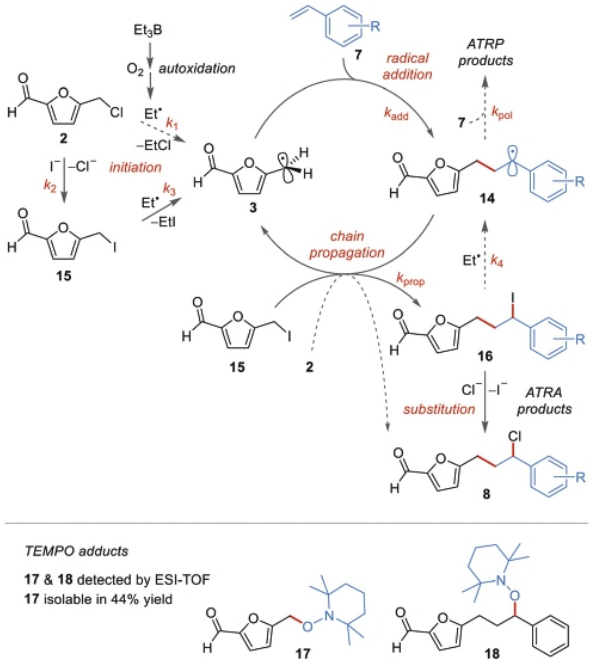

Scheme 5 Proposed reaction mechanism.

reaction with 4-methoxystyrene. The fully optimized transition state structures show that in both cases, the aromatic rings of the reactants converge in a stacked orientation, and the length of the formed bond is very similar for R = CN (2.23 Å) and OMe of 2.22 Å (also see the ESI†).

The proposed mechanism for the Et_3B/O_2-induced ATRA reactions is shown in Scheme 5. Aerobic autoxidation of Et_3B rapidly liberates reactive ethyl radicals[9] to abstract atomic iodine from iodomethylfurfural (IMF, **15**), which forms *in situ* by the reaction between CMF (**2**) and the iodide anion. Radical addition of the so-produced (2-formyl-5-furanyl)methyl radical **3** with styrenes **7** leads to the more stabilized radical adducts **14**, which react with IMF (**15**) in a chain propagation step, to give the primary ATRA products, reactive secondary benzylic iodides **16**. Nucleophilic substitution of **16** with the chloride anion finally delivers the secondary benzylic chlorides **8**.

The overall ATRA process occurs efficiently only in air; thus, when ample O_2 is available to continuously supply ethyl radicals for initiation and to sustain the short-lived radical chain, $\mathbf{14}^{\bullet} + \mathbf{15} \rightarrow \mathbf{3}^{\bullet} + \mathbf{16}$.[10] In the absence of iodide anions, direct chlorine atom abstraction from CMF (**2**) is way less efficient ($k_1 \ll k_3$). However, once IMF (**15**) is generated *in situ*, atomic iodine is easily abstracted. The radical addition of benzylic-like radical **3** with styrenes is expected to be slow,[5b] yet it is followed by a fast propagation step ($k_{prop} > k_{add}$). The formation

of chloro compounds **8** by chain propagation of adduct radicals **14** with CMF (**2**) is energetically much less likely. Furthermore, a possible polymerization of the intermediate radical adducts **14** with excess styrene molecules (atom transfer radical polymerization, ATRP)[11] is apparently of minor significance ($k_{pol} \ll k_{prop}$) based on the observed reaction yields of ATRA products **8**, which are in the range of up to *ca.* 85%. Notably, both key radical intermediates **3** and **14** could successfully be trapped by TEMPO, and their adducts **17** and **18** were unambiguously identified by ESI-TOF mass spectrometry (see the ESI†). Moreover, when CMF (**2**) alone was reacted with TEMPO and Et_3B/O_2, adduct **17** was isolated in 44% yield and could be fully characterized.

Conclusions

The derivative chemistry of the biomass-derived furan 5-chloromethylfurfural (**2**) has successfully been extended into the radical manifold. As a first demonstration, we developed efficient ATRA reactions between CMF (**2**) and styrenes, driven by the metal-free and environmentally benign initiation system of Et_3B and O_2. The key "wild type" 2-formyl-5-furfuryl radical **3** and its behavior in radical addition reactions were studied by computational chemistry approaches, and the calculated molecular and reaction parameters correlate well with the experimental outcomes of our synthetic experiments. Future approaches to utilize the radical chemistry of the furanic platform chemicals HMF (**1**) and CMF (**2**) are currently under development in our laboratories.

Experimental

General procedure for the synthesis of compounds 8

5-Chloromethylfurfural **2** (0.30 mmol, 1.0 equiv.) and tetrabutylammonium iodide (TBAI, 1.20 mmol, 4.0 equiv.) were combined in a 10 mL crimp cap vial and the vial was sealed. Dry acetone (2.00 mL) and styrene derivative **7** (3.00 mmol, 10 equiv., freshly distilled) were added and the mixture was heated to 60 °C. After 30 min, triethyl borane (Et_3B, 1.0 M solution in hexanes, 0.15 mmol, 0.5 equiv.) was added. Then, the septum was pierced with a cannula to allow the capture of oxygen from the ambient air. After 24 h of reaction time, the solvent was evaporated. The crude mixture was diluted with DCM and washed with water and brine (3 × 20 mL). The organic layer was collected and dried over anhydrous $MgSO_4$ and filtered, followed by concentration under reduced pressure. The crude mixture was subjected to column chromatography (silica gel, 230–400 mesh) to afford the desired compounds **8**.

Conflicts of interest

There are no conflicts to declare.

Acknowledgements

The authors acknowledge the financial support of this project by the strategic network funding programme of the Leibniz Association, within the project "Leibniz-WissenschaftsCampus–ComBioCat–Rostock". R. D. thanks this programme for a Ph.D. fellowship.

Notes and references

1 Selected reviews: (*a*) C. Thoma, J. Konnerth, W. Sailer-Kronlachner, P. Solt, T. Rosenau and H. W. G. van Herwijnen, *ChemSusChem*, 2020, **13**, 3544–3564; (*b*) R.-J. van Putten, J. C. van der Waal, E. de Jong, C. B. Rasrendra, H. J. Heeres and J. G. de Vries, *Chem. Rev.*, 2013, **113**, 1499–1597.

2 (*a*) M. Mascal and E. B. Nikitin, *ChemSusChem*, 2009, **2**, 423–426; (*b*) M. Brasholz, K. von Känel, C. H. Hornung, S. Saubern and J. Tsanaktsidis, *Green Chem.*, 2011, **13**, 1114–1117; (*c*) M. Mascal, *ChemSusChem*, 2015, **8**, 3391–3395.

3 Recent overviews: (*a*) Q.-S. Kong, X.-L. Li, H.-J. Xu and Y. Fu, *Fuel Process. Technol.*, 2020, **209**, DOI: 10.1016/j.fuproc.2020.106528; (*b*) D. Zhao, T. Su, Y. Wang, R. S. Varma and C. Len, *Mol. Catal.*, 2020, **495**, DOI: 10.1016/j.mcat.2020.111133; (*c*) C. Thoma, J. Konnerth, W. Sailer-Kronlachner, T. Rosenau, A. Potthast, P. Solt and H. W. G. van Herwijnen, *ChemSusChem*, 2020, **13**, 5408–5422; (*d*) B. Wozniak, S. Tin and J. G. de Vries, *Chem. Sci.*, 2019, **10**, 6024–6034; (*e*) J. G. de Vries, *Adv. Heterocycl. Chem.*, 2017, **121**, 247–293; (*f*) M. Mascal and S. Dutta, *Top. Curr. Chem.*, 2014, **353**, 41–83.

4 Reviews: (*a*) J. M. Muçoz-Molina and T. R. Belderrain, in *Science of Synthesis, C-1 Building Blocks in Organic Synthesis 2*, ed. P. W. N. M. Van Leeuwen, Thieme, Stuttgart, 2014, pp. 459–473; (*b*) T. Pintauer, *Eur. J. Inorg. Chem.*, 2010, **17**, 2449–2460; (*c*) T. Pintauer and K. Matyjaszewski, *Chem. Soc. Rev.*, 2008, **37**, 1087–1097; (*d*) K. Severin, *Curr. Org. Synth.*, 2006, **10**, 217–224.

5 Review of absolute rate constants of free-radical additions to alkenes: (*a*) H. Fischer and L. Radom, *Angew. Chem., Int. Ed.*, 2001, **40**, 1340–1371. For rate constant data of the less-reactive benzylic radicals, see: (*b*) K. Héberger, M. Walbiner and H. Fischer, *Angew. Chem., Int. Ed. Engl.*, 1992, **31**, 635–636.

6 (*a*) Y. Li, Y. Gan and C. Cao, *J. Comput. Chem.*, 2019, **40**, 1057–1065; (*b*) C. Togbé, L.-S. Tran, D. Liu, D. Felsmann, P. Oßwald, P.-A. Glaude, B. Sirjean, R. Fournet, F. Battin-Leclerc and K. Kohse-Höinghaus, *Combust. Flame*, 2014, **161**, 780–797; (*c*) L. D. Kispert, R. C. Quijano and C. U. Pittman Jr., *J. Org. Chem.*, 1971, **36**, 3837–3838.

7 Reviews: (*a*) D. Bag, H. Kour and S. D. Sawant, *Org. Biomol. Chem.*, 2020, **18**, 8278–8293; (*b*) T. M. Williams and C. R. J. Stephenson, in *Visible Light Photocatalysis in Organic Chemistry*, ed. C. R. J. Stephenson, D. W. C. MacMillan and T. P. Yoon, Wiley-VCH, Weinheim, 2018; pp. 73–92; (*c*) T. Corant and G. Masson, *J. Org. Chem.*, 2016,

81, 6945–6952; (*d*) O. Reiser, *Acc. Chem. Res.*, 2016, **49**, 1990–1996.

8 Selected overviews: (*a*) P. Renaud, in *Encyclopedia of Radicals in Chemistry, Biology and Materials*, ed. C. Chatgilialoglu and A. Studer, Wiley, New York, 2012, Vol. 1, pp. 601–628; (*b*) V. Darmency and P. Renaud, *Top. Curr. Chem.*, 2006, **263**, 71–106; (*c*) H. Yorimitsu and K. Oshima, in *Radicals in Organic Synthesis*, ed. P. Renaud and M. P. Sibi, Wiley-VCH, Weinheim, 2001, vol. 1, pp. 11–27.

9 For a recent study of the mechanism of Et_3B autoxidation, see: R. Uematsu, C. Saka, Y. Sumiya, T. Ichino, T. Taketsugu and S. Maeda, *Chem. Commun.*, 2017, **53**, 7302–7305.

10 For a detailed study on the effect of the O_2 concentration in Et_3B-initiated radical reactions, see: D. P. Curran and T. R. McFadden, *J. Am. Chem. Soc.*, 2016, **138**, 7741–7752.

11 K. Matyjaszewski and J. Xia, *Chem. Rev.*, 2001, **101**, 2921–2990.

5.2. Visible light-induced Iridium (III)-sensitized [2+2] and [3+2] photocycloadditions of 2-cyanochromone with alkenes

Rajesh Dasi, Alexander Villinger and Malte Brasholz*

Org. Biomol. Chem. **2023**, *21*, 6103-6106

DOI: 10.1039/d3ob00862b

In this work, I performed all the optimization reactions and control experiments. I performed the investigation of substrate scope, isolation, and characterization of compounds as well as writing the supporting information for the manuscript. My contribution as the first author of this paper is approximately 80%.

Organic & Biomolecular Chemistry

ROYAL SOCIETY OF CHEMISTRY

COMMUNICATION

View Article Online
View Journal | View Issue

Cite this: *Org. Biomol. Chem.*, 2023, **21**, 6103

Received 31st May 2023,
Accepted 11th July 2023

DOI: 10.1039/d3ob00862b

rsc.li/obc

Visible light-induced iridium(III)-sensitized [2 + 2] and [3 + 2] photocycloadditions of 2-cyanochromone with alkenes†‡

Rajesh Dasi, [a] Alexander Villinger [a] and Malte Brasholz *[a,b]

2-Cyanochromone (1) readily undergoes visible light-induced photocycloadditions with diverse alkene partners mediated by (Ir[dF(CF$_3$)ppy]$_2$(dtbpy))PF$_6$ as the photosensitizer. While mono-, di- and trisubstituted styrenes and acrylonitriles as the reactants lead to [2 + 2] cycloadducts with good regiocontrol and high diastereoselectivity, the use of trialkyl-substituted alkenes allows for the isolation of cyclopentenone-fused chromones resulting from a [3 + 2] cycloaddition process in moderate yields.

The continuing advancement of visible light photocatalysis has increasingly brought energy transfer-initiated reactions into focus in recent years.[1] While a growing number of tailor-made organic photosensitizers are becoming available for new applications in EnT photocatalysis,[2] among the transition-metal compounds, iridium(III) polyheteroaryl complexes in particular have proven very useful owing to their highly favourable and readily tunable photophysical properties.[3]

Triplet-sensitized photocycloadditions are among the most important transformations in EnT photocatalysis, and their implementation under visible light irradiation allows for milder conditions and frequently more selective reaction outcomes compared to direct excitation with UV light.[4]

Photocycloadditions of cyano-substituted enones, enoates and eneamides with alkenes are a particularly interesting type of reaction, and these have previously been studied under direct UV excitation, as well as with aryl ketones or acetone as sensitizers with >300 nm irradiation in several cases.[5–13] As shown in Scheme 1 for the exemplary β-cyanoenone **I**, its triplet-excitation in the presence of an alkene initially leads to a cyano-substituted triplet 1,4-biradical **II**,[14] which after inter-system crossing ring-closes to cyanocyclobutane **III**. However, in competition with the conventional [2 + 2]-cycloaddition, a 1,5-cyclization of the triplet biradical can occur, to generate a cyclic triplet nitrene intermediate **IV** as a primary product. Subsequent hydrogen transfer to the nitrene nitrogen atom, followed by a hydrogen abstraction that reinstalls the conjugated double bond, lead to a cyclopentenylimine, which upon hydrolysis gives cyclopentenone **V** as the final [3 + 2]-product. While the reactivity of α-cyanoenones and -enoates parallels that of the β-cyano compounds,[9–12] the ratio of [2 + 2]- and [3 + 2]-products generally is mostly governed by the structure of the reactants, however in a few cases it was interestingly found to be temperature-dependent.[6,7]

In a previous study, Saito *et al.* investigated photocycloadditions of 2-cyanochromone (**1**), mostly under direct UV excitation conditions, with a narrow set of alkene partners.[7] Our aim in this work was to study the behaviour of chromone **1** in the presence of visible light-absorbing triplet sensitizers, to broaden the applicability of the reaction to a larger set of

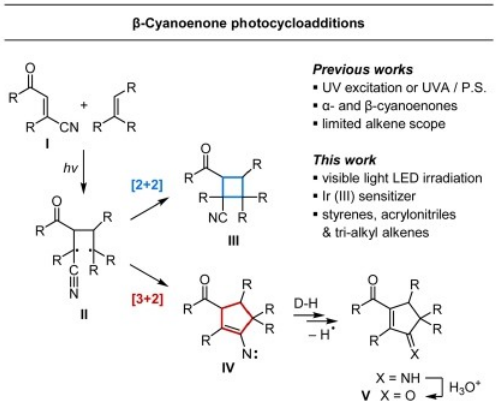

Scheme 1 [2 + 2]- and [3 + 2]-Photocycloadditions between β-cyanoenones and alkenes. P.S. = photosensitizer.

[a]*University of Rostock, Institute of Chemistry, Albert-Einstein-Str. 3a, 18059 Rostock, Germany. E-mail: malte.brasholz@uni-rostock.de*
[b]*Leibniz Institute for Catalysis e.V., Albert-Einstein-Str. 29a, 18059 Rostock, Germany*

†Dedicated to Professor Paul Margaretha.

‡Electronic supplementary information (ESI) available: Full experimental details, compound characterization data and single crystal X-ray structures. CCDC 2250461–2250465. For ESI and crystallographic data in CIF or other electronic format see DOI: https://doi.org/10.1039/d3ob00862b

alkenes, and to compare the observed selectivities between the [2 + 2] and [3 + 2] reaction channels.

We began our investigation of the visible light-mediated sensitized photocycloadditions of cyanochromone (**1**) with styrene derivatives as the alkenes, for the reason that the corresponding reactant pairs had not been reported thus far. Using styrene (**2a**), it was soon established that a range of organic and transition metal-based photosensitizers (P.S.) could promote the reaction with chromone **1** under 450 nm irradiation (30 W LED, in MeCN solvent at 30 °C), all of them to produce the *exo*-[2 + 2]-cycloadduct **3a** together with its regioisomer **3a′** as the main products (Table 1, entries 1–7; see Table ESI 1‡ for full details). Both compounds **3a** and **3a′** formed highly stereoselectively in all cases, and only trace amounts (*ca.* 5–10% combined) of other minor isomers could be detected in ^{1}H NMR spectra of the crude product mixtures, yet no [3 + 2]-adducts were present (*vide infra*). Depending on the photosensitizer, the ratio of regioisomers (r.r.) ranged from about 3 : 1 up to 5 : 1 in favour of cycloadduct **3a**, and thioxanthone (10 mol%) was by far the most effective among the organic sensitizers, with 70% conversion of chromone **1** after 24 h. Among the several Iridium(III)-complexes employed, $(Ir[dF(CF_3)ppy]_2(dtbpy))^+$ gave a result very similar to thioxanthone, however with only 2 mol% catalyst loading. From there, increasing the quantity of $(Ir[dF(CF_3)ppy]_2(dtbpy))^+$ to 3 mol%, while extending the reaction duration to 36 h as well as reducing the excess of styrene (**2a**) from 20 to 10 equiv., finally led to near-quantitative conversion of chromone **1** and allowed for the isolation of cyclobutane **3a** in 71% yield (Table 1, entries 8–10).

A scope of the Ir(III)-sensitized [2 + 2]-cycloaddition between 2-cyanochromone (**1**) and diverse alkenes is shown in Fig. 1. Under the optimized conditions, use of mono-substituted styrenes **2a–2j** led to cyclobutanes **3a–3j** in 58–76% yield, and the regioselectivity in these reactions ranged between 3.5 : 1 for compound **3c** up to 14 : 1 in the case of compound **3i**. Sterically hindered 2,6-dichlorostyrene (**2h**) gave cycloadduct **3h** in a moderate yield of 28%, while 4-cyanostyrene (**2k**) produced the corresponding [2 + 2] adducts as a mixture in only 26% yield as determined by NMR analysis.

The reactions of α-methylstyrenes **2l** and **2m** generated cycloadducts **3l** and **3m** in moderate yields of 36% and 34%, both with r.r. of 6 : 1, and in these cases the reduced yields resulted from generally less clean conversion compared to the mono-substituted styrenes. In addition, 1-arylcyclohexenes **2n–2p** could be employed, to deliver cyclobutanes **3n–3p** in 49–69% yield, as single regio- and diastereoisomers. Among the disubstituted styrenes, 1,1-diphenylethylene (**2q**) and *trans*-stilbene (**2r**) represented two unsuccessful examples, with 9% and 0% yield, respectively. Finally, use of acrylonitrile (**4a**) and methacrylonitrile (**4b**) led to their [2 + 2]-adducts **5a** and **5b** in high yields, with entire regiocontrol in both cases, however predominantly as the *endo*-diastereomers (d.r. 2 : 1 for product **5a** and 13 : 1 for compound **5b**). For all reaction products, the assignment of the relative configuration was based on NOESY spectra in addition to the single crystal X-ray structures of compounds **3a**, **3m** and **5b** (as well as those of **3d** and **3g** not enclosed in Fig. 1, see the ESI‡).[15]

With regard to the formation of [3 + 2]-cycloadducts, careful ^{1}H NMR analyses revealed that neither in case of monosubstituted styrenes, nor in the reactions with α-methylstyrenes or 1-arylcyclohexenes, any of such products could be detected under the typical conditions. In their original study of sensitizer-free photocycloadditions of 2-cyanochromone (**1**) under UV irradation, Saito *et al.* reported reactions between chromone **1** and 1-methylcyclohexene (**2t**) as well as 2-methyl-2-butene (**2u**), that gave the corresponding [2 + 2]- and [3 + 2]-cycloadducts in mixture. Further, the product ratio of the reaction with 1-methylcyclohexene (**2t**) was additionally found to be temperature-dependent (shown over a wide range from −78 to 64 °C) and with increasing temperature, selectivity shifted towards the [3 + 2] product.[7] We consequently probed these

Table 1 [2 + 2]-Cycloaddition between 2-cyanochromone (**1**) and styrene (**2a**), summary of reaction development

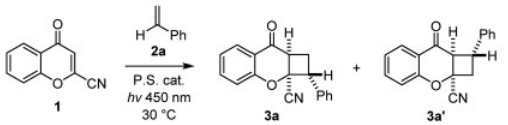

#	P.S.	mol%	*t* (h)	Conv.[a] **1** (%)	Yield[a] **3a** (%)	Yield[a] **3a′** (%)
1	1,5-Diamino-AQ	10	24	10	3	1
2	Thioxanthone	10	24	70	42	8
3	4CzIPN	2	24	40	17	5
4	Eosin Y[b]/Rose bengal[b]	2	24	18/32	0/0	0/0
5	$Ir(ppy)_3$	2	24	35	0	0
6	$[Ir(ppy)_2(dtbpy)]^+$	2	24	55	13	5
7	$(Ir[dF(CF_3)ppy]_2(dtbpy))^+$	2	24	70	43	12
8	$(Ir[dF(CF_3)ppy]_2(dtbpy))^+$	3	24	79	58	11
9	$(Ir[dF(CF_3)ppy]_2(dtbpy))^+$	3	36	80	62	13
10	$\mathbf{(Ir[dF(CF_3)ppy]_2(dtbpy))^+}$	**3**[c]	**36**	**96**	**72 (71)**[d]	**14**
11	No P.S./no light	0/3	36	4/2	0/0	0/0

Reaction conditions: 0.10 mmol of **1**, 20 equiv. of **2a**, catalytic P.S., MeCN, 450 nm LED (30 W), 30 °C. [a] Determined by ^{1}H NMR analysis against CH_2Br_2 standard. [b] 530 nm LED (30 W) used. [c] 10 equiv. of **2a** used. [d] Yield after chromatography. P.S. = photosensitizer. AQ = anthraquinone.

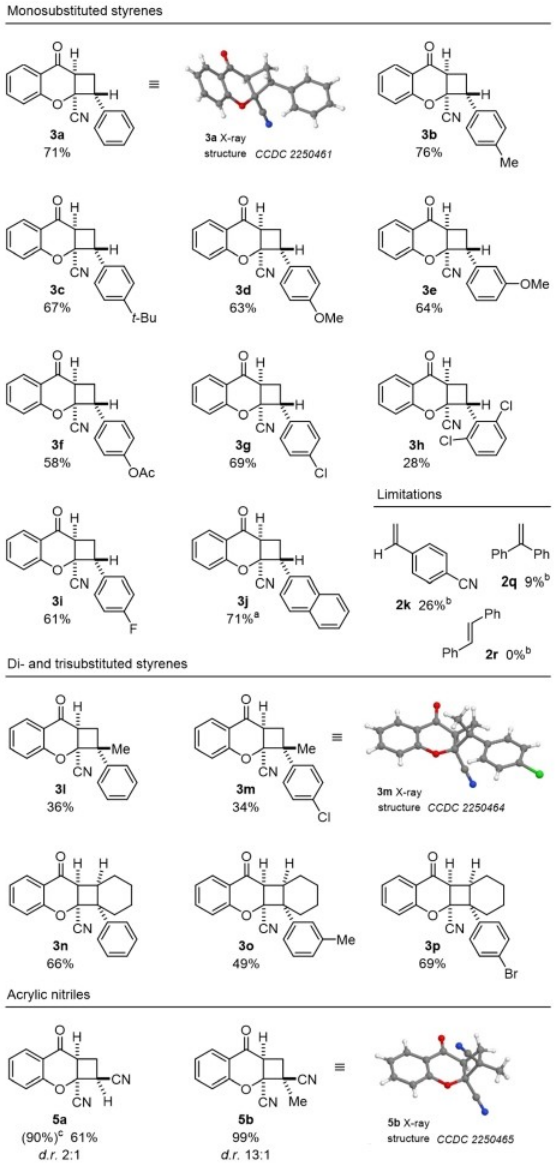

Fig. 1 Scope of the Ir(III)-sensitized [2 + 2]-photocycloaddition between 2-cyanochromone (**1**) and styrenes **2** as well as acrylonitriles **4**. Reaction conditions: 0.10 mmol of **1**, alkene **2** or **4** (10 equiv.), (Ir[dF(CF$_3$)ppy]$_2$(dtbpy))PF$_6$ (3 mol%), MeCN, 450 nm LED (30 W), 30 °C, 36 h. (a) Isolated as a 5 : 1 mixture of regioisomers. (b) Yield determined by ^{1}H NMR analysis against CH_2Br_2 standard. (c) Combined yield of both isomers determined by ^{1}H NMR analysis.

and further reactions under blue LED Irradiation, with (Ir[dF(CF$_3$)ppy]$_2$(dtbpy))$^+$ as the sensitizer and at varied temperatures (Table 2).

Under the typical reaction conditions at 30 °C, followed by treatment of the crude product mixture with dilute aqueous HCl in acetone, 1-methylcyclopentene (**2s**) gave cyclobutane **3s** and its [3 + 2]-adduct, the tetrahydro-1*H*-pentaleno[2,1-*b*]chromene-4,10-dione **6s**, in a ratio of 1 : 1.6 and in 18% and 28% isolated yield, respectively (entry 1). Both products were pure diastereomers, compound **6s** being *cis*-configured. On the other hand, using 1-methylcyclohexene (**2t**) at 30 °C produced [3 + 2]-adduct **6t** as the sole product, in 44% yield and as pure *cis*-diastereomer (entry 2). Use of 2-methyl-2-butene (**2u**) gave products **3u** (mixture of isomers) and **6u** in a ratio of 1 : 2.8 (combined yield 32%, entry 3). 2,3-Dimethyl-2-butene (**2v**) gave an improved product ratio of 1 : 3.7 in favour of the [3 + 2] adduct **6v** which was isolated in 41% yield (entry 4). Hence thus far, in comparison to the non-sensitized reactions under UV-light,[7] the new reaction conditions led to slight improvements of product selectivity in case of the previously reported [3 + 2]-cycloadducts **6t** and **6u**, however the overall yields remained moderate. Conducting the same reactions at 65 °C with alkenes **2s** and **2u** or at −10 °C for 1-methyl-cyclohexene (**2t**) however showed no effect on product ratios. Likewise, also the reaction with 1-phenylcyclohexene (**2n**) was unaffected by temperature variation, to solely produce the [2 + 2] product **6n** at 65 °C (entry 5). Similarly, using styrene (**2a**) at 65 °C gave cycloadducts **3a** and **3a′** only.

Table 2 Ir(III)-sensitized [2 + 2]- and [3 + 2]-photocycloadditions between 2-cyanochromone (**1**) and trisubstituted alkenes **2n,2s–v**

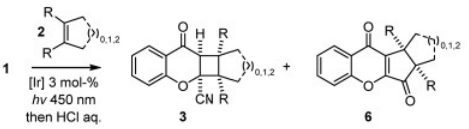

#	Alkene	T (°C)	Ratio **3** : **6**[a]	Yield[b] **3** (%)	Yield[b] **6** (%)
1	**2s**	30	**3s** : **6s** 1 : 1.6	18	28
		65[c]	**3s** : **6s** 1 : 1.6	12[d]	19[d]
2	**2t**	30	**3t** : **6t** 0 : 1	0	44
		−10[c]	**3t** : **6t** 0 : 1	0[d]	24[d,e]
3	**2u**	30	**3u** : **6u** 1 : 2.8	8	24
		65[c]	**3u** : **6u** 1 : 2.8	8[d]	26[d]
4	**2v**	30	**3v** : **6v** 1 : 3.7	11[d]	41
5	**2n**	30	**3n** : **6n** 1 : 0	66	0
		65[c]	**3n** : **6n** 1 : 0	65[d]	0[d]

Reaction conditions: 0.10 mmol of **1**, alkene **2** (10 equiv.), (Ir[dF(CF$_3$)ppy]$_2$(dtbpy))PF$_6$ (3 mol%), MeCN. 450 nm LED (30 W), 30 °C, 48 h or 450 nm LED (10 W), 65 °C, 48 h. Then HCl aq., acetone, r.t., 16 h. [a] Determined by ^{1}H NMR analysis. [b] Yield after chromatography. [c] 10 W 450 nm LED used. [d] Determined by ^{1}H NMR analysis against CH_2Br_2 standard. [e] Yield based on 76% conversion of **1**.

Hence, this study has clearly shown that benzyl cyano 1,4-biradicals **VI** fail to undergo [3 + 2] cyclization, probably owing to a reduced triplet lifetime compared to alkyl cyano 1,4-biradicals. Yet, no temperature effect on product selectivity could be observed in neither case under our reaction conditions.

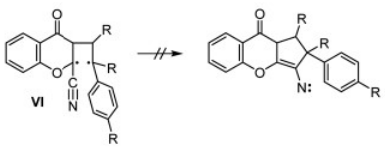

Conclusions

2-Cyanochromone (**1**) is a useful building block in visible light-induced sensitized photocycloadditions with diverse alkenes. In combination with mono-, di- and trisubstituted styrenes and acrylonitriles, [2 + 2] cycloadducts are obtained with good regiocontrol and high diastereoselectivity. Utilizing trialkyl-substituted alkenes, a competing [3 + 2] cycloaddition is observed allowing for the isolation of the corresponding cyclopentenone-fused chromones in moderate yields. A previously reported temperature-dependence of product selectivity under UV excitation remained elusive under visible light irradiation.

Conflicts of interest

There are no conflicts to declare.

Acknowledgements

The authors acknowledge financial support of this project by the Strategic Network Funding Programme of the Leibniz Association, within the project "Leibniz-WissenschaftsCampus–ComBioCat–Rostock". R. D. thanks this programme for a Ph.D. fellowship.

References

1 (*a*) J. Großkopf, T. Kratz, T. Rigotti and T. Bach, *Chem. Rev.*, 2022, **122**, 1626–1653; (*b*) Q.-Q. Zhou, Y.-Q. Zou, L.-Q. Lu and W.-J. Xiao, *Angew. Chem., Int. Ed.*, 2019, **58**, 1586–1604; (*c*) F. Strieth-Kalthoff, M. J. James, M. Teders, L. Pitzer and F. Glorius, *Chem. Soc. Rev.*, 2018, **47**, 7190–7202.

2 (*a*) A. Shiozuka, K. Sekine and Y. Kuninobu, *Synthesis*, 2022, 2330–2339; (*b*) N. F. Nikitas, P. L. Gkizis and C. G. Kokotos, *Org. Biomol. Chem.*, 2021, **19**, 5237–5253; (*c*) J. Lu, B. Pattengale, Q. Liu, S. Yang, W. Shi, S. Li, J. Hang and J. Zhang, *J. Am. Chem. Soc.*, 2018, **140**, 13719–13725; (*d*) V. Mojr, E. Svobodá, K. Straková, T. Neveselý, J. Chudoba, H. Dvořáková and R. Cibulka, *Chem. Commun.*, 2015, **51**, 12036–12039.

3 (*a*) M. R. Schreier, X. Guo, B. Pfund, Y. Okamoto, T. R. Ward, C. Kerzig and O. S. Wenger, *Acc. Chem. Res.*, 2022, **55**, 1290–1300; (*b*) Y. Wu, D. Kim and T. S. Teets, *Synlett*, 2022, 1154–1179; (*c*) R. Bevernaegie, S. A. M. Wehlin, B. Elias and L. Troian-Gautier, *ChemPhotoChem*, 2021, **5**, 217–234; (*d*) I. N. Mills, J. A. Porras and S. Bernhard, *Acc. Chem. Res.*, 2018, **51**, 352–364.

4 (*a*) M. Sicignano, R. I. Rodríguez and J. Alemán, *Eur. J. Org. Chem.*, 2021, 3303–3321; (*b*) D. Sarkar, N. Bera and S. Ghosh, *Eur. J. Org. Chem.*, 2020, 1310–1326; (*c*) S. Poplata, A. Tröster, Y.-Q. Zou and T. Bach, *Chem. Rev.*, 2016, **116**, 9748–9815; (*d*) J. Iriondo-Alberdi and M. F. Greaney, *Eur. J. Org. Chem.*, 2007, 4801–4815; (*e*) M. Zhu, X. Zhang, C. Zheng and S.-L. You, *Acc. Chem. Res.*, 2022, **55**, 2510–2525; (*f*) F. Mueller and J. Mattay, *Chem. Rev.*, 1993, **93**, 99–117; (*g*) D. I. Schuster, G. Lem and N. A. Kaprinidis, *Chem. Rev.*, 1993, **93**, 3–22; (*h*) M. T. Crimmins, *Chem. Rev.*, 1988, **88**, 1453–1473.

5 I. Saito, K. Shimozono and T. Matsuura, *J. Am. Chem. Soc.*, 1980, **102**, 3948–3950.

6 I. Saito, K. Shimozono and T. Matsuura, *J. Org. Chem.*, 1982, **47**, 4356–4358.

7 I. Saito, K. Shimozono and T. Matsuura, *Tetrahedron Lett.*, 1982, **23**, 5439–5442.

8 I. Saito, K. Shimozono and T. Matsuura, *J. Am. Chem. Soc.*, 1983, **105**, 963–970.

9 S. Andresen and P. Margaretha, *J. Chin. Chem. Soc.*, 1995, **42**, 991–993.

10 S. Andresen and P. Margaretha, *J. Photochem. Photobiol., A*, 1998, **112**, 135–138.

11 D. Schwebel, J. Ziegenbalg, J. Kopf and P. Margaretha, *Helv. Chim. Acta*, 1999, **82**, 177–181.

12 D. Schwebel, M. Soltau and P. Margaretha, *Synthesis*, 2001, 1111–1113.

13 M. Soltau, M. Göwert and P. Margaretha, *Org. Lett.*, 2005, **23**, 5159–5161.

14 For a review of the related alkyl propargyl 1,4-biradicals, see: W. C. Agosta and P. Margaretha, *Acc. Chem. Res.*, 1996, **29**, 179–182.

15 The X-ray single crystal structure data related to compounds **3a**, CCDC 2250461, **3d**, CCDC 2250462, **3g**, CCDC 2250463, **3j**, 2250464 and **5b**, CCDC 2250465 can be obtained from the Cambridge Structural Database, **https://www.ccdc.cam.ac.uk**.

5.3. Photocatalytic azetidine synthesis by aerobic dehydrogenative [2+2] cycloadditions of amines with alkenes

Rajesh Dasi, Alexander Villinger and Malte Brasholz*
Org. Lett. **2022**, *24*, 8041-8046
DOI: 10.1021/acs.orglett.2c03291

In this project, I have been involved in the design of experimental work and performed all of the optimization of reaction, investigation of substrate scope, and isolation of the compounds. I was involved in the characterization of compounds as well as writing the supporting information for the manuscript. My contribution as the first author of this paper is approximately 75%.

OL Organic Letters

pubs.acs.org/OrgLett Letter

Photocatalytic Azetidine Synthesis by Aerobic Dehydrogenative [2 + 2] Cycloadditions of Amines with Alkenes

Rajesh Dasi, Alexander Villinger, and Malte Brasholz*

Cite This: *Org. Lett.* 2022, 24, 8041−8046 Read Online

ACCESS | Metrics & More | Article Recommendations | Supporting Information

ABSTRACT: Photocatalytic dehydrogenative [2 + 2] cycloadditions between amines and alkenes were developed that allow for the stereoselective and high-yielding synthesis of functionalized azetidines. The oxidative formal Aza Paternò−Büchi reactions are induced by photoredox-catalyzed aerobic oxidation of dihydroquinoxalinones **1** as the amines, and in the presence of structurally diverse alkenes **3** intermolecular [2 + 2] cyclization to dihydro-1*H*-azeto[1,2-*a*]quinoxalin-3(4*H*)-ones **4** occurs. The utility of the method is illustrated by the selective conversion of amino acid derived dihydroquinoxalinones **1**, including oxidation-prone lysine and tryptophan derivatives.

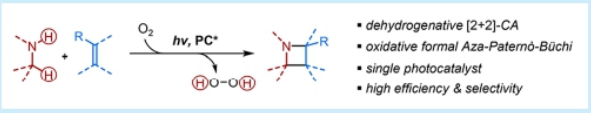

Cycloadditions are among the most powerful synthetic transformations as they allow the rapid construction of complex molecular architectures from structurally simple precursors.[1] The latter classically are unsaturated compounds, that is, alkenes and alkynes, carbonyl compounds, and imines. From the perspective of the chemical value chain, all of these components need to be made in energy-intensive processes from basic upstream feedstocks.[2] A potentially more sustainable and step-economic approach consists of dehydrogenative cycloadditions in which the unsaturated reactants are generated during the reaction by in situ dehydrogenation of the saturated precursors (Scheme 1a).

A number of compelling examples of dehydrogenative [4 + 2] cycloadditions, among them Povarov cyclizations in particular, were developed in recent years (Scheme 1a, top).

Scheme 1. (a) Concept of Dehydrogenative Cycloadditions. (b) Photocatalytic Dehydrogenative formal Aza Paternò−Büchi Reaction

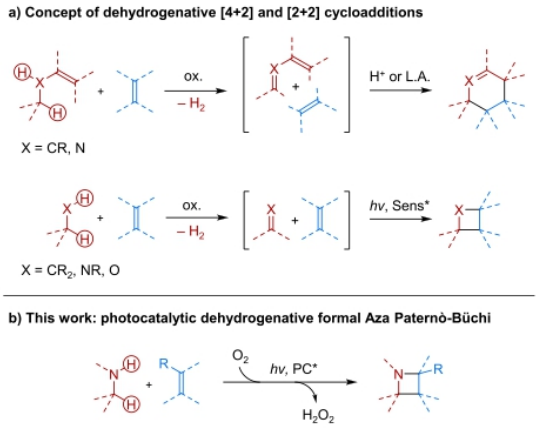

These included thermal reactions with metal and nonmetal catalysts that were catalytically active both in the dehydrogenation as well as in the cycloaddition step.[3] Subsequently, several photocatalytic variants were also reported.[4] In addition to [4 + 2] processes, dehydrogenative [3 + 2][5] and even [2 + 2 + 2][6] cyclizations have as well been demonstrated. Generally, in most of the protocols concerned, a single reactant is dehydrogenated; however, a few methods allow for double dehydrogenative cycloaddition reactions, in which both reactants are dehydrogenated.[7]

Dehydrogenative [2 + 2] cycloadditions remained largely unexplored so far. There, the challenge is to identify a catalytic system that can mediate the dehydrogenation of one or even both reactants as well as the subsequent cycloaddition, which is photochemically induced (Scheme 1a, bottom). While pursuing this idea, we examined the [2 + 2] photocycloaddition between imines and alkenes, the Aza Paternò−Büchi reaction,[8,9] for its potential implementation as a dehydrogenative process. Consequently, we succeeded in developing a method for dehydrogenative [2 + 2] cycloadditions between amines and alkenes to deliver functionalized azetidines, under purely photocatalytic conditions, and which is driven by a single photocatalyst (Scheme 1b).

Our investigations began with the consideration of several model transformations, of which the [2 + 2] photocycloaddition of quinoxalinones **2** with alkenes **3** appeared highly appealing to us (Scheme 2). This reaction was first reported by Nishio et al. in 1984,[10] and more recently, Bach and coauthors

Received: September 27, 2022
Published: October 20, 2022

https://doi.org/10.1021/acs.orglett.2c03291
Org. Lett. 2022, 24, 8041−8046

Scheme 2. Dehydrogenation of Dihydroquinoxalinones 1 and [2 + 2] Photocycloaddition between Quinoxalinones 2 and Alkenes 3

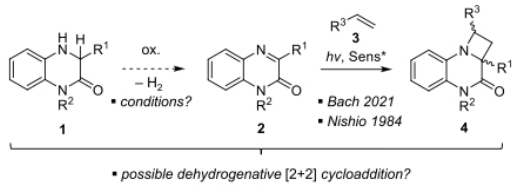

developed a highly enantioselective variant utilizing a chiral thioxanthone sensitizer.[11a,b] The sensitized reaction additionally offered excellent diastereoselectivity with styrenes as the alkene partners.[11a] For our purpose of developing a dehydrogenative version of the reaction, the 3,4-dihydroquinoxalin-2(1*H*)-ones **1** would be the required imine precursors, and their photocatalytic aerobic oxidation to quinoxalinones **2** seemed a straightforward reaction. Another persuasive advantage of this planning would be the facile preparation of structurally diverse dihydroquinoxalinones **1** by the copper-catalyzed coupling of 2-bromoaniline with abundant α-amino acids.[12]

Consequently, the 3-methyl-substituted analog **1a** and styrene (**3a**) were chosen as model substrates, and a systematic survey of the reaction conditions was initiated for each individual step as well as the one-pot photocatalytic reaction (Scheme 3). For the dehydrogenation **1a** → **2a** (step 1), we initially screened various anthraquinone dyes, potent organic photooxidants that can mediate hydrogen abstraction, photoelectron transfer, as well as energy-transfer reactions.[13] Further, thioxanthone as well as several iridium(III) complexes were employed (Table S1). All of the substituted anthraquinones tested, as well as thioxanthone, efficiently promoted the desired oxidation (10 mol % of catalyst, air or pure O_2 atmosphere, MeCN, 450 nm blue LED), and quinoxalinone **2a** was obtained in near-quantitative yields within 1−3 h. Gratifyingly, $Ir[dF(CF_3)ppy]_2(dtbpy)^+$ and $Ir(ppy)_3$ were also highly effective promoters of the oxidation **1a** → **2a** (2 mol % each). In addition, the dehydrogenation could also be achieved in high yield using rose bengal[14] (2 mol %) under 530 nm green LED irradiation (see Table S1). Of note, the catalyst-free autoxidation of compound **1a** was marginal, with just 15% conversion after 3 h of irradiation under air, while no reaction occurred in the dark. Upon examining the Aza Paternò−Büchi reaction between quinoxalinone **2a** and styrene (**3a**) (step 2), we observed that both $Ir[dF(CF_3)ppy]_2(dtbpy)^+$ and $Ir(ppy)_3$ were highly competent photosensitizers,[15] the latter being slightly superior (Table S2). When $Ir(ppy)_3$ (2 mol %) was utilized together with 20 equiv of styrene (**3a**) in MeCN solution and under 450 nm blue LED irradiation, the azetidine **4aa** could be isolated in a high yield of 89% after 24 h. As expected, the photocycloaddition was relatively insensitive to change of solvent (Table S2). Anthraquinones and thioxanthone as organic photosensitizers (10 mol % each) were comparatively less effective. 1,5-Dichloroanthraquinone (1,5-ClAQ) promoted the reaction **2a** + **3a** → **4aa** only under irradiation with 450 ± 50 nm CFL lamps to give azetidine **4aa** in a fairly low yield of 11% after 24 h. When using thioxanthone, irradiation with 370 nm centered CFL lamps led to cycloadduct **4aa** in 60% yield after 24 h. Finally, the one-pot photocatalytic reaction was examined, with $Ir[dF(CF_3)ppy]_2(dtbpy)^+$ and $Ir(ppy)_3$ as the photocatalysts (Table S3). We found that styrene (**3a**) could be added to the reaction mixture from the very beginning, and when the solution was irradiated in the presence of oxygen for 24 h, cycloadduct **4aa** formed cleanly, as a single diastereomer (*dr* > 19:1). $Ir(ppy)_3$ again gave superior results. In addition, it was verified that azetidine **4aa** was sufficiently stable to the photooxidative reaction conditions, and in a control experiment we could only observe marginal degradation of **4aa** (see the Supporting Information). After some experimentation, we developed a practical protocol whereby the reaction solution, in a 10 mL reaction vial, was exposed to ambient atmosphere for 3 h by using a cannula for gas exchange, which was then removed, and irradiation was continued in the sealed vessel for further 21 h. Hence, it was not necessary to replace air by inert gas after complete consumption of substrate **1a**, and the optimized procedure allowed for the isolation of azetidine **4aa** in 75% yield.

Scheme 3. Summary of Reaction Development[a]

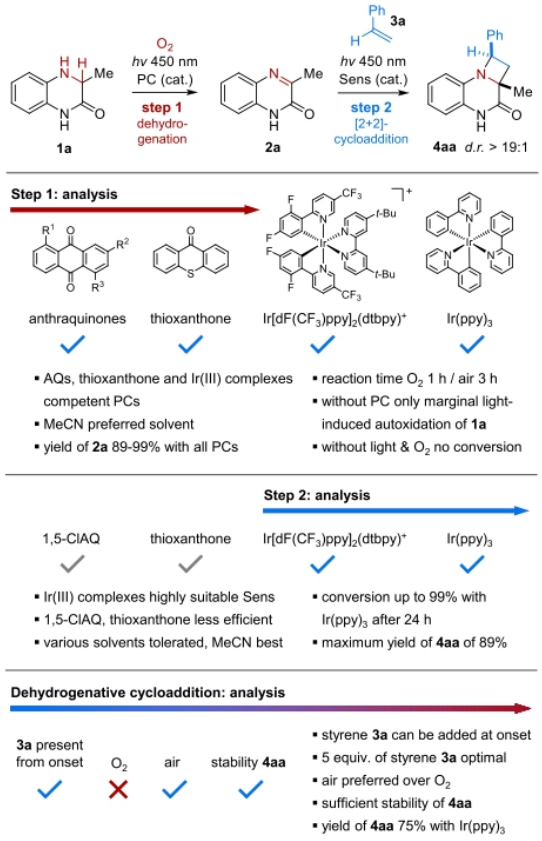

[a]Individual reaction steps were analyzed prior to the dehydrogenative photocatalytic reaction. PC = photocatalyst, Sens = photosensitizer.

A scope of the one-pot dehydrogenative [2 + 2] cycloaddition between dihydroquinoxalinones **1** and alkenes **3** is depicted in Figure 1. The racemic azetidine derivatives **4aa**−**4ah** were readily accessed from dihydro compound **1a** and *para*- as well as *meta*-substituted styrenes **3a**−**3h** in yields from 56 to 87% (Figure 1a). Even the sterically highly shielded 1,3-dichloro-2-vinylbenzene (**3i**) could successfully be employed as the alkene to give product **4ai** in 69% yield. All of the azetidines **4aa**−**4ai** were formed as single regio- and

https://doi.org/10.1021/acs.orglett.2c03291
Org. Lett. 2022, 24, 8041−8046

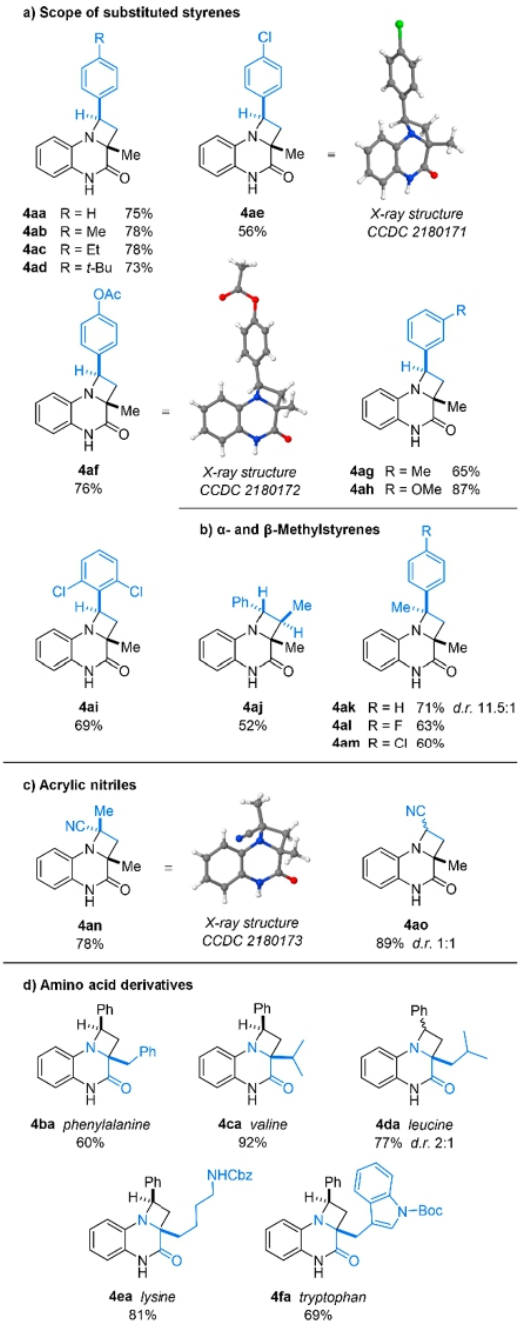

Figure 1. Scope of azetidine products **4** from the photocatalytic dehydrogenative [2 + 2] cycloaddition of dihydroquinoxalinones **1** with alkenes **3**. Reaction conditions: 0.10 mmol of **1**, 0.50 mmol of **3** (5 equiv), 2 mol % $Ir(ppy)_3$, MeCN, all components added at the beginning, 10 mL reaction vial. Irradiation with 450 nm blue LED (30 W) at 30 °C, for 3 h open to ambient air, then for 21 h in sealed vial.

diastereoisomers (*dr* > 19:1) as verified by ^{1}H NMR spectroscopic analysis of the crude reaction mixtures. In addition, the reaction between substrate **1a** and styrene (**3a**) could also be performed on a 1 mmol scale, using a slightly altered irradiation setup, to give cycloadduct **4aa** in 74% yield (see the Supporting Information for details).

α- and β-methylstyrenes were further suitable alkenes (Figure 1b), and the reaction between dihydroquinoxalinone **1a** and β-methylstyrene (**3j**) led to azetidine **4aj** in 52% yield (*dr* > 19:1). Utilization of the α-methylstyrenes **3k**–**3m** produced cycloadducts **4ak**–**4am** with yields of 60–71%. In the case of compound **4ak**, a *dr* of 11.5:1 was observed, whereas compounds **4al** and **4am** were again pure diastereomers (*dr* > 19:1). Further, acrylic nitriles could be employed (Figure 1c). The reaction between substrate **1a** and methacrylonitrile (**3n**) gave rise to cycloadduct **4an** as a single diastereomer (78% yield, *dr* > 19:1). On the other hand, use of acrylonitrile (**3o**) produced cyano-substituted azetidine **4ao** in 89% yield as a 1:1 mixture of diastereomers. A number of further alkenes were evaluated in the dehydrogenative cycloaddition with compound **1a** but found to be unsuitable reaction partners (see the Supporting Information). Finally, we employed amino acid-derived dihydroquinoxalinones **1b**–**1f** in the reaction (Figure 1d), and we were pleased to observe that the corresponding cycloadducts with styrene (**3a**), the azetidines **4ba**–**4fa**, were formed cleanly in 60–92% isolated yield. Of particular utility, the lysine- and tryptophan-derived cycloadducts **4ea** and **4fa**, both highly sensitive toward reactive oxygen species, could be obtained without any notable byproducts. Compounds **4ba**, **4ca**, **4ea**, and **4fa** were again formed as single regio- and diastereoisomers. Compound **4da**, made from the leucine-derived dihydroquinoxalinone **1d**, was however obtained as a mixture (*dr* 2:1).

A summary of experiments aimed at elucidating the reaction mechanism is given in Scheme 4, beginning with the

Scheme 4. Summary of Mechanistic Studies

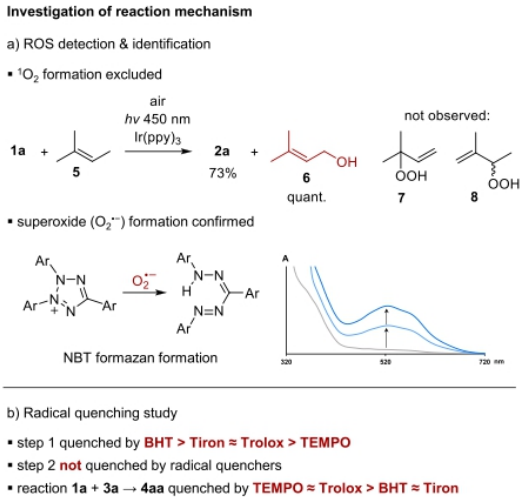

identification of the reactive oxygen species (ROS) in the dehydrogenation reaction **1a** → **2a**. When the $Ir(ppy)_3$-catalyzed reaction was performed in the presence of 2-methyl-2-butene (**5**), quinoxalinone **2a** formed cleanly, while the alkene was selectively and quantitatively converted into prenol (**6**) (Scheme 4a). This result indicated that superoxide radical anion, $O_2^{\bullet-}$, was generated which induced an oxidation reaction via radical intermediates. Notably, the allylic hydroperoxides **7** and **8** could not be detected, which ruled out a contribution of singlet oxygen ($^1O_2$). Consistent with these observations, addition of the $^1O_2$-quencher DABCO[16] to the reaction mixture had almost no effect on conversion of

https://doi.org/10.1021/acs.orglett.2c03291
Org. Lett. 2022, 24, 8041–8046

substrate **1a** (Table S4). The presence of superoxide in the $Ir(ppy)_3$-catalyzed oxidation **1a** → **2a** was additionally confirmed by the addition of nitro-blue tetrazolium (NBT)[17] to the reaction mixture, which was rapidly converted into its monoformazan as evident from UV−vis analysis (Scheme 4a and Figure S5). In order to probe for radical intermediates in the dehydrogenative reaction **1a** + **3a** → **4aa**, the individual reaction steps as well as the one-pot reaction were conducted in the presence of radical quenching agents (2 equiv each, Scheme 4b and Table S4). Consistent with the previous detection of superoxide, the dehydrogenation **1a** → **2a** was most strongly inhibited by the antioxidant butylated hydroxytoluene (BHT),[18] which reduced the conversion of substrate **1a** to 40%, followed by the superoxide scavenger Tiron (sodium 4,5-dihydroxybenzene-1,3-disulfonate)[19] and the free-radical quenchers Trolox (6-hydroxy-2,5,7,8-tetramethylchroman-2-carboxylic acid)[20] and TEMPO.[21] However, none of these agents showed any inhibition of the sensitized [2 + 2] photocycloaddition **2a** + **3a** → **4aa**. Even though this reaction proceeds via a biradical intermediate, bimolecular quenching evidently could not compete with intramolecular ring closure. Conversely, the one-pot dehydrogenative cycloaddition **1a** + **3a** → **4aa** was again strongly impacted by all quenching agents, and when using Trolox and TEMPO, large amounts of quinoxalinone **2a** were present after 24 h (42% as well as 57% relative to the fraction of azetidine **4aa**). Time/conversion monitoring of the dehydrogenative reaction **1a** + **3a** → **4aa** by NMR spectroscopy (Figure S6) showed that quinoxalinone **2a** and cycloadduct **4aa** are initially generated in parallel, and this observation pointed toward the occurrence of two product-forming pathways, one being the consecutive reaction via intermediate **2a**, while a second pathway converts substrate **1a** directly into azetidine **4aa**. The quenching experiments suggested a near equal split between them (Table S4).

The proposed mechanism is depicted in Scheme 5, for the $Ir(ppy)_3$-catalyzed reactions between dihydroquinoxalinones **1** and styrenes **3** as the alkenes (for an extended mechanism discussion, see the Supporting Information). $Ir(ppy)_3$ is excited to its triplet state by blue (450 nm) light. The excited-state reduction potential E^*_{red} of $Ir(ppy)_3$* is +0.31 V vs SCE,[22] while the oxidation potential E_{ox} of dihydroquinoxalinone **1a** was experimentally determined as +0.84 V vs SCE (see the Supporting Information), which rules out a one-electron oxidation of compounds **1** by $Ir(ppy)_3$*. Instead, $O_2^{\bullet-}$ is generated through the oxidative quench of $Ir(ppy)_3$* (E^*_{ox} = −1.73 V vs SCE)[22] by O_2 (E_{red} ($O_2/O_2^{\bullet-}$) ≈ −1.00 V vs SCE)[17a] to subsequently react with substrate **1** via hydrogen abstraction, giving the well-stabilized α-amino radical **9** and HOO^-. From radical **9**, two product-forming pathways are pursued as long as it continues to be generated from dihydro compound **1**. Path I continues with the SET oxidation of intermediate **9** by the available Ir(IV) species (E_{red} = +0.77 V vs SCE)[22] followed by deprotonation of the resulting iminium ion to give quinoxalinone **2** and H_2O_2. Pathway II comprises a radical/polar crossover cyclization[23] to azetidines **4** by the addition of radical **9** onto styrene **3**, followed by SET oxidation of the adduct **10** by Ir(IV) and cationic ring closure of benzylic cation **11**. In continuation of path I, the Ir(III)-sensitized [2 + 2]-cycloaddition between quinoxalinone **2** and styrene **3** occurs, with ring-closure via a triplet biradical intermediate. In addition to products **4**, the photodimerization products of styrenes **3**, the 1,3-diarylcyclobutanes **12**, were observed as byproducts in all of the reactions catalyzed by $Ir(ppy)_3$ as well as $Ir[dF(CF_3)ppy]_2(dtbpy)^+$. However, they formed only during the final stage of the reaction, proving that the photocycloadditions between quinoxalinones **2** and styrenes **3** proceed via selective sensitization of the heterocycles **2**.

In conclusion, we developed photocatalytic dehydrogenative [2 + 2] cycloadditions between amines and alkenes that allow for the highly stereoselective and atom-economic synthesis of functionalized azetidines. Further synthetic applications of dehydrogenative cycloadditions are currently being explored by us.

Scheme 5. Proposed Reaction Mechanism

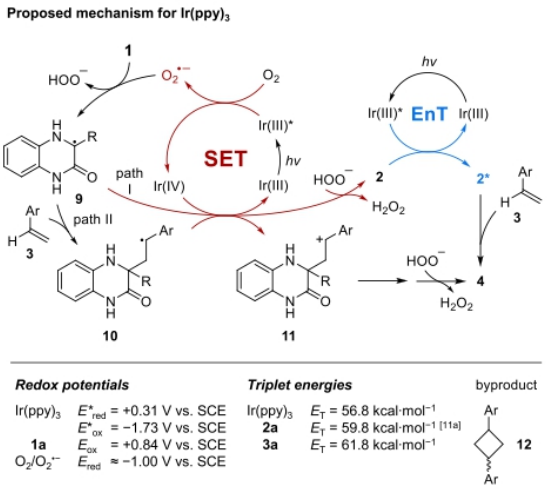

■ ASSOCIATED CONTENT

Data Availability Statement

The data underlying this study are available in the published article and its online Supporting Information.

Supporting Information

The Supporting Information is available free of charge at https://pubs.acs.org/doi/10.1021/acs.orglett.2c03291.

Full experimental details, compound characterization, and crystal data (PDF)

Accession Codes

CCDC 2180171−2180173 contain the supplementary crystallographic data for this paper. These data can be obtained free of charge via www.ccdc.cam.ac.uk/data_request/cif, or by emailing data_request@ccdc.cam.ac.uk, or by contacting The Cambridge Crystallographic Data Centre, 12 Union Road, Cambridge CB2 1EZ, UK; fax: +44 1223 336033.

■ AUTHOR INFORMATION

Corresponding Author

Malte Brasholz − *University of Rostock, Institute of Chemistry, 18059 Rostock, Germany; Leibniz-Institut für Katalyse e.V., 18059 Rostock, Germany;* orcid.org/0000-0001-8184-646X; Email: malte.brasholz@uni-rostock.de

https://doi.org/10.1021/acs.orglett.2c03291
Org. Lett. 2022, 24, 8041−8046

Authors

Rajesh Dasi − *University of Rostock, Institute of Chemistry, 18059 Rostock, Germany;* orcid.org/0000-0001-8911-7042

Alexander Villinger − *University of Rostock, Institute of Chemistry, 18059 Rostock, Germany;* orcid.org/0000-0002-0868-9987

Complete contact information is available at: https://pubs.acs.org/10.1021/acs.orglett.2c03291

Author Contributions

The manuscript was written through contributions of all authors. All authors have given approval to the final version of the manuscript.

Notes

The authors declare no competing financial interest.

■ ACKNOWLEDGMENTS

The authors acknowledge financial support of this project by the strategic network funding program of the Leibniz association, within the project "Leibniz-WissenschaftsCampus-ComBioCat-Rostock". R.D. thanks this program for a Ph.D. fellowship.

■ REFERENCES

(1) (a) Kobayashi, S., Jørgensen, K. A., Eds. *Cycloaddition Reactions in Organic Synthesis*; Wiley-VCH: Weinheim, 2001. (b) Nishikawa, N., Ed. *Methods and Applications of Cycloaddition Reactions in Organic Syntheses*; John Wiley & Sons: Hoboken, 2013.

(2) Kannegiesser, M. *Value Chain Management in the Chemical Industry*; Physica-Verlag: Heidelberg, 2008.

(3) (a) Huo, C.; Xie, H.; Wu, M.; Jia, X.; Wang, X.; Chen, F.; Tang, J. CBr_4-Mediated Cross-Dehydrogenative Coupling Reaction of Amines. *Chem.—Eur. J.* **2015**, *21*, 5723−5726. (b) Xie, Z.; Jia, J.; Liu, X.; Liu, L. Copper(II) Triflate-Catalyzed Aerobic Oxidative C-H Functionalization of Glycine Derivatives with Olefins and Organoboranes. *Adv. Synth. Catal.* **2016**, *358*, 919−925. (c) Ni, M.; Zhang, Y.; Gong, T.; Feng, B. Gold-Oxazoline Complex-Catalyzed Cross-Dehydrogenative Coupling of Glycine Derivatives and Alkenes. *Adv. Synth. Catal.* **2017**, *359*, 824−831. (d) Chen, X.; Zhang, G.; Zeng, R. Dehydrogenative Aza-[4 + 2] Cycloaddition of Amines with 1,3-Dienes via Dual Catalysis. *Org. Lett.* **2021**, *23*, 7144−7149. (e) Qi, C.; Cong, H.; Cahill, K. J.; Müller, P.; Johnson, R. P.; Porco, J. A., Jr. Biomimetic Dehydrogenative Diels−Alder Cycloadditions: Total Syntheses of Brosimones A and B. *Angew. Chem., Int. Ed.* **2013**, *52*, 8345−8348. (f) Nakao, Y.; Morita, E.; Idei, H.; Hiyama, T. Dehydrogenative [4 + 2] Cycloaddition of Formamides with Alkynes through Double C−H Activation. *J. Am. Chem. Soc.* **2011**, *133*, 3264−3267.

(4) (a) Yang, X.; Li, L.; Li, Y.; Zhang, Y. Visible-Light-Induced Photocatalytic Aerobic Oxidative Csp^3−H Functionalization of Glycine Derivatives: Synthesis of Substituted Quinolines. *J. Org. Chem.* **2016**, *81*, 12433−12442. (b) He, Y.; Yan, B.; Tao, H.; Zhang, Y.; Li, Y. Metal-free photocatalyzed aerobic oxidative Csp^3−H functionalization of glycine derivatives: one-step generation of quinoline-fused lactones. *Org. Biomol. Chem.* **2018**, *16*, 3816−3823. (c) Schendera, E.; Villinger, A.; Brasholz, M. Photoinduced iodine-mediated tandem dehydrogenative Povarov cyclisation/C−H oxygenation reactions. *Org. Biomol. Chem.* **2020**, *18*, 6912−6915. (d) Schendera, E.; Unkel, L.-N.; Huyen Quyen, P. P.; Salkewitz, G.; Hoffmann, F.; Villinger, A.; Brasholz, M. Visible-Light-Mediated Aerobic Tandem Dehydrogenative Povarov/Aromatization Reaction: Synthesis of Isocryptolepines. *Chem.—Eur. J.* **2020**, *26*, 269−274.

(5) Wang, H.-J.; Guo, L.; Zhu, C.-F.; Luo, Y.-F.; Li, Y.-G.; Wu, X. Pd/C-Catalyzed Dehydrogenative [3 + 2] Cycloaddition for the Synthesis of Functionalized Tropanes. *Eur. J. Org. Chem.* **2018**, *2018*, 5456−5459.

(6) Hore, S.; Singh, A.; De, S.; Singh, N.; Gandon, V.; Singh, R. P. Polyarylquinone Synthesis by Relayed Dehydrogenative [2 + 2 + 2] Cycloaddition. *ACS Catal.* **2022**, *10*, 6227−6237.

(7) Huo, C.; Xie, H.; Chen, F.; Tang, J.; Wang, Y. Double-Oxidative Dehydrogenative (DOD) Cyclization of Glycine Derivatives with Dioxane under Metal-Free Aerobic Conditions. *Adv. Synth. Catal.* **2016**, *358*, 724−730.

(8) Review of the Aza Paternò−Büchi reaction: (a) Richardson, A. D.; Becker, M. R.; Schindler, C. S. Synthesis of azetidines by aza Paternò-Büchi reactions. *Chem. Sci.* **2020**, *11*, 7553−7561. Selected recent examples: (b) Becker, M. R.; Wearing, E. R.; Schindler, C. S. Synthesis of azetidines via visible-light-mediated intermolecular [2 + 2] photocycloadditions. *Nat. Chem.* **2020**, *12*, 898−905. (c) Becker, M. R.; Richardson, A. D.; Schindler, C. S. Functionalized azetidines via visible light-enabled aza Paternò-Büchi reactions. *Nat. Commun.* **2019**, *10*, 5095.

(9) Reviews of the Paternò−Büchi reaction: (a) D'Auria, M.; Racioppi, R. Oxetane Synthesis Through the Paternò-Büchi Reaction. *Molecules* **2013**, *18*, 11384−11428. (b) Abe, M. Recent Progress Regarding Regio-, Site-, and Stereoselective Formation of Oxetanes in Paternò-Buchi Reactions. *J. Chin. Chem. Soc.* **2008**, *55*, 479−486. Selected recent examples: (c) Zhang, D.; Wu, C.; Zhou, H.; Ma, Y.; Zhu, Y. Photocatalyst-free, visible-light mediated Paternò-Büchi reaction between dicarbonyl compounds and olefins. *Asian J. Org. Chem.* **2022**, No. e202200561. (d) Zheng, J.; Dong, X.; Yoon, T. P. Divergent Photocatalytic Reactions of α-Ketoesters under Triplet Sensitization and Photoredox Conditions. *Org. Lett.* **2020**, *22*, 6520−6525. (e) Mateos, J.; Vega-Peñaloza, A.; Franchesci, P.; Rigodanza, F.; Andreetta, P.; Companyó, X.; Pelosi, G.; Bonchio, M.; Dell'Amico, L. A visible-light Paternò-Büchi dearomatisation process towards the construction of oxetoindolinic polycycles. *Chem. Sci.* **2020**, *11*, 6532−6538. (f) Rykaczewski, K. A.; Schindler, C. S. Visible-Light-Enabled Paternò-Büchi Reaction via Triplet Energy Transfer for the Synthesis of Oxetanes. *Org. Lett.* **2020**, *22*, 6516−6519.

(10) (a) Nishio, T. The (2 + 2) photocycloaddition of the carbon-nitrogen double bond of quinoxalin-2(1*H*)-ones to electron-deficient olefins. *J. Org. Chem.* **1984**, *49*, 827−832. (b) Nishio, T.; Omote, Y. Photocycloaddition of quinoxalin-2-ones and benzoxazin-2-ones to aryl alkenes. *J. Chem. Soc., Perkin Trans. 1* **1987**, 2611−2615.

(11) (a) Li, X.; Großkopf, J.; Jandl, C.; Bach, T. Enantioselective, Visible Light Mediated Aza Paternò-Büchi Reactions of Quinoxalinones. *Angew. Chem., Int. Ed.* **2021**, *60*, 2684−2688. (b) Recent review: Großkopf, J.; Kratz, T.; Rigotti, T.; Bach, T. Enantioselective Photochemical Reactions Enabled by Triplet Energy Transfer. *Chem. Rev.* **2022**, *122*, 1626−1653.

(12) Tanimori, S.; Kashiwagi, H.; Nishimura, T.; Kirihata, M. A General and Practical Access to Chiral Quinoxalinones with Low Copper-Catalyst Loading. *Adv. Synth. Catal.* **2010**, *352*, 2531−2537.

(13) Recent examples: (a) Unkel, L.-N.; Malcherek, S.; Schendera, E.; Hoffmann, F.; Rehbein, J.; Brasholz, M. Photoorganocatalytic Aerobic Oxidative Amine Dehydrogenation/Super Acid-Mediated Pictet-Spengler Cyclization: Synthesis of cis-1,3-Diaryl Tetrahydroisoquinolines. *Adv. Synth. Catal.* **2019**, *361*, 2870−2876. (b) Frahm, M.; von Drathen, T.; Gronbach, L. M.; Voss, A.; Lorenz, F.; Bresien, J.; Villinger, A.; Hoffmann, F.; Brasholz, M. Visible-Light Cascade Photooxygenation of Tetrahydrocarbazoles and Cyclohepta[*b*]-indoles: Access to *C,N* -Diacyliminium Ions. *Angew. Chem., Int. Ed.* **2020**, *59*, 12450−12454.

(14) Sahoo, M. K.; Jaiswal, G.; Rana, J.; Balaraman, E. Organo-Photoredox Catalyzed Oxidative Dehydrogenation of N-Heterocycles. *Chem.—Eur. J.* **2017**, *23*, 14167−14172.

(15) Reviews of energy transfer (EnT) photocatalysis: (a) Strieth-Kalthoff, F.; James, M. J.; Teders, M.; Pitzer, L.; Glorius, F. Energy transfer catalysis mediated by visible light: principles, applications, directions. *Chem. Soc. Rev.* **2018**, *47*, 7190−7202. (b) Strieth-Kalthoff, F.; Glorius, F. Triplet Energy Transfer Photocatalysis: Unlocking the Next Level. *Chem.* **2020**, *6*, 1888−1903.

(16) Ouannes, C.; Wilson, T. Quenching of Singlet Oxygen by Tertiary Aliphatic Amines. Effect of DABCO. *J. Am. Chem. Soc.* **1968**, *90*, 6527−6528.
(17) (a) Hayyan, M.; Hashim, M. A.; AlNashef, I. M. Superoxide Ion: Generation and Chemical Implications. *Chem. Rev.* **2016**, *116*, 3029−3085. (b) Wang, R.; Qu, R.; Jing, C.; Zhai, Y.; An, Y.; Shi, L. Zinc porphyrin/fullerene/block copolymer micelle for enhanced electron transfer ability and stability. *RSC Adv.* **2017**, *7*, 10100−10107.
(18) Yehye, W. A.; Rahman, N. A.; Ariffin, A.; Hamid, S. B. A.; Alhadi, A. A.; Kadir, F. A.; Yaeghoobi, M. Understanding the chemistry behind the antioxidant activities of butylated hydroxytoluene (BHT): A review. *Eur. J. Med. Chem.* **2015**, *101*, 295−312.
(19) Liubimovskii, S. O.; Ustynyuk, L. Y.; Tikhonov, A. N. Superoxide radical scavenging by sodium 4,5-dihydroxybenzene-1,3-disulfonate dissolved in water: Experimental and quantum chemical studies. *J. Mol. Liq.* **2021**, *333*, 115810.
(20) Alberto, M. E.; Russo, N.; Grand, A.; Galano, A. A physicochemical examination of the free radical scavenging activity of Trolox: mechanism, kinetics and influence of the environment. *Phys. Chem. Chem. Phys.* **2013**, *15*, 4642−4650.
(21) (a) Beckwith, A. L. J.; Bowry, V. W.; Ingold, K. U. Kinetics of Nitroxide Radical Trapping. 1. Solvent Effects. *J. Am. Chem. Soc.* **1992**, *114*, 4983−4992. (b) Kocherginsky, N.; Swartz, H. M. *Nitroxide Spin Labels. Reactions in Biology and Chemistry*; CRC Press: Boca Raton, 1995.
(22) Flamigni, L.; Barbieri, A.; Sabatini, C.; Ventura, B.; Barigelletti, F.; Balzani, V.; Campagna, S. Photochemistry and Photophysics of Coordination Compounds II. *Top. Curr. Chem.* **2007**, *281*, 143−204.
(23) Reviews: (a) Sharma, S.; Singh, J.; Sharma, A. Visible Light Assisted Radical-Polar/Polar-Radical Crossover Reactions in Organic Synthesis. *Adv. Synth. Catal.* **2021**, *363*, 3146−3169. (b) Wiles, R. J.; Molander, G. A. Photoredox-Mediated Net-Neutral Radical/Polar Crossover Reactions. *Isr. J. Chem.* **2020**, *60*, 281−293.

https://doi.org/10.1021/acs.orglett.2c03291
Org. Lett. 2022, 24, 8041−8046

5.4. Photoredox-induced deaminative radical-cationic three-component couplings with *N*-alkylpyridinium salts and alkenes

Paul Seefeldt, Rajesh Dasi, Alexander Villinger, Malte Brasholz*

Chem Photo Chem **2021**, *5*, 979-983

DOI: 10.1002/cptc.202100226

In this work, I was involved in the investigation of substrate scope, isolation, and characterization of compounds. In addition, I wrote a part of the supporting information for the manuscript. My contribution as the co-author of this paper is approximately 30%.

Check for updates

ChemPhotoChem

Communications
doi.org/10.1002/cptc.202100226

Chemistry Europe
European Chemical Societies Publishing

Photoredox-Induced Deaminative Radical-Cationic Three-Component Couplings with *N*-Alkylpyridinium Salts and Alkenes

Paul Seefeldt,[a] Rajesh Dasi,[a] Alexander Villinger,[a] and Malte Brasholz*[a, b]

In memory of Professor Klaus Hafner

N-Benzyl- and *N*-2°-alkylpyridinium salts were engaged in visible-light-driven, photoredox-induced radical-cationic three-component couplings with *N*-methylmaleimide and acrylonitrile as radical acceptors, in combination with 1,1-diarylethylenes as donor alkenes. These multicomponent coupling reactions could be achieved under mild conditions, with high efficiency, and to furnish diverse 3,4-disubstituted pyrrolidin-2,5-dione products with high stereoselectivity. In addition, 2,3-diaryl-1,3-butadienes could be utilized as alternative donor alkene components, to furnish diastereomerically pure 1,2,3-trisubstituted 1,3-butadienes as the coupling products.

Radical and radical-ionic multicomponent reactions constitute an efficient and flexible approach to rapidly generate molecular complexity from simple and readily available building blocks.[1] The choice of suitable reactants for a desired radical coupling reaction is usually guided by considering their electronic properties, that is, radical philicity,[2] and the adjuvant contribution of polar effects.[3] The reactivity of alkenes in radical multicomponent reactions is generally governed by their relative reactivity and polarizability, and in polymer synthesis, this is reflected by the *Q-e* classification, where *Q* expresses an alkene monomer's scaled reactivity and *e* its polarization.[4]

The advent of photoredox catalysis has led to a renewal of interest in the development of radical multicomponent reactions, as with its instruments, many of these protocols can now be performed under exceptionally mild and environmentally benign conditions.[5] The 1,2-difunctionalization of alkenes by photoredox catalysis[6] has emerged as a particularly prominent method for radical-cationic couplings. It involves the generation of a *C*-centered radical from a given precursor, its addition to an electron-rich alkene followed by SET oxidation. After radical-polar cross-over ('RPCO'),[7] the resulting carbenium ion may be trapped by a nucleophile Nu^- or eliminate H^+ (Scheme 1a). More recently, such reactions have also been demonstrated engaging a *C*-centered radical ('component 1') with two alkene building blocks, 'components 2 and 3' to result in radical-cationic three-component couplings (Scheme 1b).

Meanwhile, the toolbox of photoredox catalysis has been further expanded by the introduction of *N*-alkyl- and *N*-alkoxypyridinium salts as radical precursors.[8] Due to their ease of preparation, bench stability and favorable redox properties, deaminative radical coupling reactions with *N*-alkylpyridinium species are highly attractive, and they have also been extended into the area of multicomponent coupling reactions. In 2019,

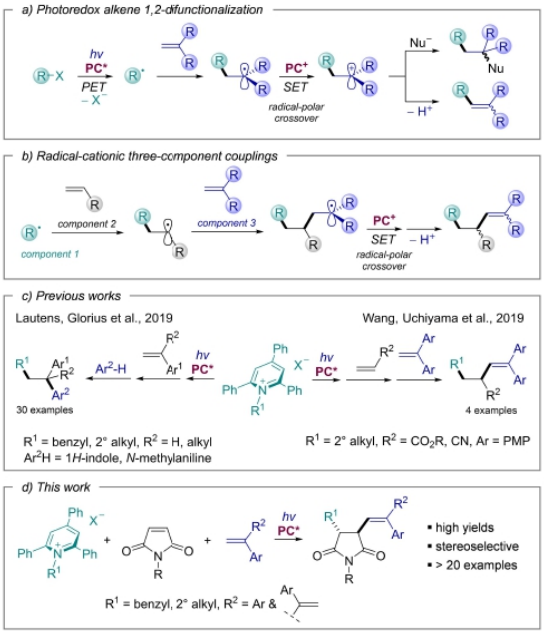

Scheme 1. Methods for photoredox radical-ionic multicomponent couplings.

[a] *P. Seefeldt, R. Dasi, Dr. A. Villinger, Prof. Dr. M. Brasholz*
Institute of Chemistry
University of Rostock
Albert-Einstein-Str. 3a
18059 Rostock (Germany)
E-mail: malte.brasholz@uni-rostock.de
[b] *Prof. Dr. M. Brasholz*
Leibniz-Institut für Katalyse e.V.
Albert-Einstein-Str. 29a
18059 Rostock (Germany)

Supporting information for this article is available on the WWW under https://doi.org/10.1002/cptc.202100226

Lautens, Glorius and co-workers developed a photoredox-induced 1,2-difunctionalization of styrenes with *N*-benzyl and *N*-alkylpyridinium salts, and arenes as nucleophiles (Scheme 1c, left).[9] In the same year, Wang and Uchiyama et al. reported photoredox radical-cationic three-component couplings of *N*-alkylpyridinium salts with acrylates and 1,1-diarylethylenes as the third component.[10]

Our interest in this area led us to investigate further potential variants of photoredox-induced radical-ionic three-component couplings, and we report here donor-acceptor-donor (DAD) couplings between *N*-alkylpyridinium salts, with maleimides and acrylonitrile as acceptors, in combination with styrene derivatives as well as 1,3-dienes as donors (Scheme 1d). The new coupling products were obtained in attractive yields, and with high stereoselectivity in case of the maleimide-derived 3,4-disubstituted pyrrolidin-2,5-diones.

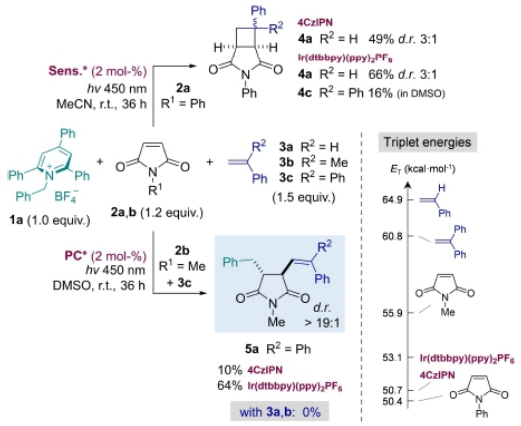

Scheme 2. Preliminary results: Photosensitized [2+2]-cycloaddition vs. photoredox-induced radical coupling pathways in the reaction between radical precursor **1a**, *N*-substituted maleimides **2a,b** and styrenes **3a–c**. Reported yields were determined by ^{1}H NMR spectroscopic analysis.

As an initial model reaction, we chose to combine pyridinium salt **1a**, precursor to the nucleophilic benzyl radical ('component 1'), with *N*-substituted maleimides **2a,b** as the electrophilic acceptor alkenes ('component 2'), along with styrenes **3a–c** as the donor alkenes ('component 3'). In the preliminary experiments shown in Scheme 2, it was soon established that when utilizing *N*-phenylmaleimide **2a**, no photoelectron transfer (PET) process occurred in the presence of the blue light-absorbing photocatalysts $[Ir(dtbbpy)(ppy)_2]PF_6$ or 4CzIPN. Instead, salt **1a** was left unreacted, and the [2+2]-cycloadducts **4a** and **4c** formed exclusively in yields between 16–66% (determined by ^{1}H-NMR analysis) as a result of energy transfer (EnT) catalysis.[11] The triplet energies E_T of $[Ir(dtbbpy)(ppy)_2]^+$ and 4CzIPN amount to 53.1 kcal·mol^{-1} and 50.7 kcal·mol^{-1} respectively,[12][13] and while those of styrene (**3a**, E_T = 64.9 kcal·mol^{-1})[14] and 1,1-diphenylethylene (**3c**, E_T = 60.8 kcal·mol^{-1})[14] are too high for them to act as energy acceptors, *N*-phenylmaleimide (**2a**, E_T = 50.4 kcal·mol^{-1})[15] is readily triplet-sensitized by both catalysts. Conversely, employing *N*-methylmaleimide **2b** in the reaction (E_T = 55.9 kcal·mol^{-1}),[15] the unwanted [2+2]-cycloaddition pathway could be suppressed, and the desired three-component radical coupling was achieved, with 1,1-diphenylethylene (**3c**) as the donor olefin, to give the 3,4-disubstituted pyrrolidin-2,5-dione **5a** in 64% yield and as a single *trans*-diastereomer. The same reaction using styrene (**3a**) or α-methylstyrene (**3b**) in place of **3c** was not feasible.

The three-component coupling **1a**+**2b**+**3c**→**5a** was subsequently further optimized as summarized in Table 1 (see also Table S1). A photocatalyst screening (entries 1–4, each used in 2 mol-% quantity) revealed that $Ru(bpy)_3^{2+}$ is even superior to $[Ir(dtbbpy)(ppy)_2]^+$ and it produced product **5a** in 81% isolated yield after 36 h reaction time. With a triplet

Table 1. Summary of the optimization of reaction conditions for the three-component coupling reaction **1a**+**2b**+**3c**→**5a**.

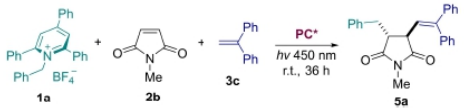

#	PC [mol-%]	solvent	equiv. (**1a**/**2b**/**3c**)	conv. **1a** [%][a]	Yield **5a** [%][b]
1	4CzIPN (2)	DMSO	(1/1.2/1.5)	68	10
2	$[Ir(dtbbpy)(ppy)_2]PF_6$ (2)	DMSO	(1/1.2/1.5)	100	64
3	$Ir(ppy)_3$ (2)	DMSO	(1/1.2/1.5)	50	45
4	$Ru(bpy)_3(PF_6)_2$ (2)	DMSO	(1/1.2/1.5)	100	82 (81)[c]
5	$Ru(bpy)_3(PF_6)_2$ (2)	MeCN	(1/1.2/1.5)	17	15
6	$Ru(bpy)_3(PF_6)_2$ (2)	DMF	(1/1.2/1.5)	100	78
7	$Ru(bpy)_3(PF_6)_2$ (2)	acetone	(1/1.2/1.5)	37	30
8	$Ru(bpy)_3(PF_6)_2$ (1)	DMSO	(1/1.2/1.5)	100	86 (82)[c]
9	$Ru(bpy)_3(PF_6)_2$ (1)	DMSO	(1/1.5/2)	77	71
10	$Ru(bpy)_3(PF_6)_2$ (1)	DMSO	(1/1.7/2.2)	77	69
11	$Ru(bpy)_3(PF_6)_2$ (1)	DMSO	(1/2/2.5)	70	66
12	none	DMSO	(1/1.2/1.5)	0	0
13	$Ru(bpy)_3(PF_6)_2$ (1)[d]	DMSO	(1/1.2/1.5)	0	0

[a] Determined by ^{1}H NMR spectroscopic analysis. [b] Determined by ^{1}H NMR spectroscopy vs internal standard. [c] Yields after chromatography. [d] Reaction run without irradiation.

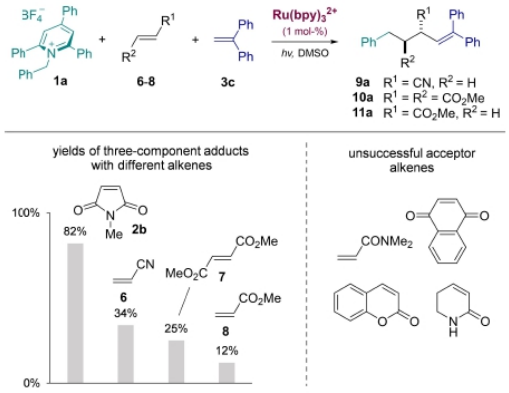

Scheme 3. Variation of 'component 2' acceptor alkenes under the optimized reaction conditions.

energy of $E_T = 48.9$ kcal·mol^{-1},[16] $Ru(bpy)_3^{2+}$ likewise cannot sensitize the [2 + 2]-photocycloaddition between **2b** and **3a–c**, which was again verified by control experiments under the reaction conditions. Comparison of solvents (entries 4–7) showed that DMSO is the optimal choice, and the catalyst loading could be lowered to 1 mol-% without any loss in overall yield (entry 8). The optimum ratio of the coupling partners **1a**/**2b**/**3c** was determined to be 1/1.2/1.5 (entries 8–11). As expected, no reaction occurred in the absence of photocatalyst nor in the dark (entries 12 and 13).

After we had identified the optimal reaction conditions for the reactant trio **1a** + **2b** + **3c**, we attempted variations of the 'component 2' acceptor alkene. As shown in Scheme 3, replacing *N*-methylmaleimide (**2b**) by acrylonitrile (**6**),[10] dimethyl fumarate (**7**) and methyl acrylate (**8**) under identical reaction conditions allowed for the isolation of the corresponding three-component adducts **9a**, *anti*-**10a** (*d.r.* > 19:1) and **11a** in moderate to fairly low yields of 34%, 25% and 12% respectively. Other acceptor alkenes like 1,4-naphthoquinone, *N,N*-dimethylacrylamide, coumarin and dihydropyridine-2-one failed to give any detectable amounts of the corresponding products.

Figure 1 depicts a broader reaction scope utilizing *N*-methylmaleimide (**2b**) as well as acrylonitrile (**6**) as the electrophilic alkenes, each under the optimized reaction conditions (Table 1, entry 8), and with variation of the alkyl radical precursor as well as the 1,1-diarylethylene coupling partner. As shown in Figure 1a, various 4-substituted arylmethylpyridinium salts gave rise to the functionalized pyrrolidin-2,5-diones **5a–5f** in 29–82% yield, generally with a high *trans*-diastereoselectivity, with the exception of compound **5c** which was obtained with a *d.r.* of 6.7:1. In contrast to the reactions involving benzyl radicals, utilization of *N*-2°-alkylpyridinium salts led to a significant decrease in yield, to produce the cyclopentyl- and isopropyl-substituted derivatives **5g** and **5h** in 20% and 27% yield respectively (in these cases, $[Ir(dtbbpy)(ppy)_2]^+$ was more efficient as the photocatalyst compared to $Ru(bpy)_3^{2+}$). Figure 1b depicts a scope of the 1,1-diarylethylene component, and upon its variation with electron-donating and -withdrawing substituents in the *para*-position of the two aromatic rings, the corresponding pyrrolidine-2,5-diones **5i-p** could be accessed in 42–87% yield. The three-component couplings involving acrylonitrile (**6**) generally provided moderate yields, both upon variation of the alkyl radical and the 1,1-diarylethylene coupling partner, to give products **9a–h** in 25–41% (Figures 1c and 1d). In all of the aforementioned experiments, *N*-2°-alkyl-substituted pyridinium salts **1** generally gave lower yields than their *N*-benzylated congeners, and their addition reactions were slightly more efficient when promoted by $[Ir(dtbbpy)(ppy)_2]PF_6$ as the photocatalyst; yields increased by about 5–10% in these cases compared to $Ru(bpy)_3^{2+}$.

Further attempts were made to identify alternative 'component 3' donor alkenes, and it was found that the 1,1-diarylethylenes **3** could be replaced by a selection 1,3-dienes. As shown in Scheme 4a, utilizing the 2,3-diaryl-1,3-butadienes **12a–d** furnished the 1,2,3-trisubstituted 1,3-dienes **13a–d** in 24–37% yield, stereoselectively, with 3,4-*trans*-configuration on the pyrrolidine ring, and with (*E*)-configured diene double bond. Other 1,3-dienes such as 1,3-cyclohexadiene and 2,3-dimethyl-1,3-butadiene did not lead to the corresponding coupling products.

The proposed reaction mechanism shown in Scheme 4b involves photoelectron transfer (PET) reduction of *N*-alkylpyridinium salt **1** by the excited state PC* of the photocatalyst, followed by its fragmentation to triphenylpyridine and the nucleophilic alkyl radical R•. Conjugate addition of the alkyl radical to maleimide **2b** and subsequent trapping of the resulting α-carbonyl radical by the electron-rich 1,3-diene gives allyl radical **14**. Single electron transfer (SET) between radical **14** and the oxidized photocatalyst PC^+ leads to allyl cation **15** and regenerates PC. In addition, cation **15** can be produced by SET between allyl radical **14** and pyridinium salt **1** in a chain

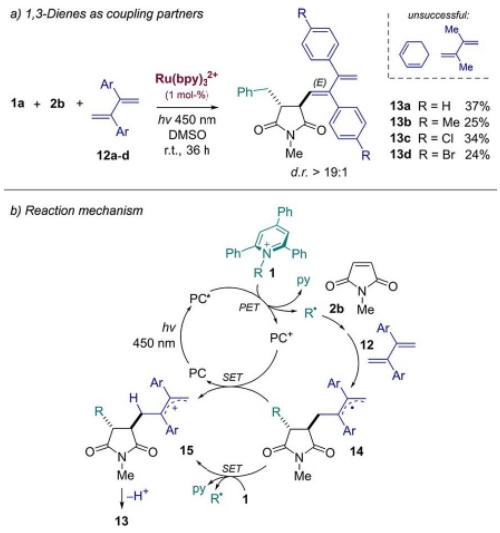

Scheme 4. a) Three-component coupling utilizing 1,3-dienes **12a–d**. b) Proposed reaction mechanism.

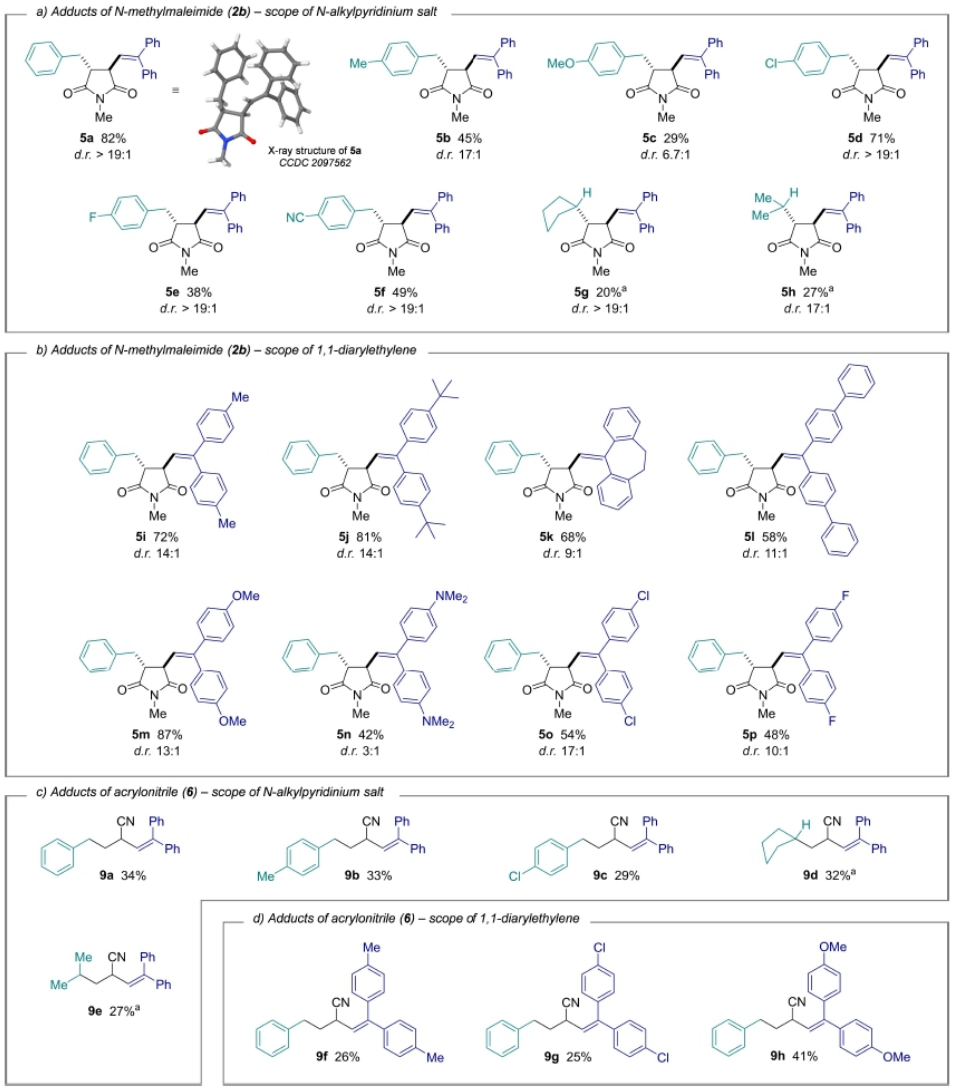

Figure 1. Scope of three component radical coupling products. Reaction conditions: $Ru(bpy)_3(PF_6)_2$ (1 mol-%), *hv* 450 nm, DMSO, r.t. 36 h, ratio of reactants **1**/**2/3** or **1/6/3** = (1/1.2/1.5). [a] $[Ir(dtbbpy)(ppy)_2]PF_6$ (1 mol-%) used.

propagation step. Loss of H^+ eventually converts cation **15** into the product **13**.

In conclusion, diverse *N*-benzyl and *N*-2°-alkylpyridinium salts were successfully engaged in photoredox-induced radical-cationic three-component couplings with *N*-methylmaleimide and acrylonitrile as radical acceptors, and 1,1-diarylethylenes as well as 2,3-diaryl-1,3-butadienes as donor alkenes. These new multicomponent reactions could be achieved under mild conditions, with high efficiency and high levels of stereoselectivity. Further extensions of this methodology are currently being investigated.

Acknowledgements

M.B. acknowledges financial support of this research by the University of Rostock. R.D. thanks the strategic network funding programme of the Leibniz association, "Leibniz-Wissenschafts-Campus-ComBioCat-Rostock" for a Ph.D. fellowship. Open Access funding enabled and organized by Projekt DEAL.

Conflict of Interest

The authors declare no conflict of interest.

Keywords: photoredox catalysis · radicals · pyridinium salts · multicomponent reactions

[1] a) E. Godineau, Y. Landais, *Chem. Eur. J.* **2009**, *15*, 3044–3055; b) V. Liautard, Y. Landais, in *Multicomponent Reactions in Organic Synthesis*; Zhu, J.; Wang, Q.; Wang, M.-X.; Eds.; Wiley-VCH, Weinheim, **2015**; pp. 401–438.
[2] F. Parsaee, M. C. Senarathna, P. B. Kannangara, S. N. Alexander, P. D. E. Arche, E. R. Welin, *Nat. Chem. Rev.* **2021**, *5*, 486–499.
[3] H. Fischer, L. Radom, *Angew. Chem. Int. Ed.* **2001**, *40*, 1340–1371; *Angew. Chem.* **2001**, *113*, 1380–1414.
[4] a) J.-F. Lutz, B. Kirci, K. Matyjaszewski, *Macromolecules* **2003**, *36*, 3136–3145; b) J. Brandrup, E. H. Immergut, Eds., *Polymer Handbook*, 4th ed.; Wiley-Interscience: New York, **1998**.
[5] a) F.-D. Lu, G.-F. He, L.-Q. Lu, W.-J. Xiao, *Green Chem.* **2021**, *23*, 5379–5393; b) S. Garbarino, D. Ravelli, S. Protti, A. Basso, *Angew. Chem. Int. Ed.* **2016**, *55*, 15476–15484; *Angew. Chem.* **2016**, *128*, 15702–15711.
[6] a) M.-Y. Cao, X. Ren, Z. Lu, *Tetrahedron Lett.* **2015**, *56*, 3732–3742; b) T. Corant, G. Masson, *J. Org. Chem.* **2016**, *81*, 6945–6952.
[7] S. Sharma, J. Singh, A. Sharma, *Adv. Synth. Catal.* **2021**, *363*, 3146–3169.
[8] Reviews: a) F.-S. He, S. Ye, J. Wu, *ACS Catal.* **2019**, *9*, 8943–8960; b) Y.-N. Li, F. Xiao, Y.-F. Zeng, *Eur. J. Org. Chem.* **2021**, 1215–1228. Selected research articles: ; c) S. Tcyrulnikov, Q. Cai, J. C. Twitty, J. Xu, A. Atifi, O. P. Bercher, G. P. A. Yap, J. Rosenthal, M. P. Watson, M. C. Kozlowski, *ACS Catal.* **2021**, *11*, 8456–8466; d) F. J. R. Klauck, M. J. James, F. Glorius, *Angew. Chem. Int. Ed.* **2017**, *56*, 12336–12339; *Angew. Chem.* **2017**, *129*, 12505–12509; e) J. Wu, P. S. Grant, X. Li, A. Noble, V. K. Aggarwal, *Angew. Chem. Int. Ed.* **2019**, *58*, 5697–5701; *Angew. Chem.* **2019**, *131*, 5753–5757.
[9] F. J. R. Klauck, H. Yoon, M. J. James, M. Lautens, F. Glorius, *ACS Catal.* **2019**, *9*, 236–241.
[10] Z.-K. Yang, N.-X. Xu, C. Wang, *Chem. Eur. J.* **2019**, *25*, 5433–5439.
[11] J. He, Q. Liu, *Synthesis* **2021**, *53*, DOI: 10.1055/a-1480–3215.
[12] P. Lundberg, Y. Tsuchiya, E. M. Lindh, S. Tang, C. Adachi, L. Edman, *Nat. Commun.* **2019**, *10*, 5307.
[13] F. Strieth-Kalthoff, M. J. James, M. Teders, L. Pitzer, F. Glorius, *Chem. Soc. Rev.* **2018**, *47*, 7190–7202.
[14] T. Ni, R. A. Caldwell, L. A. Melton, *J. Am. Chem. Soc.* **1989**, *111*, 457–464.
[15] S. Ha, Y. Lee, Y. Kwak, A. Mishra, E. Yu, B. Ryou, C.-M. Park, *Nat. Commun.* **2020**, *11*, 2509.
[16] A. A. Vlcek, E. S. Dodsworth, W. J. Pietro, A. B. P. Lever, *Inorg. Chem.* **1995**, *34*, 1906–1913.

Manuscript received: September 27, 2021
Accepted manuscript online: September 27, 2021
Version of record online: October 14, 2021

6. X-ray crystallographic data

The single crystal structure analysis were obtained by the dissolving the compound in a small amount of $CHCl_3$ and slow evaporation of solutions at room temperature. X-Ray crystal structure of following compounds published in the database of the Cambridge Crystallographic Data Centre (CCDC) and available there for retrieval.

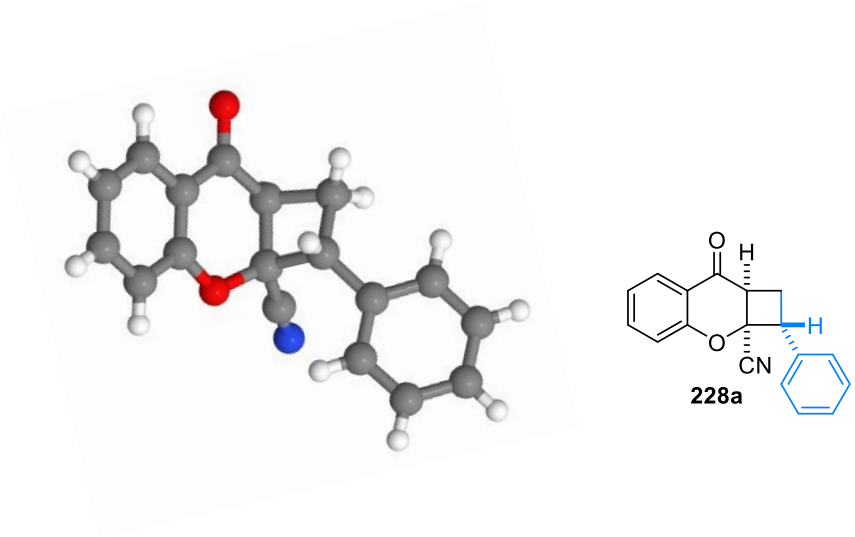

Figure 7. X-Ray crystal structure of compounds **228a.** CCDC Nr. 2250461.

Molecular Formula	$C_{18}H_{13}NO_2$
Molecular weight (g/mol)	275.29
Temperature	123 K
Crystal class	Triclinic
a; b; c (Å)	9.931 (8); 11.526 (9); 31.731 (3)
Cell angle (°)	α 90.580 (3); β 92.359 (3); γ 109.744 (3)
V (Å^3)	3414.5 (5)
Z	10
μ (mm^{-1})	0.088
Space group Hall symbol	-P 1
Space group HM symbol	P -1
Instrument	Bruker D8 QUEST

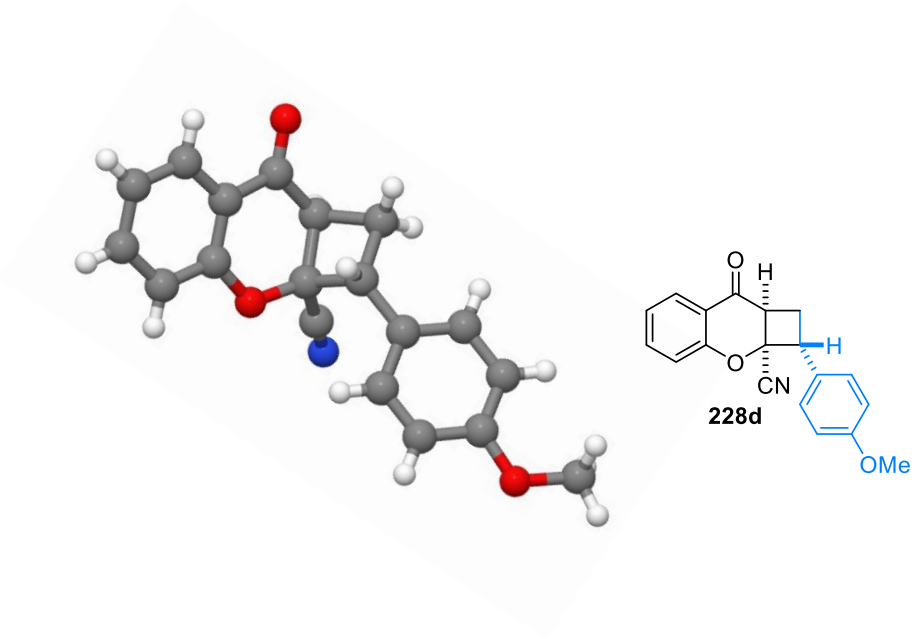

Figure 8. X-Ray crystal structure of compounds **228d.** CCDC Nr. 2250462.

Molecular Formula	$C_{19}H_{15}NO_3$
Molecular weight (g/mol)	305.32
Temperature	123 K
Crystal class	Monoclinic
a; b; c (Å)	14.6451 (9); 6.3929 (4); 17.5863 (10)
Cell angle (°)	α 90; β 112.361 (2); γ 90
V (Å^3)	1522.70 (16)
Z	4
μ (mm^{-1})	0.091
Space group Hall symbol	-P 2yn
Space group HM symbol	P 1 21/n 1
Instrument	Bruker D8 QUEST

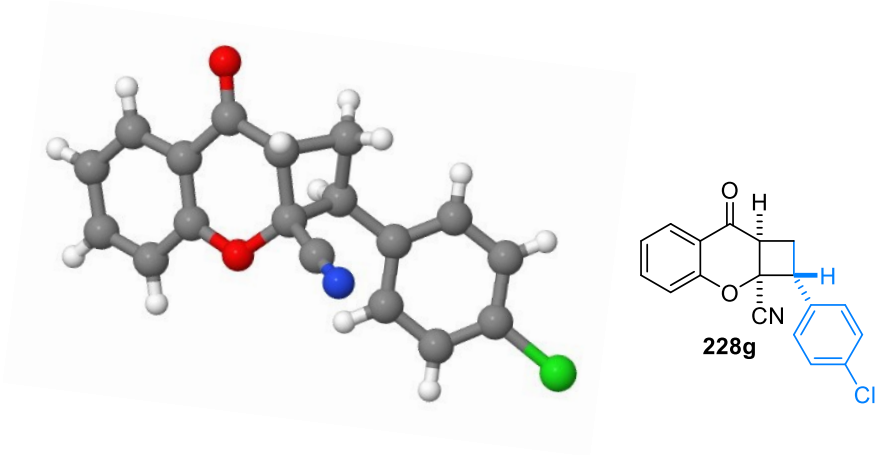

Figure 9. X-Ray crystal structure of compounds **228g.** CCDC Nr. 2250463.

Molecular Formula	$C_{18}H_{12}ClNO_2$
Molecular weight (g/mol)	309.74
Temperature	123 K
Crystal class	Triclinic
a; b; c (Å)	8.0634 (10); 9.8825 (12); 10.1049 (13)
Cell angle (°)	α 114.137 (4); β 98.043 (5) ; γ 97.708 (4)
V (Å^3)	711.10 (16)
Z	2
μ (mm^{-1})	0.275
Space group Hall symbol	-P 1
Space group HM symbol	P -1
Instrument	Bruker D8 QUEST

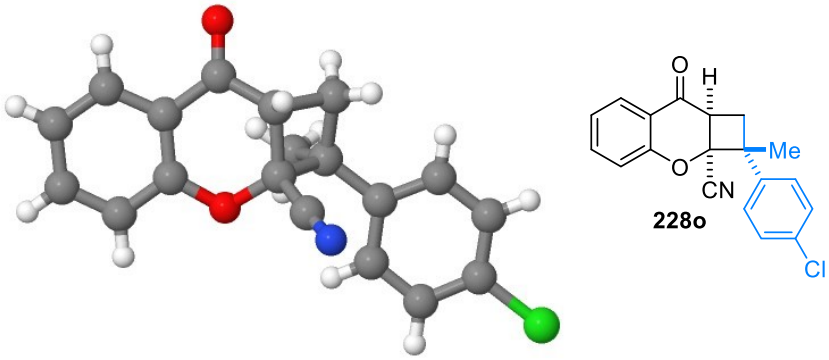

Figure 10. X-Ray crystal structure of compounds **228o.** CCDC Nr. 2250464.

Molecular Formula	$C_{19}H_{14}ClNO_2$
Molecular weight (g/mol)	323.76
Temperature	123 K
Crystal class	Monoclinic
a; b; c (Å)	9.4965 (12); 10.7884 (13); 15.316 (2)
Cell angle (°)	α 90; β 104.883 (5); γ 90
V ($Å^3$)	1516.5 (3)
Z	4
μ (mm^{-1})	0.261
Space group Hall symbol	-P 2yn
Space group HM symbol	P 1 21/n 1
Instrument	Bruker D8 QUEST

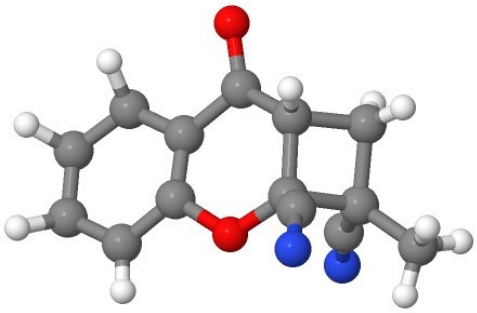

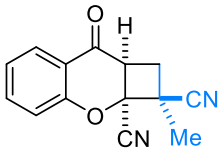

228t

Figure 11. X-Ray crystal structure of compounds **228t.** CCDC Nr. 2250465.

Molecular Formula	$C_{14}H_{10}N_2O_2$
Molecular weight (g/mol)	238.24
Temperature	123 K
Crystal class	Monoclinic
a; b; c (Å)	10.2547 (13); 6.2786 (8); 18.091 (3)
Cell angle (°)	α 90; β 100.081 (5); γ 90
V (Å^3)	1146.8 (3)
Z	4
μ (mm^{-1})	0.095
Space group Hall symbol	-P 2yn
Space group HM symbol	P 1 21/n 1
Instrument	Bruker D8 QUEST

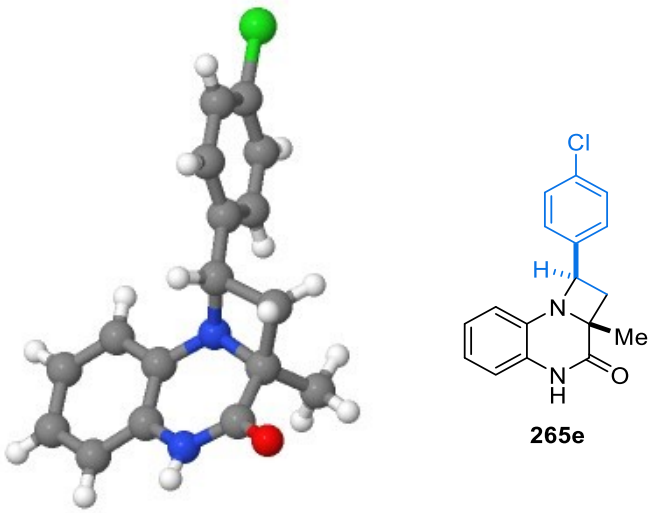

265e

Figure 12. X-Ray crystal structure of compounds **265e.** CCDC Nr. 2180171.

Molecular Formula	$C_{17}H_{15}ClN_2O$
Molecular weight (g/mol)	298.76
Temperature	123 K
Crystal class	Monoclinic
a; b; c (Å)	5.4323 (3); 7.8103 (4); 34.2274 (15)
Cell angle (°)	α 90; β 94.419 (5); γ 90
V (Å^3)	34.2274 (15)
Z	4
μ (mm^{-1})	0.264
Space group Hall symbol	-P 2ybc
Space group HM symbol	P 1 21/c 1
Instrument	Bruker D8 QUEST

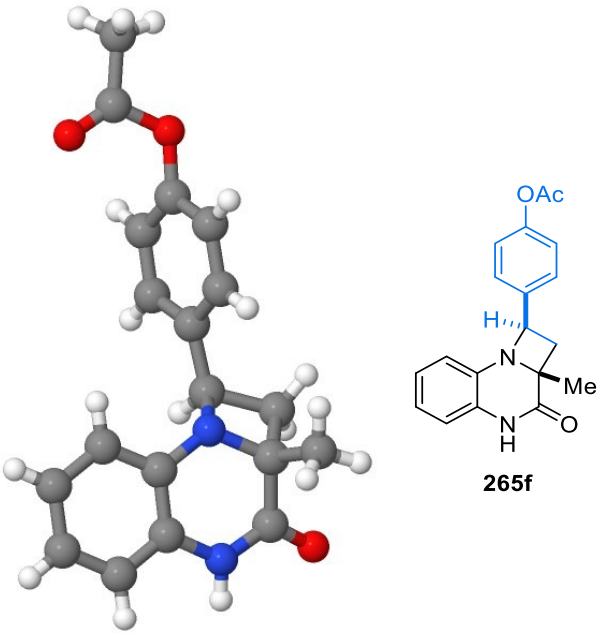

Figure 13. X-Ray crystal structure of compounds **265f.** CCDC Nr. 2180172.

Molecular Formula	$C_{19}H_{18}N_2O_3$
Molecular weight (g/mol)	322.35
Temperature	123 K
Crystal class	Triclinic
a; b; c (Å)	7.3804 (7); 9.8000 (9); 11.3168 (11)
Cell angle (°)	α 88.756 (4); β 82.784 (4); γ 82.815 (4)
V (Å^3)	805.65 (13)
Z	2
μ (mm^{-1})	0.091
Space group Hall symbol	-P 1
Space group HM symbol	P -1
Instrument	Bruker D8 QUEST

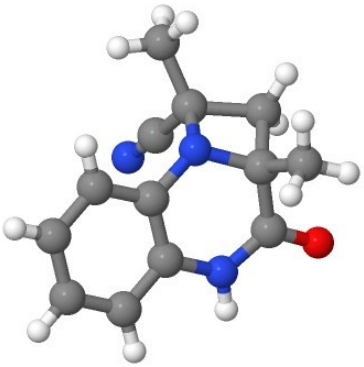

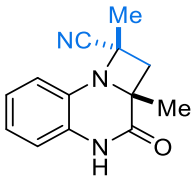

265n

Figure 14. X-Ray crystal structure of compounds **265n.** CCDC Nr. 2180173.

Molecular Formula	$C_{13}H_{13}N_3O$
Molecular weight (g/mol)	227.26
Temperature	173 K
Crystal class	Triclinic
a; b; c (Å)	6.8773(6); 7.5415(6); 11.6767(9)
Cell angle (°)	α 82.617(3); β 82.040(3); γ 79.734(3)
V (Å^3)	586.82(8)
Z	2
μ (mm^{-1})	0.085
Space group Hall symbol	-P 1
Space group HM symbol	P -1
Instrument	Bruker D8 QUEST

CURRICULUM VITAE

Rajesh Dasi geboren am 09.07.1996 in Warangal

Schwaaner Landstr. 189, 18059 Rostock

rajesh.dasi@uni-rostock.de

BERUFLICHER WERDEGANG

03/2020–08/2023 **Wissenschaftlicher Mitarbeiter, Doktorand**

Universität Rostock

AUSBILDUNG

03/2020–08/2023 **Promotionsstudium am Institut für Chemie**

Universität Rostock

- Dissertation in der Abteilung Organische Chemie
- Thema: “Thermal and photocatalytic C-C and C-N bond formation by atom-transfer radical additions and photocycloadditions”

08/2017–06/2019 **Masterstudium der Medizinischen Chemie**

National Institute of Pharmaceutical Education and Research

Masterarbeit im Fach Medizinische Chemie

- Thema: “iRGD Peptide Mediated Delivery of PLGA Nanoparticles for Targeted Delivery of Garcinol against Colon cancer”.
- Gesamtnote M.Sc.: 1.3 (GPA 8.74/10)

07/2013–06/2017 **Bachelorstudium der Pharmazie**

Jawaharlal Nehru Technological University, Hyderabad

- Bachelorarbeit im Fach Pharmazie
- Thema: “Synthesis of *N*-Acetylneuraminic acid Prodrugs”.
- Abschlusstnote B.Sc.: 2.3 (67%)

LEHRTÄTIGKEITEN

07/2019–02/2020 **Wissenschaftlicher Mitarbeiter im Bereich Organische Chemie am Pathfinder Institut für Pharmazie**

Betreuer im Grundpraktikum der organischen Chemie

- Tutor für organischen und Medizinische Chemie
- Mündliche Prüfungen
- Vorbereitung des Chemiepraktikums

PUBLIKATIONEN

[1] R. Dasi, A. Villinger, M. Brasholz, *Org. Biomol. Chem.* **2023**, *21*, 6103-6106.

[2] R. Dasi, A. Villinger, M. Brasholz, *Org. Lett.* **2022**, *24*, 8041-8046.

[3] R. Dasi, D. Schmidhuber, L.M. Gronbach, J. Rehbein, M. Brasholz, *Org. Biomol. Chem.* **2021**, *19*, 1626-1631.

[4] P. Seefeldt, R. Dasi, A. Villinger, M. Brasholz, *Chem Photo Chem* **2021**, *5*, 979-983.

[5] B. Paul, R. H. Gaonkar, D. Dutta, R. Dasi, B. Mukherjee, S. Ganguly, S. K. Das, *Biomaterial Advances*, **2022**, 134, 112714.